FLYING SAUCER 1 IS A TRANSMEMBRANE RING PROTEIN INVOLVED IN CELL WALL BIOSYNTHESIS IN THE *ARABIDOPSIS THALIANA* SEED COAT

by

Catalin Voiniciuc

B.Sc., The University of British Columbia, 2010

A THESIS SUBMITTED IN PARTIAL FULFILLMENT OF
THE REQUIREMENTS FOR THE DEGREE OF

MASTER OF SCIENCE

in

The Faculty of Graduate Studies

(Botany)

THE UNIVERSITY OF BRITISH COLUMBIA

(Vancouver)

April 2012

Abstract

The plant cell wall is a complex and dynamic network of polysaccharides and structural proteins, which lies outside the plasma membrane and provides strength and protection. The mechanical properties of the cell wall depend largely on the structure and organization of its components. Pectins form the gel matrix in which all other wall components are embedded and changes in their degree of methylesterification (DM) impact wall strength and adhesion. Low DM pectin molecules can be linked together via calcium bridges to form strong gels, but very few mutants affecting pectin methylesterification have been identified.

During my MSc research, I characterized *flying saucer 1* (*fly1*), a novel *Arabidopsis thaliana* seed coat mutant, which displays primary cell wall detachment, reduced mucilage extrusion, and increased mucilage adherence. These defects appear to result from a lower DM in mucilage, and can be intensified by addition of Ca^{2+} ions or completely rescued by treatment of seeds with cation chelators. The *FLY1* gene encodes a protein with multiple transmembrane spans that is targeted to the secretory pathway and contains a RING-H2 domain, which generally facilitates protein-protein interactions. FLY1-YFP fusion proteins localize to small intracellular compartments in seed coat epidermal cells at the stage of mucilage biosynthesis.

TUL1, a previously described FLY1 yeast ortholog, is a Golgi-localized E3 ligase involved in the trafficking of membrane proteins. I propose that FLY1 promotes pectin methylesterification in seed coat epidermal cells, potentially through interactions with pectin methyltransferase enzymes in the Golgi apparatus. Co-expression analysis suggests that *FLY1* and *FLY2*, its only paralog, may play partially redundant roles in xylem development.

These genes may be regulated by KNAT7, a transcription factor that controls secondary wall biosynthesis in both xylem and seed coat cells. The binding partners of the FLY1 protein and its precise molecular function remain to be determined.

Preface

Figure 1.1 is a modified version of a previously published image (Mendu et al., 2011). Rough and fine mapping of *FLY1* were performed by Dr. Gillian Dean and several undergraduate students: Alan Gillett, Graham Dow, Tiffany Ngai, and Andrew Karpov. Dr. Gillian Dean, Yeen Ting Hwang and Diana Young partially characterized the *fly1-1* mutant.

Dr. Gillian Dean conducted the preliminary Scanning Electron Microscopy (SEM) analysis of *fly1* dry seeds, and I subsequently replicated her results. I prepared hydrated seeds for cryo-SEM and analyzed them with the technical assistance of Derrick Horne. Jonathan Griffiths and I fixed developing seeds, and imaged seeds stained with cellulose-specific dyes together. I performed the remaining histological techniques (resin embedding and sectioning) and confocal microscopy alone. Jonathan Griffiths also operated the instruments for monosaccharide analysis in the lab of Dr. Shawn Mansfield (Faculty of Forestry, UBC), and processed the raw data. Except for one whole seed biological replicate that was prepared and analyzed by Dr. Gillian Dean, I prepared all samples alone and analyzed them in collaboration with Jonathan Griffiths.

Gabriel Lévesque-Tremblay and Patricia Lam isolated RNA and prepared cDNA from dissected siliques and other major Arabidopsis tissues respectively. I used their cDNA samples as templates for my analysis of *FLY1* and *FLY2* transcript levels. Dr. Allan DeBono provided the pGreen0229 vector containing YFP that I used to construct a *FLY1*$_{pro}$*:FLY1-YFP* transgene. Col-2 seeds expressing cytosolic YFP in the seed coat were a gift from Elahe Esfandiari. The heat map of gene expression shown in Figure 4.2 was obtained using the publicly available GENEVESTIGATOR tool (Hruz et al., 2008).

Table of Contents

List of Tables

List of Figures

List of Abbreviations

Col – columbia

Ler - landsberg erecta

FLY – flying saucer

KNAT7 – knotted-like homeobox of arabidopsis thaliana 7

TUL1 – transmembrane ubiquitin ligase 1

CESA – cellulose synthase

PME – pectin methylesterase

PMEI – pectin methylesterase inhibitor

PMT – pectin methyltransferase

GAUT – galacturonosyltransferase

CW – cell wall

PCW – primary cell wall

SCW – secondary cell wall

HG – homogalacturonan

RG-I – rhamnogalacturonan-I

GalA – galacturonic acid

Rha – rhamnose

DM – degree of methylesterification

YFP – yellow fluorescent protein

EMS – ethyl methanesulfonate

bp – base pairs

aa – amino acid

DNA – deoxyribonucleic acid

cDNA - complementary deoxyribonucleic acid

T-DNA – transfer-DNA

RNA - ribonucleic acid

mRNA – messenger ribonucleic acid

PCR – polymerase chain reaction

RT-PCR – reverse transcription polymerase chain reaction

DPA – days post-anthesis

HPAEC – high-performance anion-exchange chromatography

AIR – alcohol-insoluble residue

DIC – differential interference contrast

EDTA - ethylenediaminetetraacetic acid

S4B – pontamine fast scarlet 4b

RR – ruthenium red

BSA – bovine serum albumin

Ca^{2+} – calcium

Acknowledgements

I offer my sincere gratitude to the faculty, staff and fellow graduate students in the Botany department at UBC, who have provided the inspiration for my work in this field. I owe particular thanks to my supervisor Dr. George Haughn, whose incredible passion for genetics drove me to pursue graduate research in plant biology. Dr. Haughn's remarkable teaching and problem solving abilities have significantly facilitated my development as a scientist. I am also grateful for the guidance provided by my other committee members, Dr. Ljerka Kunst and Dr. Lacey Samuels, whose vision of science and experience helped me succeed in graduate school.

Special thanks go to my colleagues, particularly in the Haughn, Kunst and Samuels labs, who shared their technical expertise with me and patiently answered my endless questions. I would like to acknowledge and extend my gratitude to Jonathan Griffiths, who spent countless hours assisting me with microscopy, and biochemical analysis. I also thank Patricia Lam, Gabriel Lévesque-Tremblay, and Dr. Allan DeBono for their valuable advice on molecular cloning.

I greatly appreciate the assistance of the UBC Bioimaging Facility staff (Bradford Ross, Derrick Horne, Kevin Hodgson, and Garnet Martens) with my sample preparation and imaging needs. I also thank Dr. Shawn Mansfield and his lab members in the Faculty of Forestry at UBC for assistance with sugar chemistry.

Ultimately, none of this would have been possible without my close friends and family. I thank my wife, Kylin Victoria, for filling my days with happiness and my parents for their incredible support over the years.

For my friends and family in Romania

Chapter 1: Introduction

1.1 Introduction to Plant Cell Walls

1.1.1 Plant Cell Wall Polymers, Functions, and Applications

The presence of a carbohydrate-rich cell wall outside the plasma membrane is one of the fundamental features that distinguishes plant cells from other eukaryotic cells (Wojtaszek, 2001). Plant cell walls can be functionally classified as primary walls if they are synthesized while cells are growing, or as secondary walls if they are deposited after cell expansion has ceased (Carpita and Gibeaut, 1993; Liepman et al., 2010). Primary cell walls are mainly composed of the polysaccharides cellulose, hemicellulose and pectin. The cellulose network is the major load-bearing component of the cell wall, and is generally oriented perpendicular to the direction of cell expansion (Green, 1980). Crystalline cellulose microfibrils are thought to be cross-linked by hemicelluloses via multiple hydrogen bonds, forming a rigid network that is embedded in a pectinaceous gel matrix (Cosgrove, 2005; Somerville, 2006).

Pectins, particularly homogalacturonan with a low degree of methylesterification, have strong adhesive properties and are abundant in the middle lamella, the site of cell-cell attachment in plants (Lord and Mollet, 2002; Wolf et al., 2009). Due to the presence of galacturonic acid in all pectins, pectin gels are hydrophilic, a property that facilitates the diffusion of water and small molecules through the wall (Burton et al., 2010). Changes in the structure of pectin can impact the strength of the cell wall (Lord and Mollet, 2002), and the architecture of the cellulose-hemicellulose network (Pelletier et al., 2010). Current understanding of the organization of wall polysaccharides is rather limited, largely because

cell walls are dynamic structures that vary in composition over time and in different cell types (Knox, 2008).

In addition to polysaccharides, cell walls are composed of structural proteins and enzymes, while some secondary walls also contain lignin (Heredia et al., 1995). A variety of structural proteins (Keller, 1993), including arabinogalactan proteins (AGPs) (Seifert and Roberts, 2007), glycine-rich proteins (GRPs) (Ringli et al., 2001), and expansins (Sampedro and Cosgrove, 2005), have been found in plant cells walls, but their exact biological functions and molecular roles are still under investigation. Enzymes that modify polysaccharides, particularly pectin, in the apoplast are critical for cell wall remodelling and are described later in this chapter.

Cell wall polysaccharides form a mechanically strong yet dynamic structure that can play a variety of important biological functions in plants. The primary cell wall typically constrains cell shape and size, and forms a physical barrier from the environment along with the cuticle (Liepman et al., 2010). Plant cell expansion is mainly driven by turgor pressure, the outward pressure exerted by the water content of a cell (Cleland, 1971). The wall typically restricts cell expansion and must be loosened before cell size can increase and cell shape can be altered. Changes in the architecture of the pectin matrix can influence the orientation of the cellulose network, and the extent and direction of cell elongation (Chanliaud and Gidley, 1999). The maintenance of wall integrity throughout the life of a plant cell is therefore essential, although the underlying molecular signalling pathways are not well understood (Braam, 1999; Hamann and Denness, 2011; Wolf et al., 2011). Since pectins in the middle lamella normally maintain plant cell adhesion, enzymatic modification and degradation of their structure is necessary for stamen abscission, and the dehiscence of

anthers and siliques to occur (Micheli, 2001; Pelloux et al., 2007; Lashbrook and Cai, 2008; Ogawa et al., 2009).

In addition to providing mechanical support, extracellular oligosaccharides can act as signals (Mohnen and Hahn, 1993; Hamant et al., 2010), which are required in cell morphogenesis (Szymanski and Cosgrove, 2009) and biotic/abiotic stress responses (Popper, 2008; Hématy et al., 2009). Cell wall polysaccharides also function as antigravitational compounds that enable land plants to withstand the intense mechanical load exerted on their bodies (Volkmann and Baluska, 2006). Without cell walls, majestic trees that reach great heights above the ground would be reduced to mere slime molds (Cosgrove, 2005).

On top of their important roles in plant physiology, wall polysaccharides also serve as raw materials in many industries that manufacture desirable products for human use. Cellulose fibers have a very high economic value and are used in the production of paper, textiles, and biofuels (Showalter, 1993), while pectins are employed as gelling agents in a variety of food and pharmaceutical products (Thakur et al., 1997). In the last decade, pectins with a low degree of methylesterification have been successfully applied as a carrier for oral drug delivery to the colon in humans (Liu et al., 2003; Sande, 2005; Itoh et al., 2007; Sriamornsak, 2011). Since the plant cell wall represents the most abundant source of renewable biomass on the planet (Liepman et al., 2010), its industrial applications will likely increase in the near future as the availability of non-renewable resources declines. Despite the great biological and commercial value of plant cell walls, the synthesis and subsequent modification of their polysaccharide components, particularly pectin, are poorly understood processes (York et al., 1986). I am therefore interested in isolating mutants with defects in

pectin and other wall polysaccharides in order to identify new genes involved in cell wall biosynthesis and modification.

1.1.2 Overview of Cell Wall Polysaccharide Biosynthesis

The availability of the genome sequence of *Arabidopsis thaliana* (hereafter Arabidopsis), an important model system for flowering plants, opened the door for the identification of large families of genes involved in cell wall biogenesis (Arabidopsis Genome Initiative, 2000). Nevertheless, after more than a decade of research, the functions of the vast majority of genes encoding putative cell wall-related enzymes have yet to be determined (Somerville, 2006; Mutwil et al., 2008).

Cellulose is a deceptively simple, linear polymer composed of 1,4-β-D-glucan chains that can form extensive hydrogen bonds resulting in the crystallization of multiple parallel chains into insoluble microfibrils (Saxena and Brown, 2005; Joshi and Mansfield, 2007; Taylor, 2008). Cellulose biosynthesis occurs at the plasma membrane via rosette complexes composed of cellulose synthase (CESA) proteins (Mutwil et al., 2008). At least three different CESA subunits are believed to be required for a functional complex, and different combinations are involved in primary cell wall and secondary cell wall biosynthesis (Somerville, 2006). In Arabidopsis, *CESA1*, *CESA3*, *CESA6* and the closely related *CESA2*, *CESA5*, and *CESA9* are essential for cellulose synthesis in the primary wall, while *CESA4*, *CESA7*, and *CESA8* are required for secondary cell wall biosynthesis (Guerriero et al., 2010).

Unlike cellulose, the matrix polysaccharides hemicellulose and pectin are synthesized within the Golgi apparatus and are then secreted to the apoplast (Reiter, 2002). Xyloglucan, the most abundant hemicellulose in the primary walls of higher plants, has a 1,4-β-D-glucan backbone decorated with 1,6-α-D-xylose residues (Hayashi and Kaida, 2011). Recent studies

have shown that some *CELLULOSE SYNTHASE-LIKE* (*CSL*) genes are required for synthesizing the backbone of hemicelluloses (Cosgrove, 2005), while glycosyltransferases are responsible for adding the side branches (Scheible and Pauly, 2004).

Even less is known about the synthesis of pectin, one of the most structurally and functionally complex polysaccharides found in nature (Mohnen, 2008). About one third of the primary cell wall consists of the polymers homogalacturonan (HG, typically 65% of pectin), rhamnogalacturonan-I (RG-I, 25-35%), and rhamogalacturonan-II (RG-II, less than 10%) (Willats et al., 2001a; Zandleven et al., 2007; Mohnen, 2008). These galacturonic acid-rich polysaccharides are not thought to be separate molecules but are proposed to form a high-molecular weight complex via multiple covalent bonds (Harholt et al., 2010). HG is the simplest pectin component, consisting of unbranched chains of 1,4-α-D-galacturonic acid, while RG-II has the same backbone but is a highly substituted polymer. In contrast, the RG-I backbone is made of alternating 1,4-α-D-galacturonic acid and 1,2-α-L-rhamnose units that have a variable number of branches containing arabinose, fucose, galactose, and glucuronic acid. Although pectin biosynthesis is predicted to require at least 67 different glycosyltransferases, methyltransferases, and acetyltransferases, only a small number of enzymes are currently known and adequately characterized (Mohnen, 2008; Harholt et al., 2010) . The isolation of the first pectin biosynthetic enzyme GAUT1, an HG 1,4-α-galacturonosyltransferase (Sterling et al., 2006), has recently led to the identification of a HG biosynthetic complex with GAUT1 and GAUT7 at its core, and 12 associated proteins including two putative methyltransferases (Atmodjo et al., 2011). HG is thought to be methylated by pectin methyltransferase (PMT) enzymes in the Golgi and is secreted to the cell wall in a highly methylesterified form (Pelloux et al., 2007). Once secreted to the

apoplast, pectins form a dynamic gel matrix that can be further modified through changes in the degree of methylesterification (DM) of HG polymers. The identification of novel mutants that specifically affect pectin biosynthesis or modification is necessary to increase our understanding of this complex polysaccharide (Bouton et al., 2002; Wolf et al., 2009).

1.1.3 Enzymes Involved in Pectin Modification

Pectin modification is a complex process that can increase the rigidity of the wall when cell elongation needs to stop, or maintain wall flexibility for growth or cell separation to occur. Although pectins are synthesized as fully methylesterified polymers in the Golgi apparatus, HG with different DM has been visualized across the cell wall using monoclonal antibodies (Willats et al., 2001c). Changes in pectin methylesterification are thought to impact the strength of pectin gels, which form through calcium cross-links between unesterified regions of two or more homogalacturonan molecules (Willats et al., 2001a). Pectin methylesterases (PMEs) are secreted to the apoplast and typically remove methyl groups from chains of galacturonic acids in a block-wise fashion, thereby leaving more carboxyl groups available to form bonds with Ca^{2+} ions (Moustacas et al., 1991; Goldberg et al., 1996; Wolf et al., 2009). Linear de-methylesterification has been shown to strengthen pectin gels, and is required to maintain cell-cell adhesion and to limit cell elongation (Derbyshire et al., 2007). In contrast, non-linear removal of methylester groups by certain PMEs can render HG polymers more susceptible for degradation by enzymes such as polygalacturonases that play essential roles in stamen abscission, and anther and silique dehiscence (Micheli, 2001; Pelloux et al., 2007; Lashbrook and Cai, 2008; Ogawa et al., 2009). PMEs are also involved in fruit softening, so further understanding of their biochemical roles may provide new avenues for the genetic manipulation of the ripening

process, and may lead to significant agricultural breakthroughs (Steele et al., 1997; Prasanna et al., 2007).

Since the pectin gel matrix embeds all other wall polysaccharides, modification of pectins by PMEs can have profound influences on the overall functions of the cell wall. Some pathogens exploit this mechanism by secreting PMEs and pectinases that preferentially cleave unesterified HG polysaccharides, in order to penetrate plant cells and to use the cell wall as a carbon source (Juge, 2006). However, research over the past decade has uncovered a plant-pathogen arms race for the control of pectin methylesterification. Proteinaceous PME inhibitors (PMEIs) have been identified in several plant species and are proposed to bind PMEs in the cell wall and block their access to HG substrates (Jolie et al., 2010). The existence of large *PME* and *PMEI* gene families in the Arabidopsis genome highlights the importance and the complexity of pectin modification (Somerville, 2006).

1.2 The Seed Coat Is a Model System for Cell Wall Research

1.2.1 Arabidopsis Seed Coat Structure and Function

The variability of cell wall polysaccharide composition across different Arabidopsis cell types complicates the identification and characterization of pectin-related genes (Somerville et al., 2004). Combined with the structural complexity of the polymers themselves, these technical challenges suggest that the best approach to study pectin biosynthesis and modification may be to focus on a single cell type. The ideal cell type would not be required for plant viability but would produce large amounts of pectin.

Fortunately, in recent years, the Arabidopsis seed coat epidermal cells have been successfully employed as a model system for the synthesis, secretion and modification of cell wall components, particularly pectin (Arsovski et al., 2010). The seed epidermal cells

produce large amounts of cell wall polysaccharides but are dispensable under laboratory growth conditions (Western et al., 2001). The epidermis of mature dry seeds features three morphologically and biochemically distinct structures: a thin primary cell wall, a donut-shaped pocket of mucilage, and a volcano-shaped secondary cell wall known as the columella (Western et al., 2000). The outer primary cell wall envelops the thick mucilage ring, which surrounds the central columella. Hydration of mature seeds triggers the rapid expansion of pectin, which ruptures the primary wall, and releases a thick layer of mucilage around the seed. This gel-like capsule can be easily visualized using Ruthenium Red, Calcofluor White and other polysaccharide-binding dyes (Western et al., 2000; Macquet et al., 2007a). The analysis of mutants defective in seed coat development has facilitated the characterization of several novel cell wall-related genes (Western et al., 2001; Haughn and Chaudhury, 2005).

Although the genetic disruption of Arabidopsis seed coat epidermal cells does not compromise plant viability in laboratory growth chambers, mucilage may play several important biological roles in the wild (Western et al., 2000, 2001). The reduced germination efficiency under low water conditions of *myb61*, *bxl1*, and *sbt1.7* seeds, which have mucilage defects, suggests that mucilage may aid water uptake and germination under drought conditions (Penfield et al., 2001; Willats et al., 2001c; Rautengarten et al., 2008; Arsovski et al., 2009). Moreover, mucilage may promote seed dispersal by protecting seeds from animal digestion and by facilitating the attachment of seeds to moving organisms through the adhesive properties of its pectin components (Young and Evans, 1973; Sorensen, 1986). Since the Arabidopsis seed coat epidermis is a dispensable cell layer that synthesizes large

amounts of wall polysaccharides, it provides an excellent genetic system for studying cell wall biogenesis.

1.2.2 Development of Seed Coat Epidermal Cells

Between 5 and 8 Days Post-Anthesis (DPA), the Arabidopsis seed coat epidermal cells secrete large amounts of pectin between the primary cell wall and the plasma membrane, forming a donut-shaped pocket of mucilage around a cytoplasmic column (Western et al., 2000). Although mucilage is deposited in an asymmetric manner to the apoplastic space at the junction of the outer tangential and radial cell walls, the underlying mechanisms for this polarized secretion are unknown (McFarlane et al., 2008; Young et al., 2008). The epidermal cells then synthesize a volcano-shaped secondary wall (9 to 11 DPA), which protrudes through the center of the mucilage pocket and forms connections to the primary wall (Figure 1.1). Hydration of mature seeds triggers the rapid expansion of pectins, and the rupture of the outer tangential primary wall from the radial wall. Interestingly, large fragments of tangential wall remain attached to the columella after mucilage extrusion from wild type seeds (Figure 1.1), but the factors that mediate this specific attachment have not been identified.

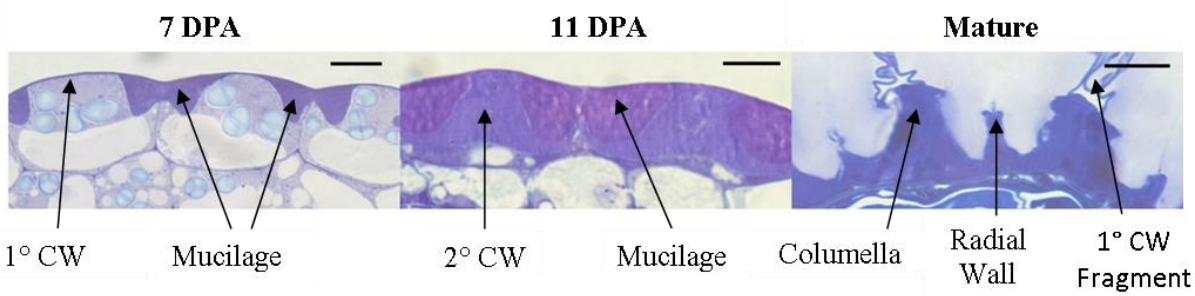

Figure 1.1: Morphology of Developing Seed Coat Epidermal Cells.
Sections of Col-0 cryo-fixed young seeds and aqueous glutaraldehyde-fixed mature seeds are stained with Toluidine Blue. Outer tangential primary cell walls (1º CW), secondary cell walls (columella; 2º CW), mucilage and radial walls are indicated. This figure is a modified version of a previously published image (Mendu et al., 2011). Scale bars = 10 µm.

1.2.3 Known Mutants with Seed Mucilage Defects

The isolation of Arabidopsis mutants with defective seed mucilage extrusion has led to the functional characterization of several genes that are involved in cell wall biosynthesis. Three key transcription factors, *GL2*, *TTG2* (Western et al., 2001; Johnson et al., 2002), and *MYB61* (Penfield et al., 2001; Western et al., 2004), are proposed to regulate independent pathways that affect mucilage extrusion, but their downstream targets are largely unknown. Loss-of-function mutations in genes encoding enzymes required for the biosynthesis of the pectin (*MUM4*, *GAUT11*) (Western et al., 2004; Caffall et al., 2009), or for pectin modification after secretion (*MUM2*, *BXL1*, *SBT1.7*) have also been shown to cause reduced mucilage production and release (Dean et al., 2007; Rautengarten et al., 2008; Arsovski et al., 2009).

Mucilage-Modified 4 (MUM4/RHM2) was the first seed coat cell wall enzyme identified. MUM4 coverts UDP-D-glucose to UDP-L-rhamnose, a key initial step in the biosynthesis of RG-I (Usadel et al., 2004a; Western et al., 2004; Oka et al., 2007). *BXL1* encodes an α-L-arabinofuranosidase that removes arabinan residues located on the side chains of RG-I (Arsovski et al., 2009), while *MUM2* encodes a putative β-D-galactosidase (BGAL6) that removes RG-I galactose side chain residues (Dean et al., 2007; Macquet et al., 2007b). Aside from a recent screen of T-DNA insertions in 13 of the 15 Arabidopsis GAUT genes that found one mutant (*gaut11*) with a mucilage defect (Caffall et al., 2009), very little is known about the genes involved in HG biosynthesis in the Arabidopsis seed coat.

In the last two years, researchers have made significant findings concerning cellulose biosynthesis in the seed coat epidermis. Cellulose synthesized by CESA5/MUM3 has been shown to play an essential role in mucilage adherence to the seed, while cellulose

synthesized by CESA2, CESA5 and CESA9 reinforces the structure of the secondary wall in the seed coat (Stork et al., 2010; Harpaz-Saad et al., 2011; Mendu et al., 2011; Sullivan et al., 2011). Additional CESA subunits are likely to participate in cellulose biosynthesis in the mucilage pockets but their identities are currently unknown.

1.3 Isolation of the *flying saucer 1* Mutant

The *flying saucer 1-1* (*fly1-1*) line was isolated from an EMS-mutagenized Col-2 population during a screen for mucilage-defective mutants in the Haughn Lab. Although the *fly1-1* mutant seeds release mucilage when hydrated in water, they can be easily distinguished from wild type seeds by the presence of unusual disc-like structures at the periphery of the extruded mucilage (Figure 1.2). A test-cross segregation ratio of 3:1 was observed in the F_2 generation indicating that the *fly1-1* phenotype is caused by a single recessive mutation. Crosses performed by various Haughn lab members over the past ten years revealed that *fly1-1* complements all previously known seed coat mutants, including *ap2*, *ttg1*, *gl2* (all regulators of *MUM4*) (Western et al., 2004), *ats* (Leon-Kloosterziel et al., 1994), *mum1-1* (Huang et al., 2011), *mum2* (Dean et al., 2007), *mum3*/*cesa5* (Western et al., 2001; Sullivan et al., 2011), *mum4*, *mum5* (Western et al., 2001, 2004), *myb61* (Penfield et al., 2001), *ttg2* (Johnson et al., 2002), and *bxl1* (Arsovski et al., 2009). Dr. Gillian Dean partially characterized the *fly1-1* mutant phenotype and conducted several experiments to investigate if the unusual discs are detached primary cell walls and/or unexpanded mucilage rings. Her experimental results suggest that the discs released by the *fly1-1* mutant consist of detached primary cell walls bound to mucilage. The position of the *fly1-1* mutation was fine-mapped using insertions/deletions (indels) between Col-2 and Ler ecotypes to a 180 kb region near the end of chromosome IV, which contains 60 protein-coding genes. The precise

identity of the *FLY1* gene was not determined since no further indels are present in this small region and the probability of observing more recombination events is very low.

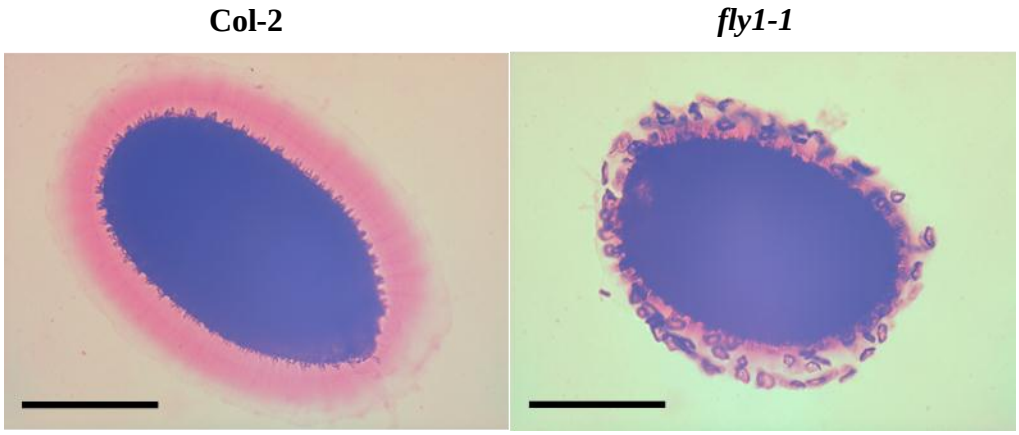

Figure 1.2: Mucilage Phenotype of Col-2 and *fly1-1* Hydrated in Water.
Light micrographs of seeds shaken in water and stained with Ruthenium Red.
Scale bars = 250 µm.

1.4 Research Outline and Goals

My MSc research utilizes the Arabidopsis seed coat as a model system to study the molecular foundations of plant cell wall biosynthesis. Analyses of mucilage-defective mutants has led to the identification of several genes required for cell wall biogenesis, but many other players involved in this process remain to be discovered. The majority of my work was devoted to carefully characterizing the complex phenotype of the *fly1-1* mutant, cloning the *FLY1* gene, and investigating its function in seed coat epidermal cells (Chapter 3). A secondary goal was to use the *FLY1* gene to identify homologous or co-expressed genes that may play similar biological functions (Chapter 4). Overall, my thesis project was driven by three major research objectives:

1. To characterize the seed mucilage phenotype of the *fly1* mutant, to determine the composition of the discs and to discover the underlying cause for these defects.

2. To clone the *FLY1* gene, to confirm its identity, and to analyze its expression, as well as the subcellular localization and the putative functions of the encoded protein.

3. To identify additional genes involved in cell wall biosynthesis, which are related to *FLY1* through sequence homology or co-expression.

These objectives were completed using a combination of forward and reverse genetics, molecular biology, light and electron microscopy, analytical chemistry and bioinformatics. To address the first objective, I focused my research on confirming that *fly1* discs contain detached primary cell walls, and that the mucilage extruded from mutant seeds is more compact and adherent than wild type. I also aimed to uncover when and why the discs are released, and to explain how the discs and the mucilage extrusion defects are related. For the second objective, I cloned the *FLY1* gene by position, determined its expression pattern, and investigated the phenotype of multiple *fly1* T-DNA insertional mutants. I also complemented the *fly1-1* mutant with a wild type copy of the *FLY1* gene, and analysed the expression and subcellular localization of FLY1-YFP fusion proteins. My findings in Chapter 3 confirm that the *fly1* discs contain detached primary cell walls bound to mucilage that contains more unesterified HG than wild type. My results suggest that FLY1 is an intracellular transmembrane protein that positively regulates pectin methylesterification, possibly through protein-protein interactions with PMT enzymes in the Golgi. To better understand the role of FLY1, I identified homologous genes in Arabidopsis and other species and investigated their function. I also conducted a screen for T-DNA insertional mutants in the top genes co-expressed with *FLY1* to identify additional players involved in mucilage biosynthesis. In Chapter 4, I analyze the functions of the yeast ortholog (*TUL1*), the

Arabidopsis paralog (*FLY2*), and the top co-expressed gene (*KNAT7*), and describe their connections to *FLY1*.

Chapter 2: Materials and Methods

2.1 Plant Materials and Growth Conditions

All the plants used in this study, except the mapping population (see section below), were descended from the *Arabidopsis thaliana* Columbia wild type. The Col-2 line was obtained from a Col-0 seed propagated through five generations of single seed descent by Shauna Somerville. The *fly1-1* line was isolated from an EMS-mutagenized Col-2 population and was backcrossed to Col-2 four times to remove background EMS mutations. Seeds bearing SALK (Alonso et al., 2003), SAIL (Sessions et al., 2002) or WiscDsLox (Woody et al., 2007) T-DNA insertions in the Col-0 background were obtained from the Arabidopsis Biological Resource Center (ABRC) in Columbus, Ohio, and from the Nottingham Arabidopsis Stock Centre (NASC) in Loughborough, United Kingdom. Although I examined more than 120 T-DNA lines (Appendices A and B), a list of the most important mutant lines described in this study is presented below:

Table 2.1: The Most Important Mutant Lines Characterized.

Allele	**Locus**	**Polymorphism**
fly1-1	At4g28370	ems mutation
fly1-2	At4g28370	SALK_067290
fly1-3	At4g28370	SALK_144822
fly1-4	At4g28370	SALK_139156
fly1-5	At4g28370	SALK_000015
fly1-6	At4g28370	SALK_062423
fly2-1	At2g20650	SALK_140887
fly2-2	At2g20650	SALK_023653
knat7-1	At1g62990	SALK_002098C
knat7-3	At1g62990	SALK_110899C

Seeds were germinated on plates with AT medium (Haughn and Somerville, 1986) and 7% (w/v) agar, and seedlings were transferred to soil (Sunshine Mix 4; SunGro,

Kelowna, British Columbia) after 7 to 10 d. Plants were grown in chambers with continuous fluorescent illumination of 80-140 $\mu Em^{-2}s^{-1}$ at 20-22ºC. Seeds were harvested from individual plants when tracking segregation ratios and screening the phenotype of mutants for the first time. For Col-2, and confirmed homozygous mutant lines, bulk seeds from multiple plants with the same genotype were collected and used for microscopy and/or chemical analysis.

Developing seeds were staged using a previously described method (Western et al., 2001), where flowers are marked with nontoxic, water-soluble paint at 0 Days Post-Anthesis (DPA) just as they start opening and long stamens grow over the gynoecium.

2.2 Preparation of Seed Coat Sections

Developing seeds at 4 and 7 DPA were fixed using high pressure freezing and freeze substitution, embedded in Spurr's resin and sectioned according to previously described methods (Rensing et al., 2002; Mendu et al., 2011). Siliques staged at 4 and 7 DPA were dissected using a sharp razor blade. The seed coat was punctured with either an insect pin or a razor blade to later facilitate resin infiltration. Seeds were then transferred onto copper hats (Ted Pella; Redding, California) containing 1-hexadecene and fixed using a Leica EM HPM 100 High Pressure Freezer (Leica; Germany). Copper hats were then transferred to frozen cryovials containing freeze substitution medium consisting of 2% (w/v) osmium tetroxide in acetone with 8% (v/v) dimethoxypropane. The freeze substitution was performed at -80°C for 6 d by incubation in a Leica EM AFS chamber (Leica; Germany), followed by an incubation at -20°C for 20 h to allow for reaction of the fixatives. The temperature was then increased to 4°C, after which, samples were removed from the copper hats and rinsed in anhydrous acetone several times and slowly infiltrated and embedded in Spurr's epoxy resin

over a period of 4 d (Canemco; Lakefield, Quebec) (Spurr, 1969). Samples were thick sectioned (0.5 µm) using a Reichert Ultracut E microtome (Reichert; Seefeld, Germany) and stained with 1% (w/v) Toluidine Blue O in 1X (w/v) sodium borate (pH 11). Samples with well-preserved seed coats were examined by light microscopy.

2.3 Genotypic and Phenotypic Screening of Mutant Lines

2.3.1 Genomic DNA Extraction

DNA was isolated from rosette leaves using a previously published one-step protocol (Kasajima et al., 2004). However, instead of using plastic rods to crush plant cells, samples were quickly ground using 1.0 mm zirconia/silica beads (Biospec Products; Bartlesville, Oklahoma) and a Precellys 24 (Bertin Technologies, France) tissue homogenizer (Verollet, 2008). The supernatant was used immediately (1µL of DNA solution in 20 µL PCR reaction) or was stored at -20ºC until needed.

2.3.2 Genotyping of SALK T-DNA Insertions

Left (LP) and right (RP) gene-specific primers were selected using the SALK T-DNA Primer Design tool (http://signal.salk.edu/tdnaprimers.2.html) and are listed in Table 2.2. The LBb1.3 primer (ATTTTGCCGATTTCGGAAC) was used as the insert-specific primer. PCR reactions were set up with LP+RP+LBb1.3, LP+RP, and RP+LBb1.3 primer combinations. Wild type amplicons of 1 kb were observed from RP+LP, while smaller insert-specific fragments of 500-800bp were obtained using RP+LBb1.3 and DNA from plants containing at least one T-DNA insert in the gene of interest. When the LP+RP+LBb1.3 primer mix was used, plants homozygous for the insertion showed only a single band (500-800bp), while heterozygous lines displayed both the insert-specific band and the larger wild type amplicon.

Table 2.2: Gene-Specific Primers Used for T-DNA Genotyping.

Allele	Left Primer	Right Primer
fly1-2	CGCAAGTTCAGATGCTAATGC	AAAAAGGAACCGACAAACCTG
fly1-3	AGGCACAAATAAGCATCCATG	ATGAACAAAATGTGGGTGGTG
fly1-4	TCTGCTAATGGCTTGTTTGATG	ACGGGTTGCTTTCCATATAGC
fly1-5	TTTTCACTAGAAGCCACACGG	CTTGCAGTGGCTCTTTGGTAG
fly1-6	GCACTCAAGATTCAGTGCAGG	ATGACGGAGATTGTTTTTCCC
fly2-1	AACTGCACCCTGTTCACATTC	ACTCCGACATTCCAAGTTTCC
fly2-2	CGATTCCTAAGGAACCAAAGG	TTCTTGTATACAAGGGTGCCG
knat7-1	GAGATTAGTGTTTGCGCTTGG	TATGCGTAAGGGCATATCAGG
knat7-3	TTGCCACCAATTTTTCAAGAC	GCTTCAAAGAACAGCTGCAAC

2.4 Transmitted Light Microscopy

Mature dry seeds were typically hydrated in distilled water, 50mM $CaCl_2$, or 50mM ethylenediaminetetraacetic acid (EDTA) solution for 1 to 2h, rinsed with once with water, and stained with 0.01% (w/v) Ruthenium Red (Sigma-Aldrich; USA) for 1 h while shaking on a rotator. Brightfield micrographs of stained samples were taken with QCapture software and digital camera (QImaging; Surrey, British Columbia) equipped on a Zeiss AxioSkop 2 upright light microscope (Carl Zeiss AG; Germany). The contrast of unstained seeds was enhanced with either phase contrast or DIC components.

Videos of seed mucilage extrusion were captured using Olympus stereomicroscope equipped with a high resolution digital camera (Olympus; Richmond Hill, Ontario). Dry seeds attached to a glass slide with double-sided tape were hydrated with a single drop of distilled water, 50mM $CaCl_2$, or 50mM ethylenediaminetetraacetic acid (EDTA).

Xylem cell integrity was assessed by analyzing hand-cut sections from the stem base according to the method used to screen for *irx* mutants (Turner and Somerville, 1997). Sections were stained with one drop of saturated phloroglucinol in 20% HCl solution (Sigma-Aldrich; USA) or with one drop of 0.05% (w/v) Toluidine Blue solution (Sigma-

Aldrich; USA) in water (Parker et al., 1982). Transmitted light micrographs were analysed and processed with ImageJ (Abramoff et al., 2004), or with Photoshop (Adobe Systems; San Jose, California).

2.5 Electron Microscopy

Dry seeds were mounted on stubs and coated with gold-palladium in a SEMPrep2 sputter coater (Nanotech; Worcester, Massachusetts). Images were taken with a Hitachi S4700 scanning electron microscope (Hitachi High-Technologies; Canada).

For cryo-SEM, seeds were hydrated with a drop of distilled water and were quickly transferred to stubs topped with Tissue-Tek mounting medium (Sakura Finetek; Torrance, California) and small squares of filter paper to absorb excess water. Once mounted on the stubs, seeds were immediately frozen in liquid nitrogen. Samples were analyzed under high vacuum at liquid nitrogen temperatures with a Hitachi S-4700 Field Emission Scanning Electron Microscope (FESEM; Hitachi High-Technologies; Canada) equipped with a Leica VCT 100 cryo transfer system and cryo stage control (Leica; Germany). Electron micrographs were processed and measured with ImageJ (Abramoff et al., 2004). Image panels were made using Photoshop (Adobe Systems; San Jose, California).

2.6 Confocal Microscopy

2.6.1 Whole Seed Staining with Calcofluor White and Pontamine S4B

Seeds were mixed with water on an orbital shaker for 2 h, then stained with 0.01% (w/v) Pontamine Fast Scarlet S4B (Sigma-Aldrich Rare Chemical Library, #S479896; USA) and 50 to 150mM NaCl for 1 h (Anderson et al., 2010; Mendu et al., 2011). Seeds were then rinsed twice with distilled water and imaged using a 561 nm laser on either a Zeiss 510 Meta Laser Scanning Confocal Microscope (Carl Zeiss AG; Germany) or a PerkinElmer Ultraview

VoX Spinning Disk Confocal system (PerkinElmer; Waltham Massachusetts). Calcofluor staining and imaging was carried out using a previously described method (Willats et al., 2001b). All confocal micrographs were processed and measured with ImageJ (Abramoff et al., 2004). Image panels were made using Photoshop (Adobe Systems; San Jose, California).

2.6.2 Whole Seed Immunolabeling with M36, JIM5, JIM7, 2F4

The immunochemistry techniques used closely resemble two previously described protocols (Young et al., 2008; Harpaz-Saad et al., 2011). The specificities of the four monoclonal antibodies used have been extensively described (Knox et al., 1990; Knox, 1997; Willats et al., 2001b; Macquet et al., 2007a; Young et al., 2008; Pattathil et al., 2010; Xu et al., 2011). For CCRC-M36, JIM5 and JIM7 (CarboSource; Athens, Georgia) immunolabeling (Pattathil et al., 2010), seeds were sequentially washed with the solutions described in Table 2.3 while rotating on an orbital shaker at room temperature.

Table 2.3: Summary of the Sequential Washes for Whole Seed Immunolabeling.

Step	Solution	Volume (µL)	Duration (min)
1	phosphate buffer (PB, pH 7.4)	800	30
2	PB with 5% (w/v) Bovine Serum Albumin (BSA)	100	30
3	Primary antibody (M36, JIM5 or JIM7) diluted 1/10 in 1% BSA in PB	50	90
4	PB (this step is repeated 5 times in total)	800	10 (each wash)
5	Secondary antibody diluted 1/100 in 1% BSA in PB (incubation in dark)	100	90
6	PB (this step is repeated 5 times in total)	800	10 (each wash)

The 2F4 antibody (PlantProbes; Leeds, England) does not work with the conventional phosphate buffer (Liners et al., 1989), and was used with the following buffer: 20 mM Tris-HCl pH 8.2, 0.5 mM $CaCl_2$, 150 mM NaCl. The secondary antibodies used against JIM5 and JIM7 were goat-anti-rat conjugated to AlexaFluor488, and goat-anti-mouse conjugated to

AlexaFluor488 (Molecular Probes, Invitrogen; Carlsbad, California) against CCRC-M36 and 2F4. The immunolabeling method was carried out without primary antibody as a negative control. Seeds were imaged using a 488 nm laser (antibody fluorescence) and 561 nm laser (seed intrinsic fluorescence, background) on a Zeiss 510 Meta Laser Scanning Confocal Microscope (Carl Zeiss AG; Germany) or a PerkinElmer Ultraview VoX Spinning Disk Confocal system (PerkinElmer; Waltham Massachusetts). All confocal micrographs were processed and measured with ImageJ (Abramoff et al., 2004). Image panels were made using Photoshop (Adobe Systems; San Jose, California).

2.6.3 YFP Expression and Subcellular Localization

Seeds were removed from developing siliques of Basta-resistant transgenic plants. Seed coats were separated from embryos using crossing forceps and a dissecting microscope. Seeds and dissected tissues were imaged using a 514nm laser (YFP fluorescence) and transmitted light (for contrast, since 561 nm laser was unavailable) on a PerkinElmer Ultraview VoX Spinning Disk Confocal system (PerkinElmer; Waltham Massachusetts). FLY1-YFP expression driven by the native *FLY1* promoter in different cell types was examined with a 20x oil immersion objective, while subcellular localization of the FLY1-YFP signal was investigated with a 63X oil immersion objective. The negative controls used were untransformed Col-2 and *fly1-1* seeds, and Col-2 seeds transformed with the empty pGreenII0229 YFP vector.

2.7 Determination of Monosaccharide Composition by HPAEC

The protocol described here is a modified version of previously published procedures (Dean et al., 2007; Mendu et al., 2011). The average weight of Col-2 and *fly1-1* seeds was determined by carefully weighing three replicates of 100 seeds for each genotype. To prepare

the mucilage extraction samples for High-Performance Anion-Exchange Chromatography (HPAEC), four technical replicates of 25mg of Col-2 or *fly1-1* seeds (exact weight recorded) were mixed with 1.4 mL of distilled water and 10 µL of 5 mg/mL D-erythritol (internal standard). These samples were gently shaken using a tube rotator for 1 h. The mucilage in the supernatant of the first extraction was transferred (1mL) to a glass tube and dried at 60ºC under nitrogen gas. The same seeds were then rinsed twice with 700 µL of water, and shaken vigorously with a vortex mixer on the highest setting for 2 h, in 1.4 mL of water and 10 µL of 5 mg/mL D-erythritol. The supernatant was transferred to a glass tube and dried as described for the first extraction.

Serial dilutions (1 mM, 0.5 mM, 0.25 mM, and 0.125 mM) of neutral sugar standards (fucose, arabinose, rhamnose, galactose, glucose, mannose, and xylose) and acid sugar standards (galacturonic acid) in distilled water were transferred (0.5 mL) to glass tubes, mixed with 10 µL of 5 mg/mL D-erythritol (internal standard), and dried under nitrogen gas at 60ºC.

All mucilage samples and sugar standards were hydrolyzed simultaneously, using the following method. After drying under nitrogen gas, samples were treated with 17.4 µL of 72% (w/v) sulphuric acid for 2 h and shaken vigorously every 30 min with a vortex mixer. 482.6 µL of distilled water was then added to each glass tube to give a final concentration of 2.5% sulphuric acid, and all samples and standards were autoclaved for 60 min at 121ºC before being filtered through 0.45-mm nylon syringe filters.

For the HPAEC analysis of whole seeds, tubes were filled with 5 mg of seeds (exact weight recorded), frozen in liquid nitrogen, and ground to a fine powder using pestles. The powder was resuspended in 1 mL of 70% (w/v) ethanol and heated at 65ºC for 10 min to

inactivate enzymes. Three 30 min washes in 1 mL 70% ethanol were then performed on an orbital shaker in order to remove small soluble sugars. The Alcohol-Insoluble Residue (AIR) was collected with a microcentrifuge between washes, and was then dried under nitrogen gas. The dried AIR was weighed, transferred to glass tubes containing 10 mL of 5 mg/mL D-erythritol, and dried once again. The AIR samples were hydrolyzed as described for the mucilage samples, except that that larger volumes of sulphuric acid were used. After 2 h in 70 μL 72% (w/v) sulphuric acid, 1.93 mL water was added to each sample to give a final concentration of 2.5% sulphuric acid. The AIR samples were autoclaved at the same time as the mucilage samples and the sugar standards.

2.8 Positional Cloning of the *FLY1* Gene

The *fly1-1* mutant line (backcrossed twice to Col-2) was crossed to the Landsberg *erecta* (L*er*) ecotype to generate an F2 mapping population. The *fly1-1* mutation was rough mapped to the chromosome IV using insertion/deletion (indel) polymorphisms between the Arabidopsis accessions Col-0 and L*er* (Jander et al., 2002). The position of the *fly1-1* mutation was narrowed to a 180 kb region (13.94 to 14.12 mb) that contains 60 protein-coding genes. Using the SIGnAL T-DNA Express: Arabidopsis Gene Mapping Tool (http://signal.salk.edu/cgi-bin/tdnaexpress), I selected T-DNA insertions in the exons, 5' UTRs or introns (in decreasing order of preference) of the 60 *FLY1* candidate genes from At4g28070 to At4g28570 (Appendix A). T-DNA insertions were available in all candidates except for At4g28088, a low temperature and salt responsive protein, and At4g28280, a LORELEI-like-GPI-anchored protein that may play a role in fertilization (Tsukamoto et al., 2010). I ordered multiple T-DNA insertions from ABRC for the candidate genes that were preferentially expressed in the seed coat in the Arabidopsis eFP Browser

(http://bar.utoronto.ca/efp/cgi-bin/efpWeb.cgi; Winter et al., 2007). In total, I grew approximately 100 different T-DNA mutant lines in one growth chamber (Appendix A), collected seeds from individual plants, and analyzed their mucilage phenotype when hydrated in water and stained with 0.01% Ruthenium Red.

2.9 Bioinformatic Analysis

2.9.1 Analysis of Gene and Protein Structure

All genes analysed in this study were first investigated using the *Arabidopsis* Information Resource (TAIR) (http://arabidopsis.org; Swarbreck et al., 2007; Lamesch et al., 2011). The SignalP 4.0 Server (http://www.cbs.dtu.dk/services/SignalP) was used to detect the presence of a signal peptide in an amino acid sequence (Petersen et al., 2011). Analysis of transmembrane alpha helices was conducted using the TMHMM Server v. 2.0 (http://www.cbs.dtu.dk/services/TMHMM; Krogh et al., 2001), and the ARAMEMNON database (http://aramemnon.botanik.uni-koeln.de), which integrates the predictions of 18 individual programs (Schwacke et al., 2003). *FLY1* homologs were identified manually using nucleotide and protein BLAST programs (http://blast.ncbi.nlm.nih.gov/Blast.cgi), and were verified using the Phytozome (http://www.phytozome.net; Goodstein et al., 2012), PLAZA (http://bioinformatics.psb.ugent.be/plaza; Van Bel et al., 2012), and the InParanoid 7 databases (http://InParanoid.sbc.su.se; Ostlund et al., 2010). I investigated how the two Arabidopsis paralogs arose using the Plant Genome Duplication Database (PGDD; http://chibba.agtec.uga.edu/duplication; Tang et al., 2008) .

Functional domains were identified using the InterProScan (http://www.ebi.ac.uk/Tools/pfa/iprscan; Quevillon et al., 2005), and PROSITE databases (http://prosite.expasy.org; Sigrist et al., 2010). I also searched for homologous protein

architectures using the Conserved Domain Architecture Retrieval Tool (CDART; http://www.ncbi.nlm.nih.gov/Structure/lexington/lexington.cgi; Geer et al., 2002), and for additional conserved footprints using the Conserved Domain Database (CDD; http://www.ncbi.nlm.nih.gov/Structure/cdd/wrpsb.cgi; Marchler-Bauer et al., 2011).

2.9.2 *FLY1* and *FLY2* Transcript Analysis

Transcript structure and levels in plants was first investigated with AceView (http://www.ncbi.nlm.nih.gov/IEB/Research/Acembly; Thierry-Mieg and Thierry-Mieg, 2006). Expression patterns in specific Arabidopsis organs and cell types, and in response to biotic/abiotic stress, were visualized with the eFP browser (http://bar.utoronto.ca/efp/cgi-bin/efpWeb.cgi; Winter et al., 2007) and corroborated with GENEVESTIGATOR (https://www.genevestigator.com/gv/plant.jsp; Hruz et al., 2008).

The presence of *FLY1* and *FLY2* transcripts throughout the plant was confirmed by RT-PCR using cDNA samples prepared from RNA extracted from Arabidopsis tissues. RNA was extracted from Col-0 seedlings, roots, leaves, stems, and flowers using TRIzol (Invitrogen; Carlsbad, California) as per manufacturer's protocol. Col-2 siliques were dissected using fine forceps and RNA was isolated from the silique wall, embryo, and developing seed coat using the RNeasy Mini Kit (QIAGEN; Toronto, Ontario) according to the manufacturer's instructions. RNA quantification was performed using a NanoDrop 8000 (Thermo Scientific; Nepean, Ontario). 500ng of total RNA was treated with DNaseI (Fermentas; Burlington, Ontario) and then used for first strand cDNA synthesis using iScript RT supermix (Bio-Rad; Mississauga, Ontario). RT-PCR was conducted using a typical PCR reaction containing Taq Polymerase (Invitrogen; Carlsbad, California) and the following pairs of intron-spanning primers. The *FLY1* RT-PCR forward and reverse primers are

TGTAGAGCCCAACAAGGTTTG and GATCAATAGCGGTCATGCAG, while TTTGAAGAACGCAGCTGTTG and TTTATTGATCCGGCAAATGG were used for *FLY2*. Amplicons of approximately 200bp were expected after intron splicing, while amplicons over 300bp would be observed if the cDNA templates were contaminated with genomic DNA.

2.9.3 Identifying Genes with Similar Expression Patterns

The top genes expressed simultaneously with *FLY1* and/or *FLY2* were selected using GeneCAT (http://genecat.mpg.de; Mutwil et al., 2008), and ATTED-II (http://atted.jp; Obayashi and Kinoshita, 2010; Obayashi et al., 2011). Gene association was also investigated with AraNet (http://www.functionalnet.org/aranet/search.html; Lee et al., 2010) and GeneMANIA (http://www.genemania.org; Warde-Farley et al., 2010), although these two bioinformatic tools failed to predict likely candidates for cell wall biosynthesis.

2.10 Cloning of the *FLY1*$_{pro}$:*FLY1-YFP* Construct

2.10.1 Manipulation of Arabidopsis DNA and Bacterial Vectors

Amplification of *FLY1* (At4g28370) was performed using Phusion High-Fidelity DNA Polymerase (Thermo Fisher Scientific; Nepean, Ontario) and genomic DNA isolated from Col-2 leaves. The 5156 bp *FLY1*$_{pro}$:*FLY1* amplicon starts 690 bp upstream of the 5' UTR of *FLY1* [123 bp away from the 5' UTR of its upstream neighbour (At4g28365) that lies on the opposite DNA strand] and includes the complete *FLY1* coding region, except for the translation stop codon. The forward primer used (containing a KpnI restriction enzyme digestion site) was gcgGGTACCtctcacaaacaaacatttctcactc, while the reverse primer was tactcgagTGCTGGAGGAAGAGACCGCCGACAA and contained an XhoI site.

The constructs were fused with a yellow fluorescent protein (YFP) tag in order to investigate the expression of At4g28370 in various tissues and to determine the subcellular

localization of the FLY1 protein. Citrine was selected since it has superior photostability compared to green fluorescent proteins (GFP) and other YFP variants, and can fluoresce in the acidic environment of the apoplast (Griesbeck et al., 2001).

The *FLY1*$_{pro}$*:FLY* amplicons and a previously constructed pGreenII0229 vector with Citrine (DeBono, 2012) were each double digested with KpnI High Fidelity (HF) and XhoI restriction enzymes (New England Biolabs; Pickering, Ontario) at 37ºC for 1 h. Complete digestion was confirmed by obtaining only a discrete band of the correct size when products were separated by agarose gel electrophoresis. The digested amplicons were purified using a QuickClean II PCR Extraction Kit (GenScript; Piscataway, New Jersey), while the digested vector was first dephosphorylated with Antarctic Phosphatase (New England Biolabs; Pickering, Ontario) before being purified. Cohesive end ligations were performed for 1 h at room temperature using T4 DNA Ligase (New England Biolabs; Pickering, Ontario) and various insert to vector molar ratios. I inactivated the Ligase by incubating the reaction at 65ºC for 10 min and proceeded with the transformation.

2.11 Preparation and Transformation of Competent Cells

2.11.1 *Escherichia coli* (DH5α)

E. coli cells were treated with cold 50mM $CaCl_2$ for 20 min, and resuspended in 100 mM $CaCl_2$ with 20% glycerol. Competent cells were transferred in 50µL volumes to Eppendorf tubes, frozen immediately in liquid nitrogen, and stored at -80ºC. For transformation, 5µL of ligated product was added to 50µL of competent cells, and the solution was thawed on ice for 30 min. Cells were heat shocked at 42ºC for 1 min, allowed to recover on ice for at least 2 min, and shaken vigorously at 37ºC for 1 h after addition of 450µL of liquid LB media. 200 to 500 µL of the cell suspension was spread on plates with

LB media, 14% (w/v) agar, and 50 µg/ml Kanamycin and grown overnight at 37ºC. All *E. coli* liquid cultures were grown at 37ºC for 18-22 h. Plasmid DNA was isolated using EZ-10 Spin Column Plasmid DNA MiniPreps Kit (Bio Basic Inc.; Markham, Ontario) according to the manufacturer's instructions. The presence of the correct *FLY1* genomic DNA insert in the plasmid was confirmed by BglII restriction enzyme digestion and DNA sequencing.

2.11.2 *Agrobacterium tumefaciens* (GV3101 with pMP90 and pSOUP)

Competent *A. tumefaciens* GV3101 bearing mutually compatible plasmids pMP90 and pSOUP were prepared by treating cells with cold 50mM $CaCl_2$ before resuspending them in 50mM $CaCl_2$ with 15% (v/v) glycerol. Aliquots of 50µL were transferred to Eppendorf tubes, frozen in liquid nitrogen and stored at -80ºC. For transformation, 2 to 5 µL of plasmid DNA was added to frozen cells, and the mixture was thawed at 37ºC for 5 min. Cells were vigorously shaken in 500 µL liquid LB media for 3 h at 30ºC, and were then spread on plates with LB media, 14% (w/v) agar, and 25 µg/ml Gentamycin, 15 µg/ml Tetracycline, and 50 µg/ml Kanamycin. Plates were incubated at 30ºC for 2 to 3 nights, while liquid cultures were grown at 30ºC overnight. Plasmid DNA was isolated using EZ-10 Spin Column Plasmid DNA MiniPreps Kit (Bio Basic Inc.; Markham, Ontario), following to the manufacturer's protocol. BglII restriction enzyme digestion was used to verify that plasmids contained $FLY1_{pro}$*:FLY1-YFP* inserts.

2.12 Isolation of Arabidopsis Transgenic Lines

Pots of flowering *fly1-1* or Col-2 Arabidopsis plants were transformed using *Agrobacterium tumefaciens* and the previously described floral dip method (Clough and Bent, 1998). Transgenic plants were selected by spraying the leaves of plants germinated on soil with 200mM Basta herbicide solution every 2 to 3 d for two weeks or until most

seedlings turned yellow. Around 1% of T_1 plants were Basta-resistant, and developing seeds from several independent plants were analyzed with confocal microscopy for YFP fluorescence.

Chapter 3: Analysis of the Role of *FLY1* in Cell Wall Biosynthesis

3.1 Synopsis

The *fly1-1* mutant was isolated from an EMS-mutagenized Col-2 population during a screen for mutants with altered mucilage. The *fly1-1* mutant releases unusual disc-like structures upon hydration in water. Using light microscopy of unstained seeds and S4B-labelling of cellulose microfibrils in seeds, I demonstrated that the discs are outer tangential primary cell walls that detach from the columella of seed coat epidermal cells upon mucilage extrusion. Although *fly1-1* does not display significant changes in epidermal cell morphology in young or mature seeds, or in whole seed monosaccharide levels, mucilage extrusion is reduced in the mutant while mucilage adhesion is increased. Further investigation of the mucilage hydration properties revealed that *fly1* is more sensitive to Ca^{2+} ions than Col-2. Calcium bridges are required for cross-links between unesterified homogalacturonan (HG) molecules and can increase the strength of pectin gels. Hydration of seeds in a $CaCl_2$ solution significantly impairs the release of *fly1* mucilage compared to wild type. On the other hand, hydration in EDTA, a cation chelator, completely rescues the mutant phenotypes suggesting that *fly1* mucilage contains more calcium cross-links than wild type. Whole seed immunolabeling with three anti-HG antibodies indicate that *fly1* mucilage has a lower degree of methylesterification relative to Col-2.

The FLY1 gene was cloned by position and encodes a protein with multiple membrane spans and a RING-H2 domain for protein-protein interactions. YFP signal appears only in the epidermal cell layer of seeds expressing a *FLY1*$_{pro}$:*FLY1-YFP* transgene. FLY1-YFP fusion proteins are primarily localized in small intracellular bodies, at the stage of mucilage biosynthesis. I propose that FLY1 positively regulates the level of pectin

methylesterification in seed mucilage by interacting with pectin methyltransferase enzymes in the Golgi apparatus.

3.2 Introduction

Despite being studied intermittently for more than a decade, the *flying saucer 1-1* (*fly1-1*) mutant was only partially characterized and the identity of *FLY1* gene was unknown when I joined the Haughn lab. My goals were to confirm the composition of the discs-like structures and the reduced mucilage extrusion phenotype of the *fly1-1* mutant, and to discover the underlying cause for the *fly1-1* mucilage defects. In this chapter, I characterize the seed coat phenotype of the *fly1-1* mutant in detail and identify the *FLY1* gene using map-based cloning. I also investigate the phenotype of multiple *fly1* T-DNA insertional mutants, and analyse the expression and subcellular localization of FLY1-YFP fusion proteins.

3.3 Characterization of the *fly1-1* Seed Coat Phenotype

3.3.1 Water-Imbibed *fly1-1* Seeds Release Disc-Like Structures

The *fly1-1* mutant line was isolated while screening an EMS-mutagenized Col-2 population for mucilage-defective mutants. Hydration of dry Col-2 seeds in water triggers the expansion of the pectin gel matrix in seed coat epidermal cells, which ruptures the outer tangential primary cell wall from the radial wall and releases a large amount of mucilage (Western et al., 2000). Mature Col-2 seeds that are hydrated in water and stained with Ruthenium Red (RR), which binds the free carboxyl groups of pectin molecules (Hanke and Northcote, 1975; Western et al., 2000), are surrounded by a pink gel-like capsule (Figure 3.1). In contrast to Col-2, hydrated *fly1-1* seeds appear to release smaller RR-stained mucilage halos, surrounded by a large number of darkly stained small rings (Figure 3.1). Besides *fly1-1*, no previously isolated seed coat mutant displays discs in the extruded

mucilage. Although the precise number of discs released is technically difficult to determine, large gaps separate many of the discs suggesting that not every *fly1-1* seed coat epidermal cell releases such a structure. The discs also appear to be separated from the pink mucilage halo by a layer that is not stained by Ruthenium Red (Figure 3.1).

Mucilage extruded from wild type seed coat epidermal cells is not homogeneous but consists of an outer, non-adherent layer that is easily washed off with water and an inner fraction which remains attached to the seed after shaking (Figure 3.1 A; Western et al., 2000). Since most of the inner mucilage layer is not removed by prolonged shaking (Macquet et al., 2007a), I decided to investigate if the attachment of *fly1-1* discs to the seed coat parallels that of the inner mucilage layer. Although the discs are at a distance from the surface of *fly1-1* seed coat epidermal cells, they are not detached after 24 h of mechanical agitation with an orbital rotator (Figure 3.1 C and D). This suggests that the discs are strongly bound to the adherent mucilage. In addition, *fly1-1* seeds hydrated in water appear to have more compact mucilage halos compared to Col-2, a phenotype that is enhanced when dry seeds are stained directly in Ruthenium Red (data not shown). These results suggest that mucilage extrusion from the *fly1-1* mutant is reduced compared to wild type.

When hydrated Col-2 seeds are not stained with RR or other polysaccharide-binding dyes, the mucilage halo is very difficult to observe with light microscopy (Figure 3.2 A). Interestingly, *fly1-1* discs are easily observed without staining unlike the mucilage extruded by the mutant or wild type seeds (Figure 3.2 B), suggesting that the rings are more than just mucilage donuts that do not expand properly.

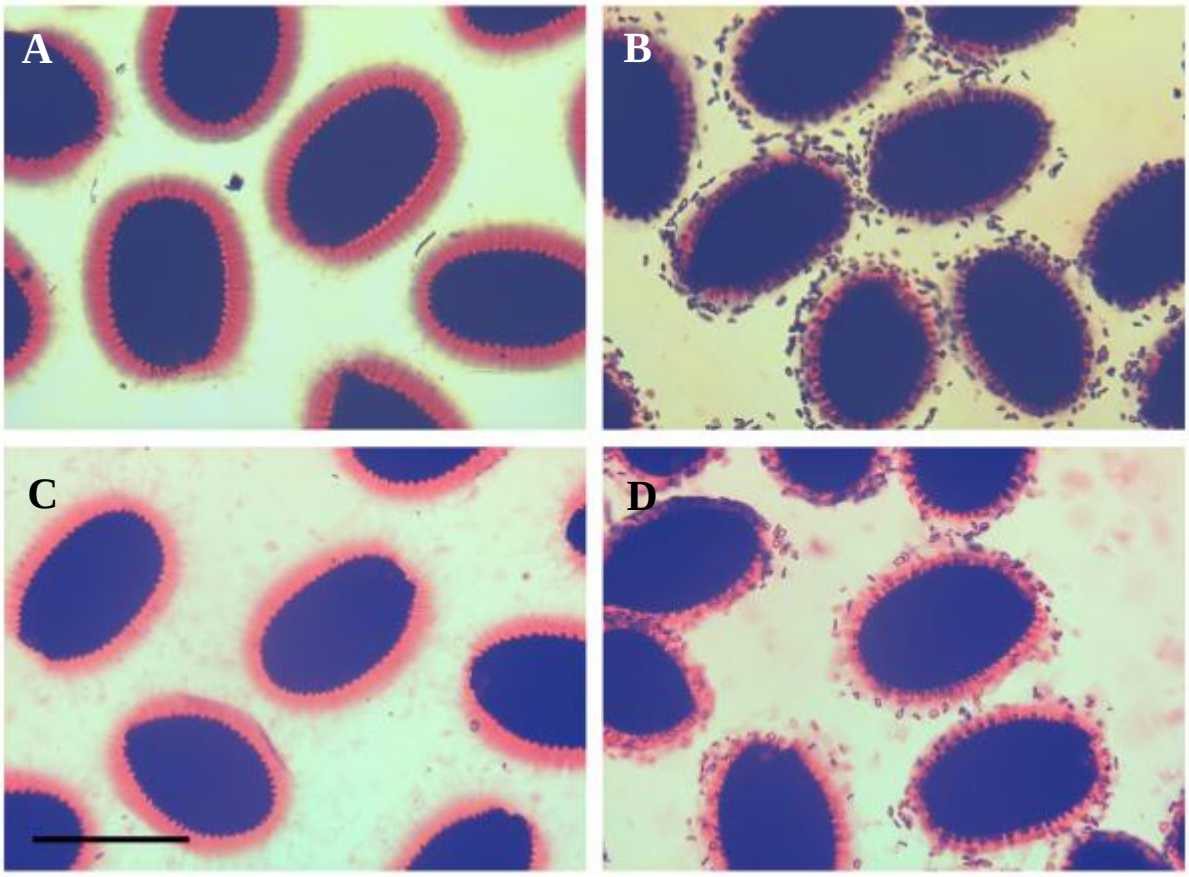

Figure 3.1: Ruthenium Red Staining of *fly1-1* Seeds Shaken in Water.
Col-2 (A) and (C), and *fly1-1* (B) and (D) seeds were shaken in distilled water for 2 h (A) and (B), or 24 h (C) and (D). Inner, adherent mucilage capsules were stained with Ruthenium Red for 30 min. Scale bar = 500 µm.

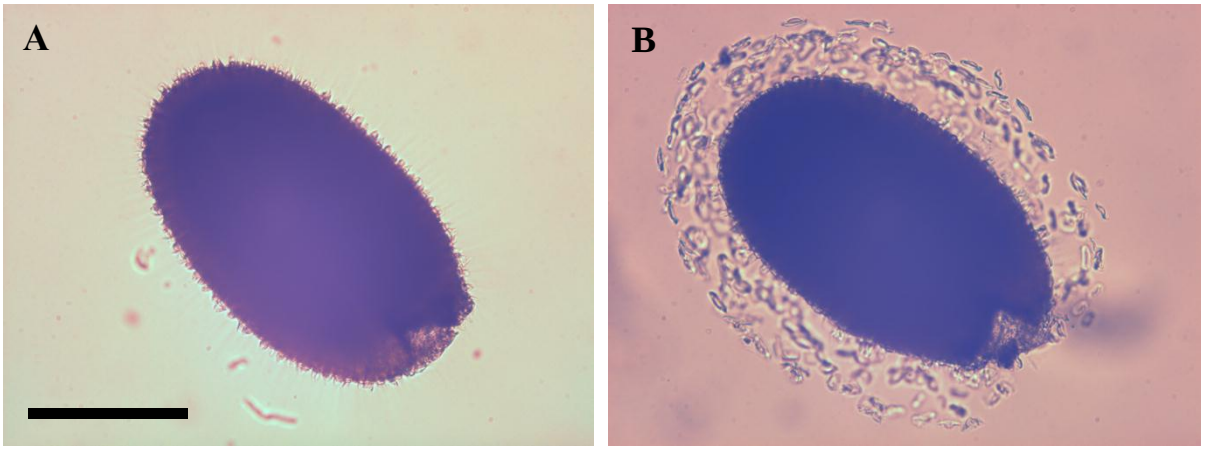

Figure 3.2: Discs, Unlike Mucilage, Can Be Seen Without Staining.
Col-2 (A) and *fly1-1* (B) seeds were hydrated in distilled water and imaged using a light microscope with phase contrast components. Scale bar = 250 µm.

3.3.2 Primary Cell Walls Detach From *fly1-1* Seed Coat Epidermal Cells

By the end of their development, seed coat epidermal cells contain three morphologically and chemically distinct cell walls (Figure 1.1). Comparing the shape and size of *fly1-1* discs to the morphology of the primary cell wall, the mucilage donut and the columella of a seed epidermal cell, can provide clues about the biochemical make-up of the unusual structures observed in the mutant (Figure 3.3). Preliminary analysis of the *fly1-1* mutant seeds by Dr. Gillian Dean supports the hypothesis that the discs have both primary cell wall and mucilage components. The polygonal discs appear similar in shape and size to the outer tangential primary cell walls and the mucilage rings of seed coat epidermal cells (Figure 3.3). Since primary cell wall fragments normally remain attached to the columella after mucilage extrusion from hydrated seeds (Figure 1.1), and the discs can be observed without staining (Figure 3.2), I decided to determine the location of primary wall remnants in Col-2 and *fly1-1* seeds shaken in water. While every Col-2 seed coat epidermal cell has primary cell wall attached to the columella, many *fly1-1* cells display naked columellae, without primary wall fragments (Figure 3.4).

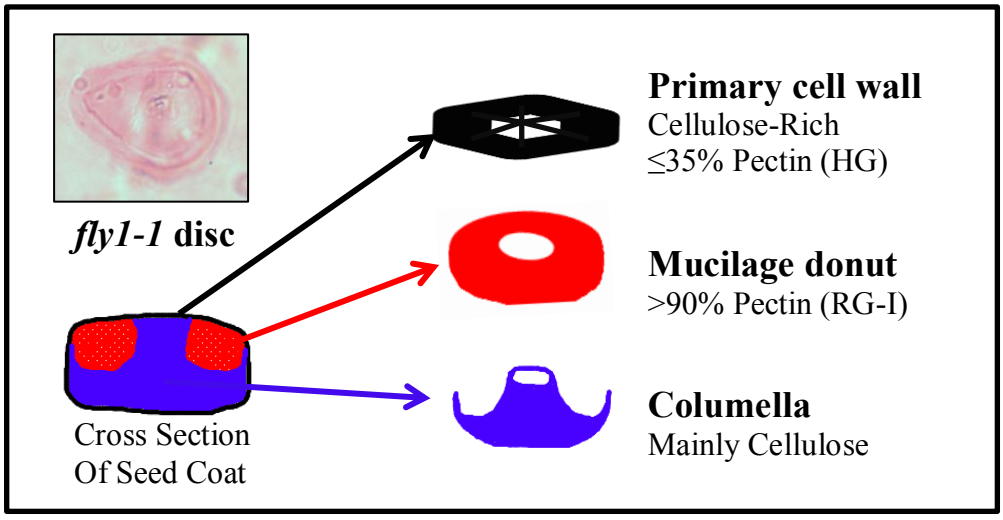

Figure 3.3: Comparison of *fly1-1* Discs with the Walls of Seed Epidermal Cells.

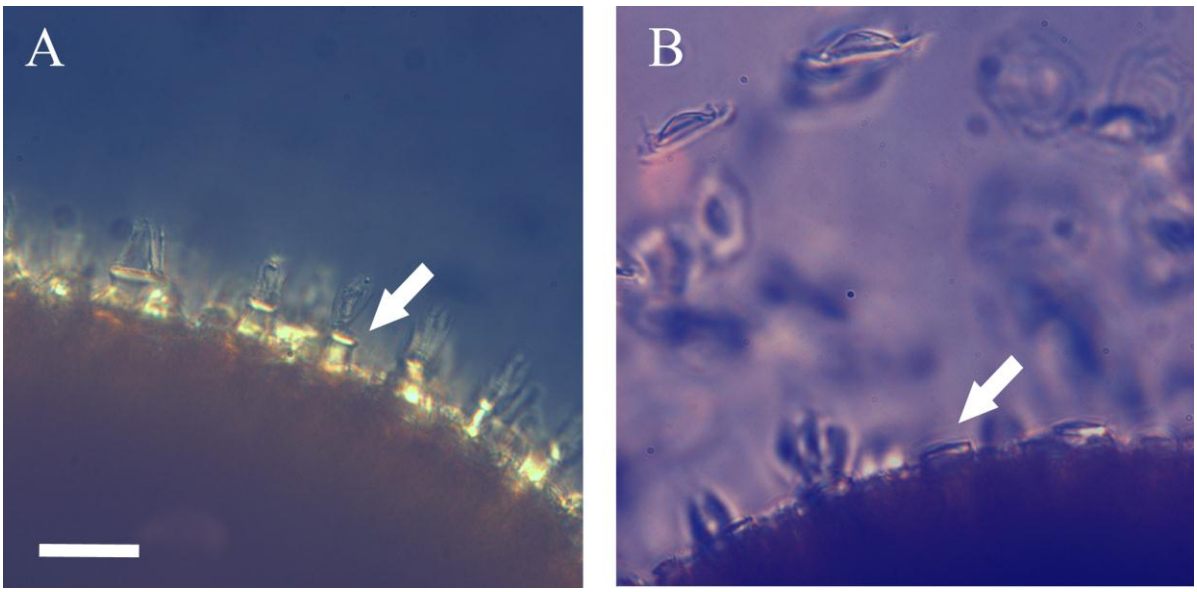

Figure 3.4: Location of Primary Cell Wall Fragments in Unstained Col-2 and *fly1-1*. (A) Col-2 and (B) *fly1-1* water-hydrated seeds analyzed using differential interference contrast (DIC) microscopy. Arrows indicate the position of columellae. Note the attachment of primary cell wall fragments to columellae in (A), and the absence of attached wall fragments in (B). Scale bar = 30 μm.

The position of the *fly1-1* discs appears to correlate with the location of columellae that lack primary cell wall attachment (Figure 3.4). This suggests that the discs, which are at the edge of the mucilage halo, may be composed of outer tangential primary walls that detach from columellae when *fly1-1* seeds are hydrated in water. To confirm that the detached rings indeed contain primary cell walls, I labelled seeds hydrated in water with Pontamine Fast Scarlet 4B (S4B), a dye that fluoresces specifically when bound to cellulose microfibrils (Anderson et al., 2010). S4B-stained Col-2 seeds show intense fluorescence from the tangential cell wall fragments atop the columella of every wild type seed coat epidermal cell (Figure 3.5), consistent with the observations made using unstained seeds in water (Figure 3.4). Diffuse S4B signal is also observed in the inner layer of the Col-2 mucilage, consistent with a previously proposed role for cellulose microfibrils in the attachment of the adherent

mucilage to the seed (Macquet et al., 2007a; Mendu et al., 2011). Interestingly, many *fly1-1* seed epidermal cells do not have S4B-labelled tangential walls fragments attached to the columella but instead had S4B-stained thin discs floating above them. Although the release of a large number of discs can obscure their exact location of origin (Figure 3.4), there is a strong correlation between the position of discs and columellae lacking attached primary cell walls (Figure 3.5). Similar results were obtained for seeds hydrated in water and stained with Calcofluor White (data not shown), a more general fluorescent probe for β-glycans that has been used to indicate the presence of cellulose in mucilage (Hughes and McCully, 1975; Macquet et al., 2007a; Anderson et al., 2010). Col-2 and *fly1-1* seeds showed similar patterns of S4B labelling in the inner mucilage layer, consistent with a wild type level of cellulose in *fly1-1* mucilage (Figure 3.5). The intense labeling of the discs by cellulose-binding dyes combined with the loss of primary cell wall attachment in *fly1-1* seed coat epidermal cells indicate that the discs are, at least in part, outer tangential primary cell walls that detach from the columellae upon mucilage extrusion.

To obtain further evidence that *fly1-1* discs include detached primary cell walls, I closely examined the shape and size of these structures using scanning electron microscopy (SEM). SEM provides an excellent view of the surface morphology of dry seeds, but fails to reveal any obvious differences between Col-2 and *fly1-1* seed coat epidermal cells (Figure 3.6 A and B). Col-2 and *fly1-1* seeds display outer tangential cell walls and columellae that are similar in shape and size. Since mucilage consists mainly of gelatinous pectins that are extruded only after seed hydration, its morphology cannot be visualized with conventional SEM techniques, which require dry samples.

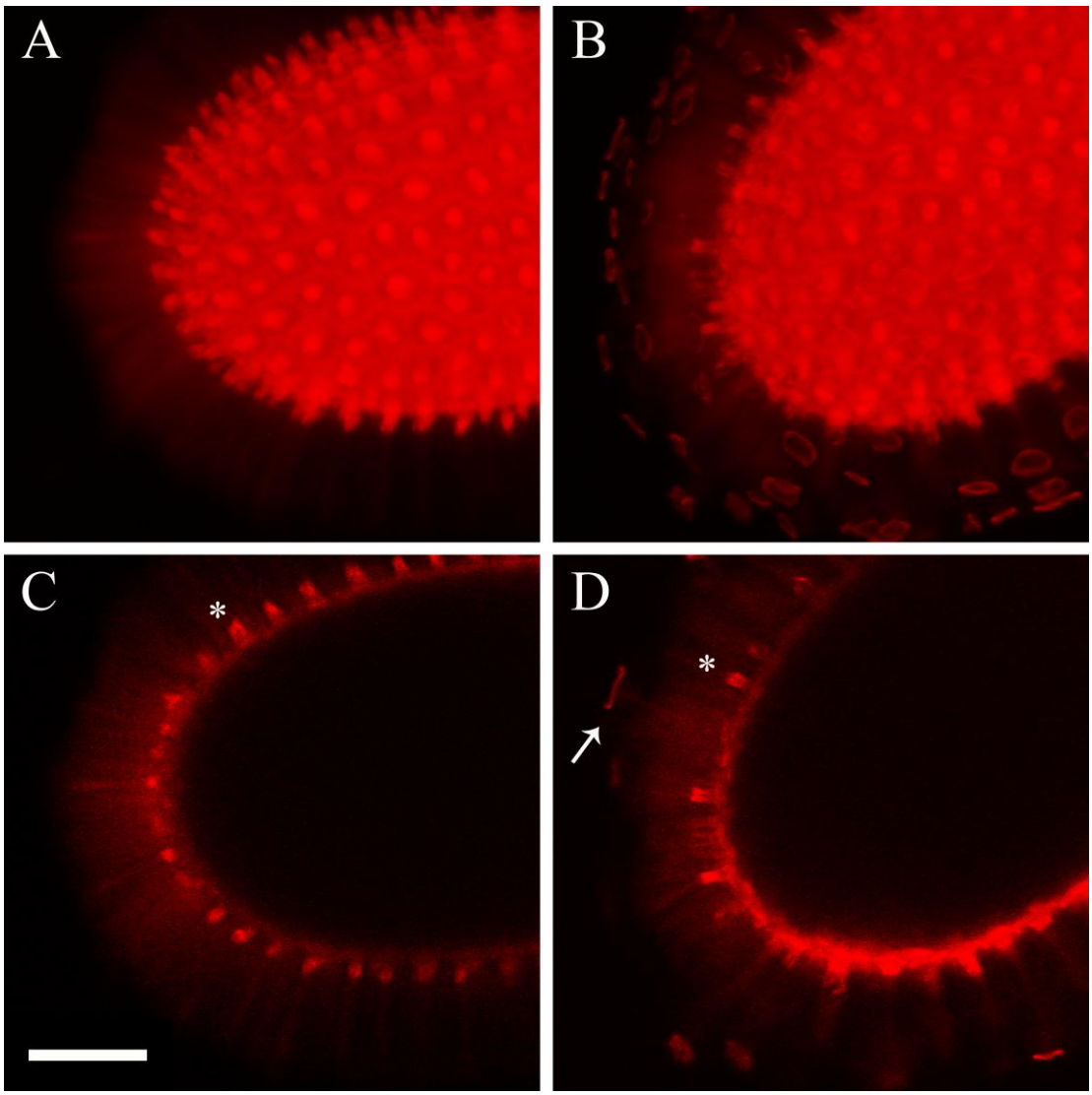

Figure 3.5: S4B Staining of Cellulose in Water-Imbibed Col-2 and *fly1-1* Seeds. Col-2 (A) and (C), and *fly1-1* (B) and (D) were shaken in water for 2 h and then stained with S4B. (A) and (B) are whole seed images containing the S4B signal of multiple optical slices (rendered using ImageJ, Z-project standard deviation method). (C) and (D) are optical slices through the middle of seeds. The asterisks indicate S4B-labelled primary cell wall fragments atop columellae. The absence of attached primary cell fragments correlates with the position of S4B-stained discs, arrow in (D). Scale bar = 100 μm.

To investigate the structure of extruded mucilage, Col-2 and *fly1-1* seeds hydrated in water were immediately frozen in liquid nitrogen and analyzed with cryo-SEM. Both Col-2 and *fly1-1* hydrated seeds display an intricate mesh-like network of mucilage in cryo-SEM images (Figure 3.6 C to F). However, only the mutant seeds show electron-dense discs on top of the extruded mucilage matrix (Figure 3.6 D and F), similar to the position of RR-stained discs at edge of the *fly1-1* mucilage halo in light micrographs (Figure 3.1 B). Consistent with *fly1-1* discs containing detached primary cell walls, the structures observed with cryo-SEM have similar dimensions with the outer tangential cell walls seen in dry seed SEM (Figure 3.6 A and B) and with the RR-stained rings in light micrographs (Figure 3.1 B).

Quantitative data on cell morphology was obtained by measuring the diameter of primary walls and discs observed with different techniques (>30 different samples measured in each category). Since the outer tangential primary cell walls and the discs resemble polygons, the diameter was measured as the maximum distance between any two points on the wall or the disc. The mean diameter of *fly1-1* outer tangential primary cell walls observed with SEM (32.95 ± 0.69 µm) is very similar to that of RR-stained discs (32.98 ± 0.88 µm; P-value=0.98). The diameter of discs seen with cryo-SEM (30.88 ± 0.70 µm) was statistically different from that of walls in SEM of dry seeds (P-value=0.038 < 0.05), but not from the diameter of RR-stained discs (P=0.066 > 0.05). Overall, the results in this section demonstrate that in *fly1-1*, many outer tangential primary cell walls detach from the secondary cell walls (columellae) when seeds are hydrated in water and mucilage is extruded. Nevertheless, the molecular factors that anchor the primary cell wall to the columella in a wild type seed coat epidermal cell remain unknown.

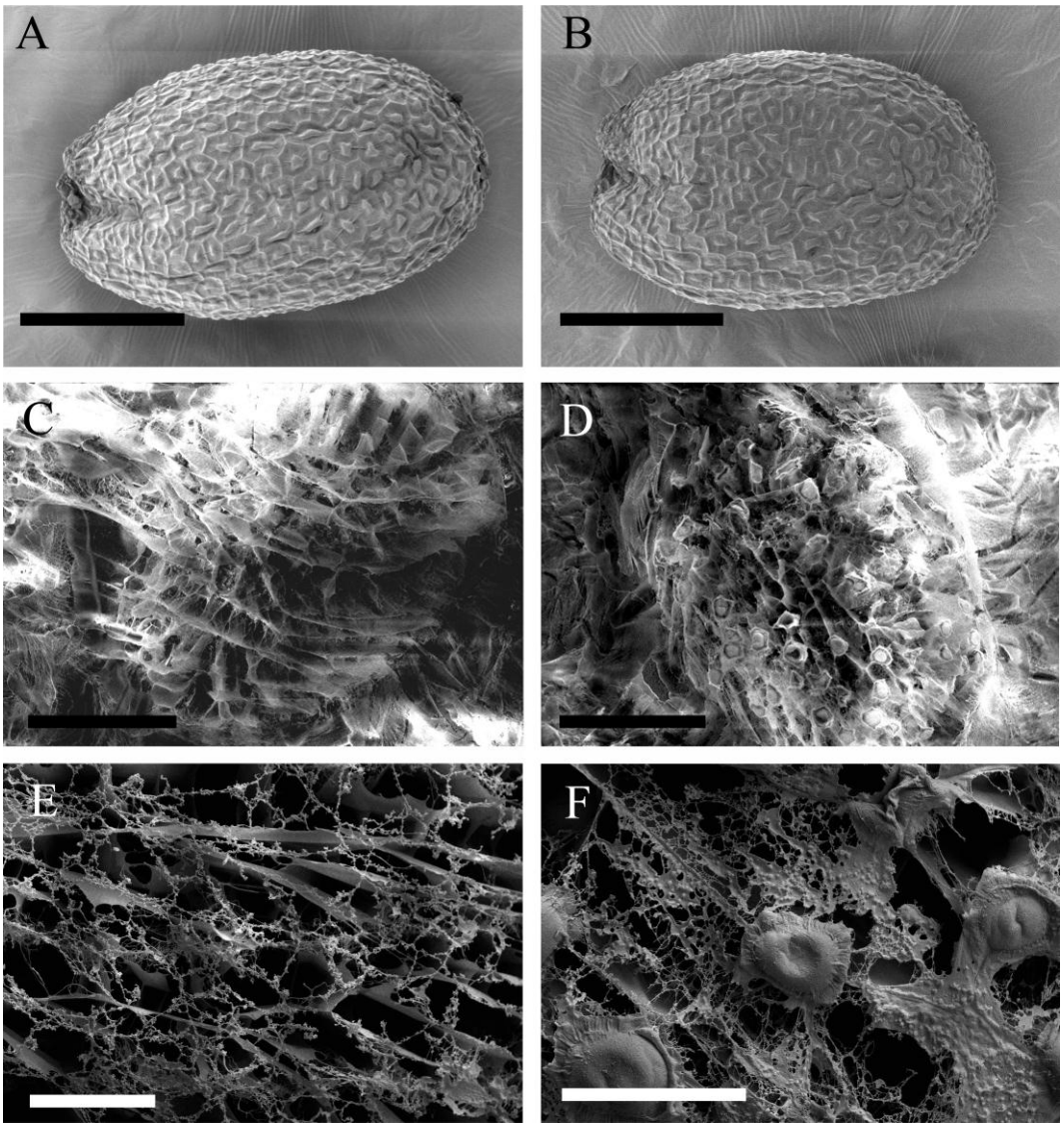

Figure 3.6: Analysis of Dry and Hydrated Seeds by SEM and cryo-SEM.
Col-2 (A) and *fly1-1* (B) dry mature seeds appear similar when viewed with SEM. cryo-SEM of Col-2 seeds hydrated in water showed an irregular mucilage matrix before (C) and after sputter coating (E). cryo-SEM of hydrated *fly1-1* seeds revealed discs on top of the mucilage matrix before (D) and after sputter coating (F). Scale bars = 200 µm (A) to (D), and 50 µm (E) and (F).

Despite the detachment of primary cell walls from the *fly1-1* columellae (Figures 3.4, 3.5 and 3.6), the primary wall-containing *fly1-1* discs are not dislodged from the extruded mucilage even after 24 h of shaking (Figure 3.1 D). The mechanical properties of discs may be accounted for if, as previously suggested, the detached primary cell walls are strongly bound to the adherent mucilage capsule. Since the primary cell wall detachment phenotype could result from altered mucilage extrusion, the remaining phenotypic experiments investigate the properties of *fly1-1* mucilage and seek to address why they differ from those of wild type.

3.3.3 Col-2 and *fly1-1* Have Similar Epidermal Cell Morphology

To determine if seed coat epidermal cell development is compromised by the *fly1-1* mutation, I analyzed fixed sections of young seeds using light microscopy. The *fly1-1* mutant displayed similar seed coat morphology to wild type at 4 and 7 Days Post-Anthesis (DPA), and also deposited large amounts of mucilage in a polarized manner (Figure 3.7). The *fly1-1* mucilage pockets at 7 DPA were not smaller than wild type as seen in mutants that synthesize less mucilage such as *mum4* (Western et al., 2004). In addition, SEM of *fly1-1* and Col-2 dry mature seeds showed no obvious differences in the size and shape of seed coat epidermal cells (Figure 3.6). The unaltered cell morphology of the *fly1-1* mutant, despite reduced seed mucilage extrusion and cell wall detachment, suggests that the disruption of *FLY1* does not result in the loss of a major cell wall polysaccharide.

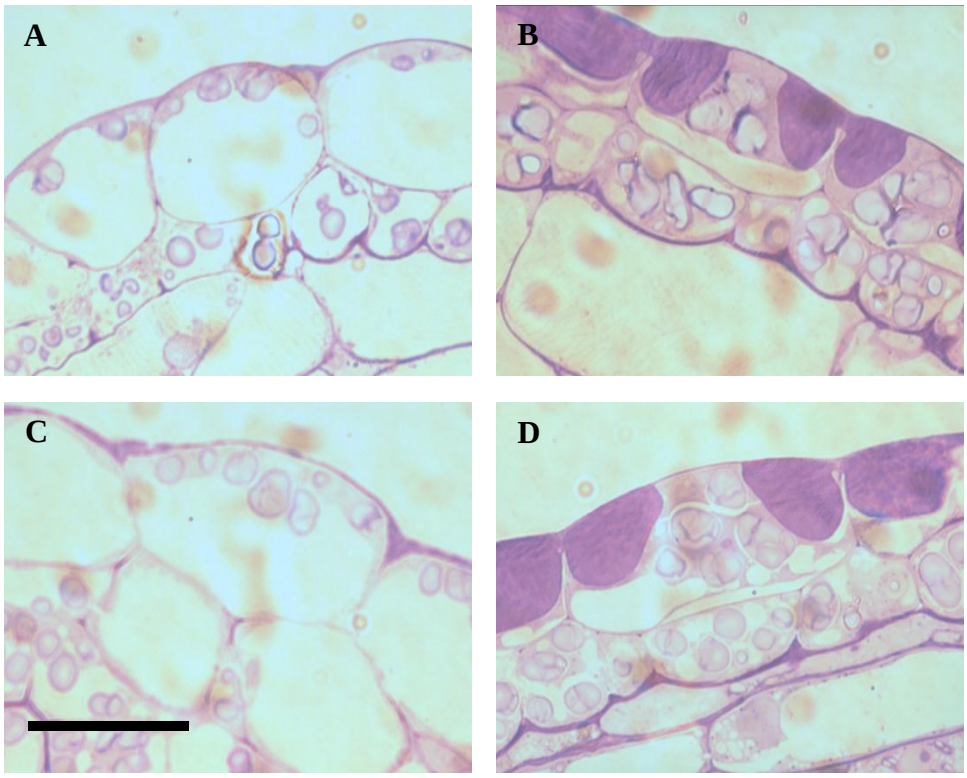

Figure 3.7: Sections of Developing Col-2 and *fly1-1* Seed Coat Cells. Cryo-fixed samples were resin-embedded, sectioned (0.5 µm) and stained with Toluidine Blue. Sections were analyzed with light microscopy. Col-2 seed coat epidermal cells at 4 DPA (A) and 7 DPA (B) are similar in morphology to *fly1-1* at 4 DPA (C) and 7 DPA (D) respectively. Scale bar = 25 µm.

3.3.4 Col-2 and *fly1-1* Have Similar Whole Seed Sugar Levels

The monosaccharide composition of Col-2 and *fly1-1* whole seeds was quantified with High-Performance Anion-Exchange Chromatography (HPAEC) to further investigate if *FLY1* is required for the biosynthesis of a major cell wall component. Analysis of the Alcohol-Insoluble Residue (AIR) prepared from dry mature seeds did not reveal any significant differences between *fly1-1* and wild type (Figure 3.8, verified with two additional biological replicates). These results resemble those previously obtained for *bxl1* and *mum2*

mutants that are defective in pectin modification rather than pectin biosynthesis (Dean et al., 2007; Arsovski et al., 2009).

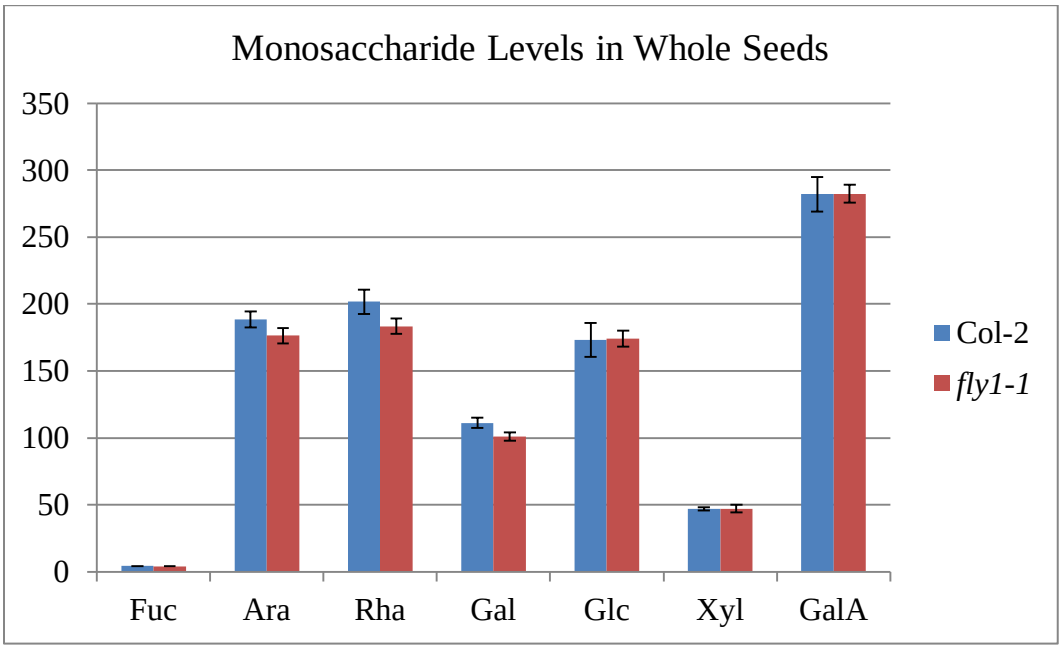

Figure 3.8: Monosaccharide Composition of Col-2 and *fly1-1* Whole Seeds.
Values are the mean ± Standard Error of four samples and are expressed as nmol sugar normalized to mg of Alcohol-Insoluble Residue (AIR).

3.3.5 The *fly1-1* Mucilage is More Adherent Than Col-2

Although *fly1-1* whole seeds did not show altered monosaccharide levels, the mutant phenotype could be masked by sugars from additional cell layers if *FLY1* is specifically involved in mucilage biosynthesis. An advantage of studying seed coat cells is that mucilage can be easily extracted and analysed, providing quantitative data for mutants that affect the release or the adherence of mucilage. Although *fly1-1* discs are not detached from the seed epidermis by light to moderate shaking even after 24 h (Figure 3.1), they can be removed along with some of the adherent mucilage by prolonged exposure to vigorous mechanical agitation using a vortex mixer (Figure 3.9). By changing the shaking intensity, mucilage fractions with or without discs can be isolated from *fly1-1* seeds and used for chemical

analysis. Sequential mucilage extractions were therefore performed to determine the monosaccharide composition of the loose mucilage without discs (extraction 1, gentle shaking in water for 1 h) and that of the adherent mucilage and discs (extraction 2: vigorous shaking in water for 2 h). The second extraction removes a visible portion of the adherent mucilage for both Col-2 and *fly1-1*, and the majority of discs from *fly1-1* seeds (Figure 3.9). Despite their dissociation from the seed, the discs maintain their shape and are still closely bound to mucilage (Figure 3.9 D, arrows).

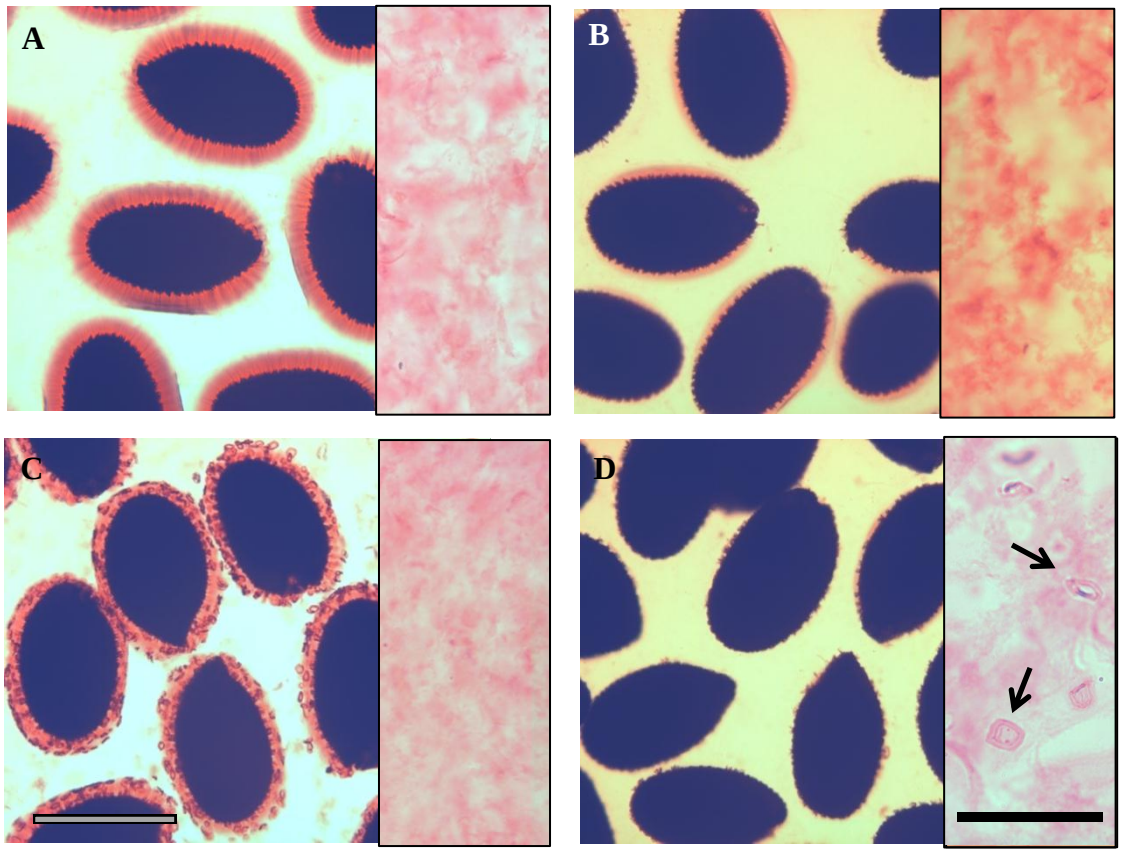

Figure 3.9: Ruthenium Red Staining of Sequential Mucilage Extractions.
(A) and (B) represent Col-2 seeds, while (C) and (D) show *fly1-1* seeds. The first extraction (A) and (C) consisted of 1 h of gentle shaking, while the second extraction was obtained by vigorously shaking the same seeds for another 2 h (B) and (D). Inset micrographs show the mucilage in the supernatant solutions collected after each extraction and used for HPAEC analysis. Disc-like structures are only removed from *fly1-1* seeds that are vigorously shaken, arrows in (D). Scale bar = 500 µm for all images except inset in (D) which is 125 µm.

HPAEC monosaccharide analysis of the first extraction showed that there was a strong reduction of Rhamnose (Rha) and Galacturonic Acid (GalA) in *fly1-1* relative to Col-2 (Figure 3.10), while the subsequent extraction obtained by more vigorous shaking revealed almost twice as much Rha and GalA in *fly1-1* compared to Col-2 (Figure 3.11). All other monosaccharides detected in the sequential mucilage extractions had trace amounts compared to Rha and GalA, but showed similar trends to the more abundant sugars. In addition, both extractions displayed a molar ratio of approximately 0.9 Rha to 1 GalA, consistent with mucilage containing about 90% rhamnogalacturonan I (RG-I), whose backbone is made of repeating Rha and GalA units (Western et al., 2000; Macquet et al., 2007a). Since the whole seed monosaccharide levels were unaltered (Figure 3.8), the lower sugar levels obtained in the first *fly1-1* mucilage extraction (Figure 3.10) reflect changes in the extrusion or adherence of mucilage. The reduced extractability of *fly1-1* mucilage was partially rescued by more vigorous mechanical agitation (Figure 3.11), suggesting that *fly1-1* has a more adherent mucilage capsule than wild type.

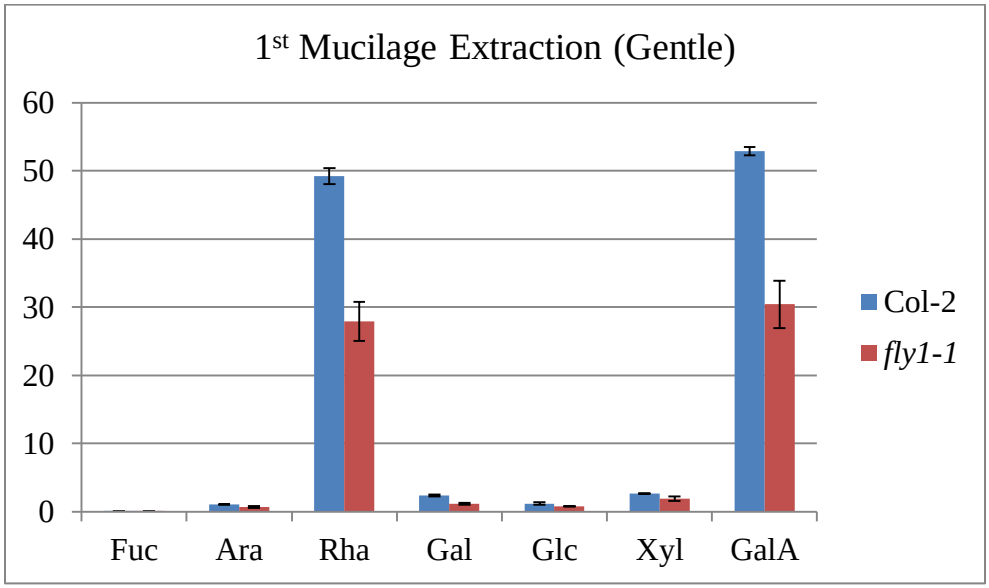

Figure 3.10: Monosaccharide Analysis of Col-2 and *fly1-1* Loose Mucilage.
Values are the mean ± Standard Error of four samples and represent nmol sugar per mg seed.

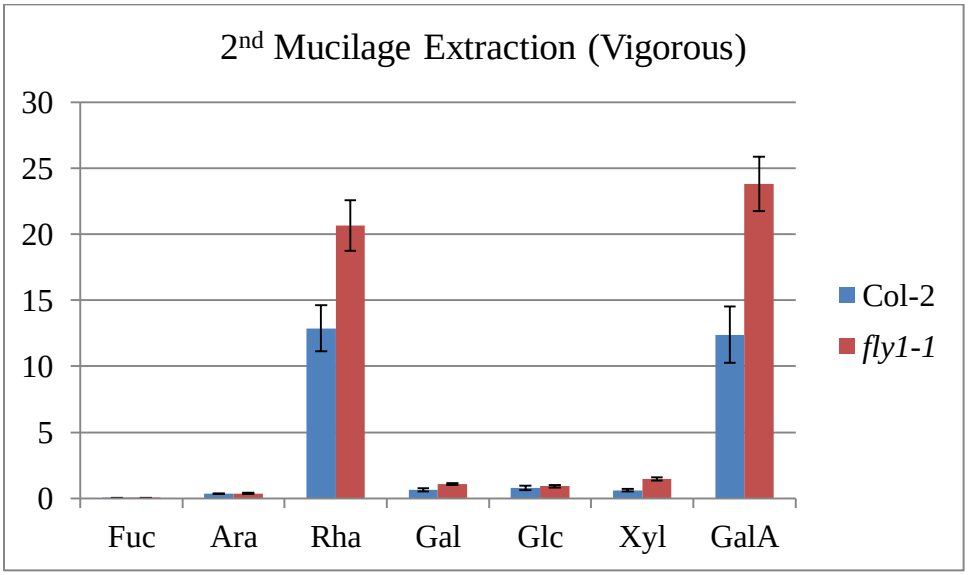

Figure 3.11: Monosaccharide Analysis of *fly1-1* Disc-Rich Mucilage Fraction.
Values are the mean ± Standard Error of four samples and represent nmol sugar per mg seed.

3.3.6 Mucilage Extrusion from *fly1-1* Is Calcium-Dependent

Although the *fly1-1* mutant does release mucilage in water, videos of seed hydration indicate that the extrusion of mucilage occurs more slowly in the mutant than in wild type (data not shown). In addition, the *fly1-1* mucilage halo appears to be more compact (Figures 3.1, and 3.12 A and B) and more adherent than wild type (Figures 3.10 and 3.11). To investigate why mucilage expansion is reduced in the *fly1-1* mutant, I examined the effects of hydrating seeds in a $CaCl_2$ solution. Ca^{2+} ions are required for the formation of cross-links between unesterified regions of homogalacturonan (HG), and can therefore strengthen the pectin gel matrix. Interestingly, hydration of seeds directly in a 50 mM $CaCl_2$ solution almost completely impairs mucilage extrusion from the *fly1-1* mutant, but not from Col-2 seeds, which show only a small reduction in mucilage halo size (Figure 3.12 C and D). This suggests that pectin molecules in *fly1-1* mucilage can form more calcium cross-links than wild type, and implies that HG molecules are likely to have a lower degree of methylesterification. Relatively few $CaCl_2$-hydrated *fly1-1* seed epidermal cells release mucilage but they all appear to have discs atop their compact mucilage columns (Figure 3.12 D). These results are consistent with the discs resulting from abnormal mucilage extrusion and being strongly bound to the pectin matrix.

In contrast to the addition of Ca^{2+} ions, pectin gels are loosened by treatment with EDTA, a cation chelator that disrupts the calcium bridges necessary for cross-links between chains of unesterified HG. EDTA was previously used to rescue the phenotypes of mutants such as *bxl1* that have reduced mucilage extrusion (Arsovski et al., 2009). Hydration of seeds in a 50 mM EDTA solution completely rescued the *fly1-1* mutant phenotype, resulting in equally large Col-2 and *fly1-1* mucilage capsules without any visible discs (Figure 3.12 E and

F). Although the disappearance of the discs after EDTA treatment requires further investigation, these results suggest that both the release of discs and the reduced mucilage halo are caused by increased calcium cross-links in the *fly1-1* mutant.

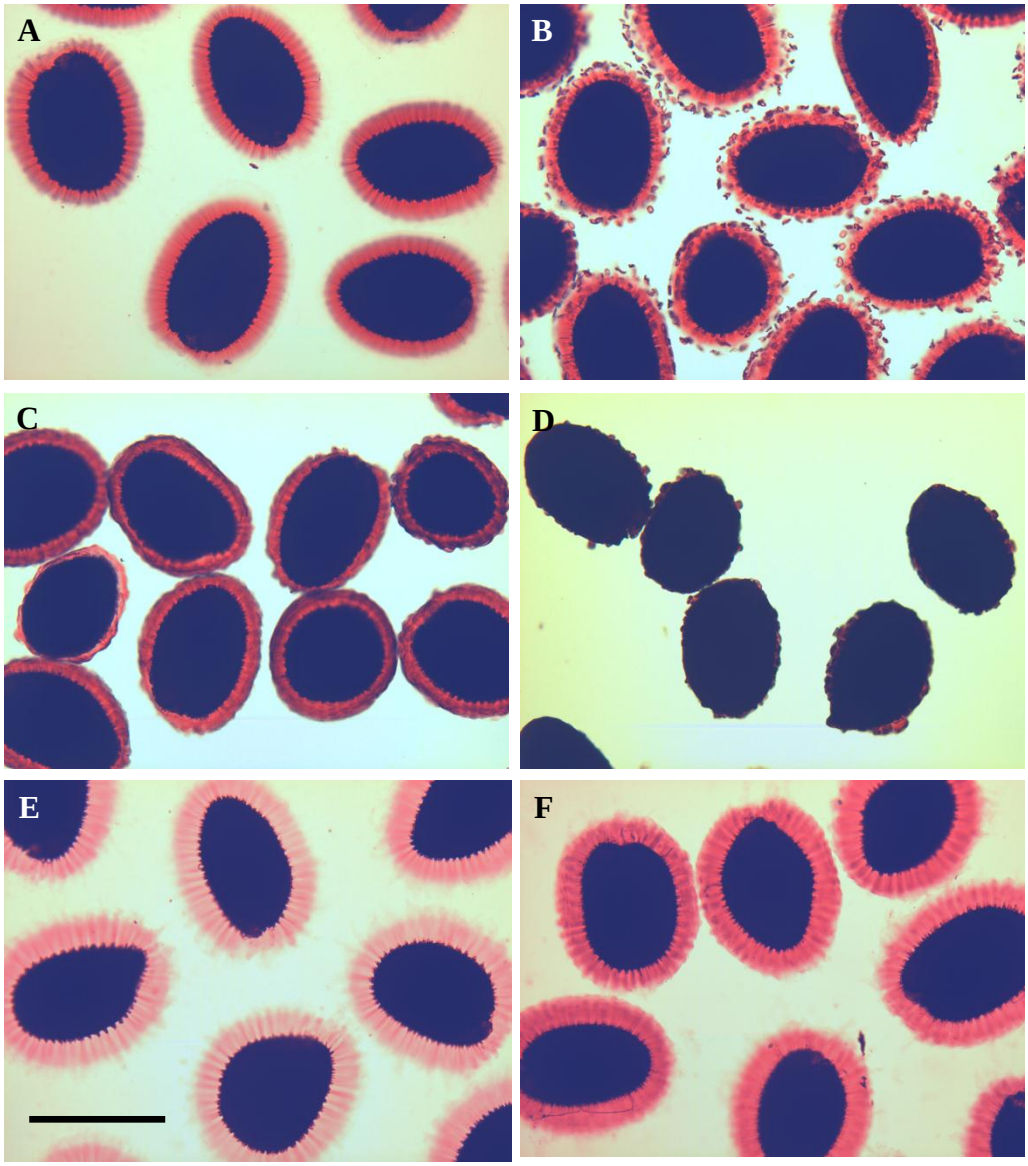

Figure 3.12: Effects of Ca^{2+} and EDTA on *fly1-1* Mucilage Extrusion. Col-2 (A), (C) and (E), and *fly1-1* (B), (D) and (F) seeds were shaken first with water (A) and (B), 50mM $CaCl_2$ (C) and (D), or 50mM EDTA (E) and (F) for 45 min, and then stained with 0.01% Ruthenium Red for 30 min. Addition of Ca^{2}+ ions almost completely inhibits mucilage release from the *fly1-1* mutant (D). EDTA rescues the mucilage defects of the *fly1-1* mutant (F). Scale Bar = 500 μm.

3.3.7 EDTA-Treated *fly1-1* Does Not Release Discs

Since the loss of RR-stained discs in EDTA-hydrated *fly1-1* seeds was an unexpected result, I decided to investigate if primary cell wall detachment still occurs in this treatment. Surprisingly, unstained *fly1-1* seeds hydrated directly in EDTA look identical to Col-2 seeds and have primary cell wall fragments attached to all columellae (Figure 3.13 A and B). Confocal micrographs of S4B-stained seeds treated first with EDTA also indicate that removal of Ca^{2+} ions prevents the detachment of primary cell walls from the columellae (Figure 3.13 C and D), and fully rescues the *fly1-1* mucilage defects.

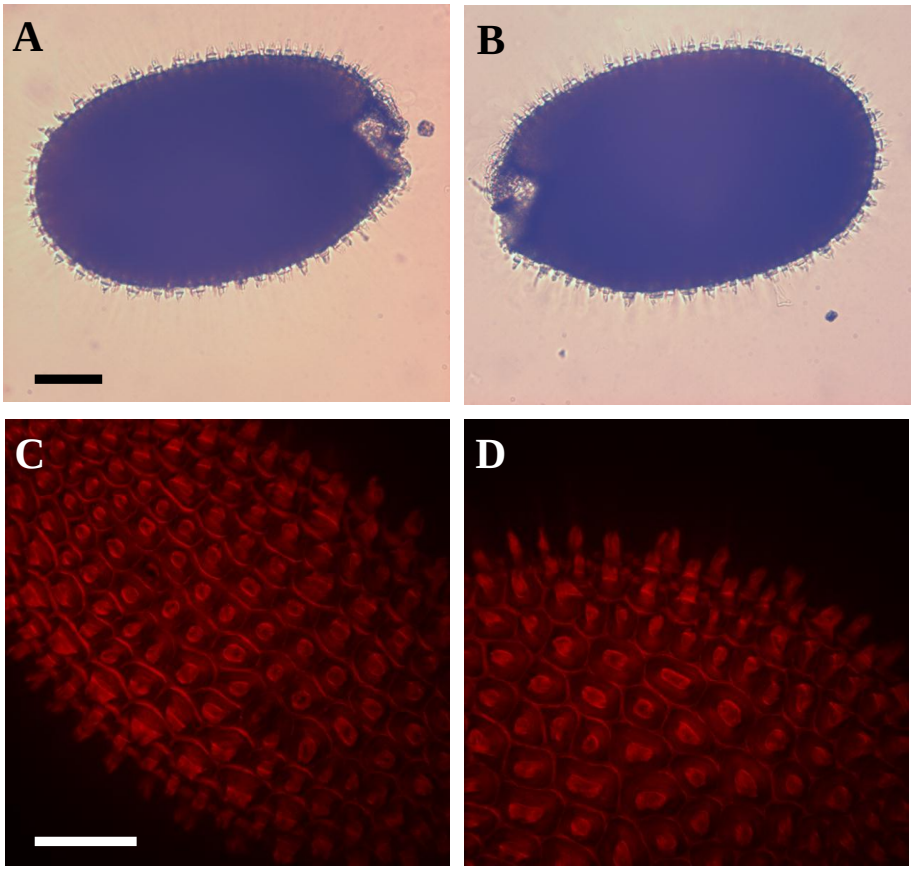

Figure 3.13: Cell Wall Attachment in EDTA-Hydrated Col-2 and *fly1-1* Seeds. EDTA-hydrated Col-2 seeds (A) and (C) appear identical to EDTA-hydrated *fly1-1* seeds (B) and (D). (A) and (B) panels show unstained seeds observed with phase contrast microscopy, while (C) and (D) depict confocal micrographs containing S4B signal from multiple optical slices (rendered using ImageJ, Z-project max intensity method). All columellae have primary cell walls attached to them. Scale bars = 100 μm.

3.3.8 The *fly1-1* Mucilage Has More Unesterified HG Than Col-2

Since the *fly1-1* mutant phenotypes are very sensitive to the presence of Ca^{2+} ions, *fly1-1* mucilage is likely to contain more unesterified galacturonic acid residues compared to Col-2. In contrast to cellulose biosynthesis at the plasma membrane, pectins are thought to be assembled into fully methylesterified polymers in the Golgi apparatus, which are subsequently modified and secreted to the apoplast (Lerouxel et al., 2006). Pectins with different degrees of methylesterification (DM) have been visualized across the primary cell wall and seed mucilage using monoclonal antibodies raised against HG (Willats et al., 2001c).

Whole seed immunolabeling with three anti-HG antibodies was conducted to determine if the pattern of methylesterification in *fly1-1* mucilage differs from wild type. 2F4, an antibody that specifically binds unesterified blocks of HG cross-linked by Ca^{2+} ions, only labeled primary cell wall material in Col-2 seeds (Figure 3.14), including the outer tangential wall remnants attached to columellae and the radial walls. For *fly1-1* seeds, 2F4 signal was detected in both the primary cell wall and in the extruded mucilage. The 2F4 labeling is consistent with *fly1-1* discs containing detached primary cell walls bound to cohesive mucilage. Given that 2F4 only recognizes pectin molecules with the egg-box conformation, the absence of 2F4 epitopes in Col-2 mucilage combined with their abundance in *fly1-1* mucilage supports the proposed increase of unesterified HG in the mutant (Figure 3.14). Unesterified pectins in discs and the underlying mucilage columns are likely to facilitate connections between the two structures, and may account for the effects of $CaCl_2$ and EDTA treatments on *fly1-1* mucilage and disc release (Figures 3.12 and 3.13).

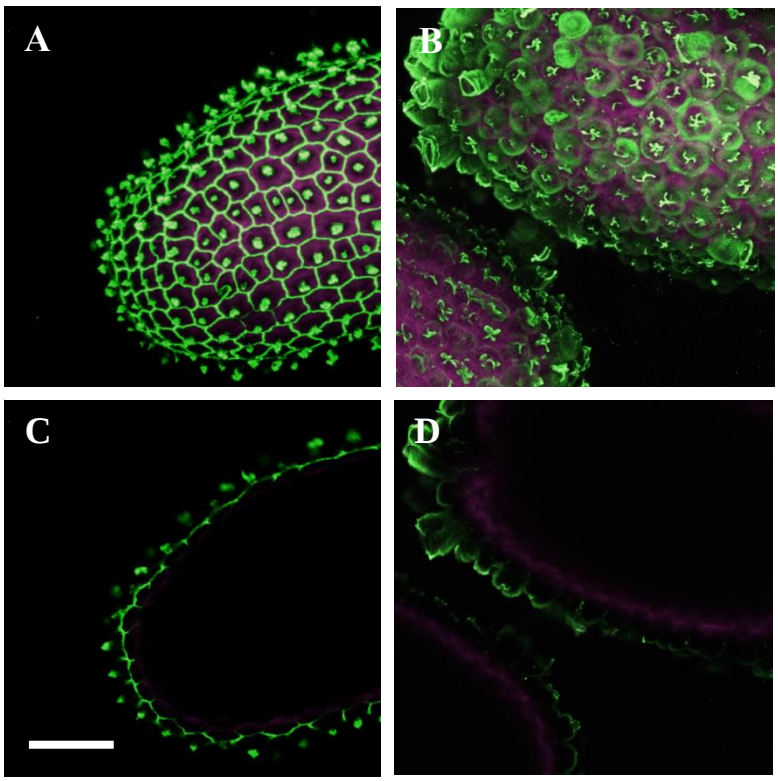

Figure 3.14: 2F4 Labeling of Unesterified HG in *fly1-1* Seeds.
Green represents the 2F4 signal, while magenta is the seed intrinsic fluorescence. 2F4 labels mucilage in *fly1-1* (B) and (D), but not in Col-2 (A) and (C). (A) and (B) contain 2F4 signal from multiple optical sections (rendered using ImageJ, Z-project max intensity method), while (C) and (D) are single slices through the middle of seeds. Scale bar = 100 µm.

Two additional antibodies with broader specificities were also used to characterize the *fly1-1* mucilage: JIM7, which binds to heavily (35 to 81%) methylesterified HG (Knox et al., 1990), and JIM5, which binds partially (up to 40%) methylesterified HG (VandenBosch et al., 1989). JIM5 and JIM7 recognize partially overlapping domains of seed mucilage, and both labelled larger regions of the *fly1-1* mucilage halo compared to Col-2 (Figure 3.15), consistent with the mutant containing lower DM pectin.

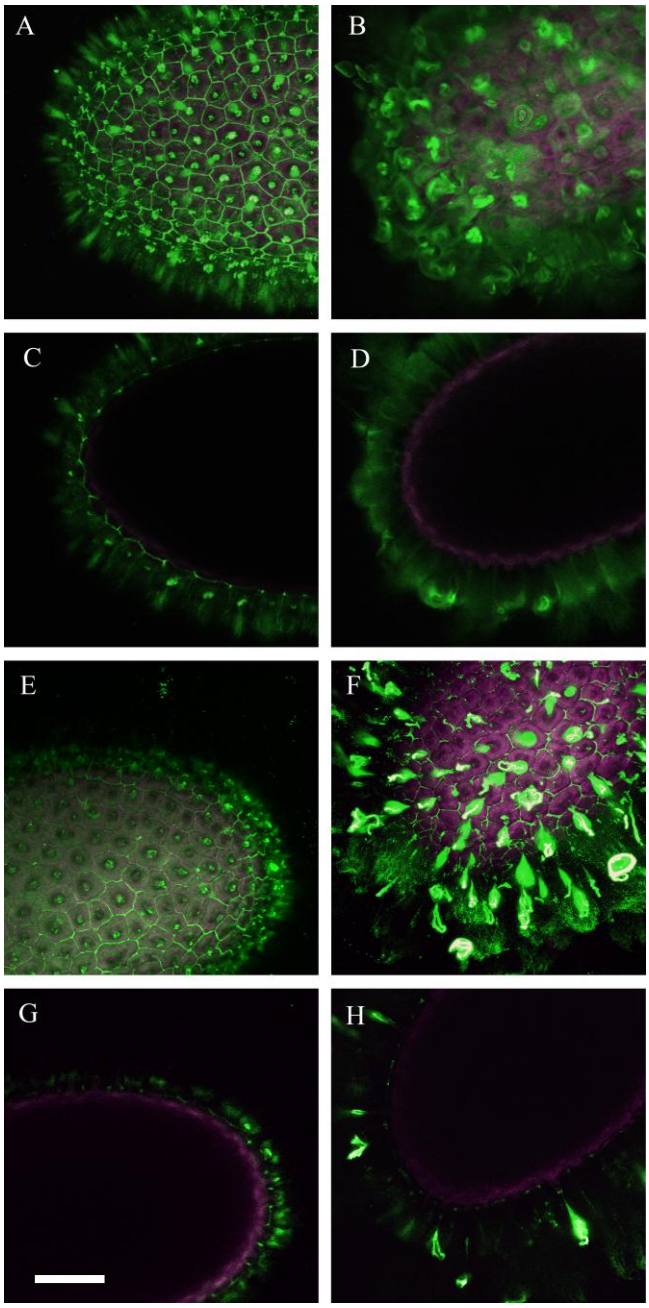

Figure 3.15: JIM5 and JIM7 Labeling of Partially Methylesterified HG in Seeds. JIM5 (A) to (D) and JIM7 (E) to (H) antibody signals are shown in green, and intrinsic seed fluorescence in magenta. Note increased labeling of *fly1-1* mucilage (B), (D), (F) and (H) compared to Col-2 (A), (C), (E), and (G). The images in (A), (B), (E) and (F) show fluorescent signals from multiple optical slices (rendered using ImageJ, Z-project max intensity method). (C), (D), (G) and (H) represent single optical sections through the middle of seeds. Scale bar = 100 µm.

CCRC-M36, a monoclonal antibody that binds to the RG-I backbone, is an excellent marker for seed mucilage and was previously shown to label the entire mucilage pocket but not the primary cell walls in seed coat epidermal cells (Young et al., 2008). In contrast with the results of the three anti-HG antibodies, CCRC-M36 labelled equally large regions of the mucilage halo in both *fly1-1* and Col-2 seeds (Figure 3.16). The even distribution of CCRC-M36 epitopes throughout the extruded mucilage is consistent with a role for FLY1 in the modification of HG rather than RG-I. CCRC-M36-labeled mucilage extruded from *fly1-1* seeds appears to have a more regular structure and partially maintains its original donut shape, as expected if the mutant has a more compact pectin gel matrix compared to Col-2.

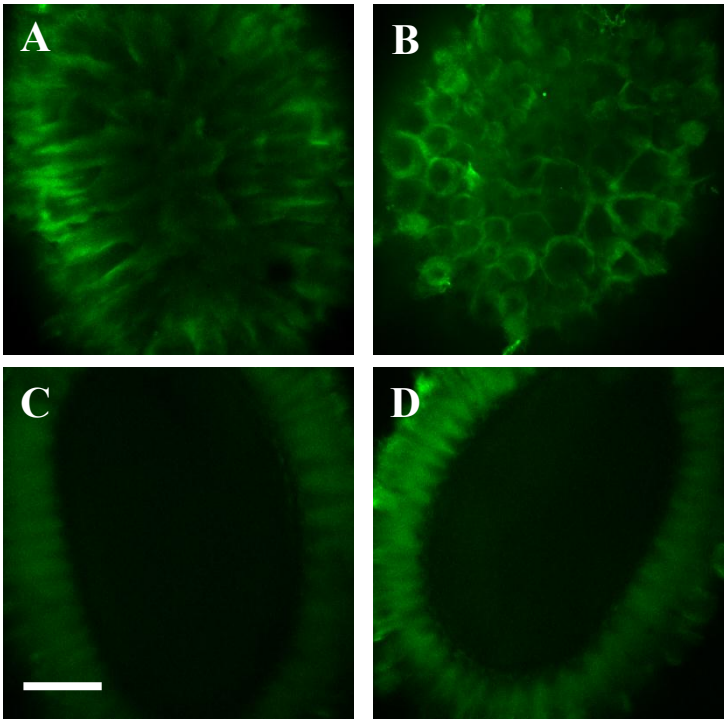

Figure 3.16: CCRC-M36 Labeling of RG-I in Seed Mucilage.
CCRC-M36 (green) labeling patterns for Col-2 (A) and (C) and *fly1-1* (B) and (D) seeds. (A) and (B) contain signals from multiple optical slices (rendered using ImageJ, Z-project max intensity method), while (C) and (D) are single optical sections through the middle of seeds. Scale bar = 100 µm.

Overall, the characterization of the *fly1-1* mutant seed coat epidermal cells revealed two major cell wall phenotypes. First, I observed that hydration of *fly1-1* seeds results in the detachment of many outer tangential primary cell walls from the columellae of epidermal cells. These cell wall discs are tightly bound to the extruded mucilage and are not removed even after 24 h of moderate shaking. Surprisingly, the cell wall detachment phenotype is completely rescued if *fly1-1* seeds are imbibed directly in EDTA, a cation chelator that removes Ca^{2+} ions that are required for strong pectin cross-links. The other major phenotype of the *fly1-1* mutant, the smaller mucilage halo, can also be rescued by treatment with EDTA, while addition of Ca^{2+} ions almost completely impairs mucilage release. Results from immunolabeling experiments indicate that *fly1-1* mucilage contains more unesterified HG bound by Ca^{2+} ions, and pectin methylesterification than wild type, suggesting that *FLY1* positively regulates the DM of pectin.

3.4 Analysis of the *FLY1* Gene and the Protein It Encodes

3.4.1 Positional Cloning and Expression Analysis of *FLY1*

The *fly1-1* phenotype was shown to segregate as a single recessive mutation, and the mutant was backcrossed to Col-2 four times to remove background EMS mutations. The position of the *fly1-1* mutation was previously mapped to a 180 kb region containing 60 genes near the end of the *Arabidopsis thaliana* chromosome IV. Since no additional insertions/deletions were available in this genomic region to facilitate further map-based cloning using Col-0/L*er* polymorphism markers, I decided to screen T-DNA insertional mutants affecting all the candidate genes for mucilage defects (Appendix A). I obtained nearly 100 different T-DNA mutants affecting 58 of the 60 genes from the Arabidopsis Biological Resource Center (ABRC) and from the Nottingham Arabidopsis Stock Centre

(NASC), and examined multiple alleles for candidates that are preferentially expressed in the seed coat. Seeds obtained from the stock centers were planted, and the progeny seeds were hydrated in water, stained with RR, and screened for mucilage extrusion defects. Only three T-DNA mutants (*fly1-2*, *fly1-3*, and *fly1-4*) produced seeds that showed discs and reduced mucilage extrusion (Figure 3.18 C to E), and all three independent lines had homozygous insertions in the At4g28370 gene (Figure 3.17). This gene encodes a previously uncharacterized protein that is annotated as a RING (Really Interesting New Gene) finger superfamily protein in The Arabidopsis Information Resource database (TAIR 10, Lamesch et al., 2011). Sequencing of At4g28370 in the *fly1-1* mutant background revealed a G-to-A transition, consistent with EMS mutations, at 3903 bp that changes the amino acid Trp (residue 460) to a stop codon. The early stop codon truncates the peptide encoded by the *FLY1* gene, resulting in the loss of the RING finger domain that may to facilitate protein-protein interactions (Kosarev et al., 2002).

In total, five independent T-DNA insertional mutants (*fly1-2* to *fly1-6*) affecting the *FLY1* gene were obtained from the ABRC stock center (Figure 3.17). Since most of the lines received were not confirmed homozygous mutants for the desired T-DNA insertion, the mutants were genotyped using PCR and a combination of T-DNA and gene-specific primers. Homozygous plants for all five lines produced seeds with identical mucilage defects, while heterozygous plants produced wild type seeds, consistent with the T-DNA insertions being recessive loss-of-function mutations. All five *fly1* T-DNA mutants closely resembled *fly1-1* seeds hydrated in water and stained with RR (Figure 3.18 B to G). Two of the alleles, *fly1-2* and *fly1-3*, were characterized in greater detail and were shown to be indistinguishable from *fly1-1* with cryo-SEM, S4B staining, and anti-HG immunolabeling (data not shown).

Complementation tests between *fly1-1*, *fly1-2* and *fly1-3* failed to rescue the mutant phenotype, consistent with the mutations occurring in same gene.

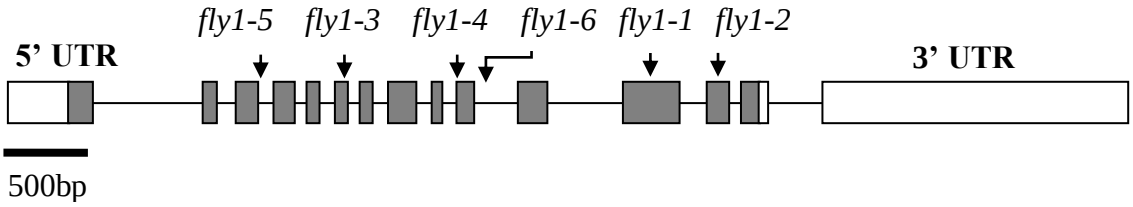

Figure 3.17: *FLY1* Gene Structure and Position of Mutations.
The 15 exons of At4g28370 are shown in boxes. Protein coding regions are shaded and introns are denoted by the connecting lines. Arrows indicate the position of the *fly1-1* EMS mutation and the sites of T-DNA insertions (*fly1-2* to *fly1-6*).

Analysis of *FLY1* gene expression using the Electronic Fluorescent Pictograph (eFP) browser revealed very high transcript levels in seeds relative to other major Arabidopsis organs, and preferential expression in the seed coat compared to the endosperm and embryo (Schmid et al., 2005; Winter et al., 2007; Le et al., 2010). This expression profile is consistent with the abnormal seed mucilage phenotype of the *fly1* mutant alleles. According to AceView, a curated database containing all public mRNA sequences, *FLY1* is moderately expressed and has 34.9% of the transcript levels of the average Arabidopsis gene (Thierry-Mieg and Thierry-Mieg, 2006). Interestingly, BLAST search revealed that *FLY1* has only one paralog in Arabidopsis, At2g20650 (hereafter called *FLY2*), which encodes a protein with 84.5% amino acid (aa) identity (Huang and Miller, 1991). *FLY2* is expressed at 19.0% of the average gene in the AceView database (Thierry-Mieg and Thierry-Mieg, 2006), and has a lower expression in developing seeds than *FLY1*, although its transcripts are still more abundant in the seed coat compared to the embryo (Zimmermann et al., 2004; Winter et al., 2007; Le et al., 2010). However, T-DNA insertions in *FLY2* do not cause any obvious

morphological defects or abnormal seed mucilage release (Figure 3.18 H and I). The expression of *FLY1* and *FLY2* is not limited to the seed coat since RT-PCR analysis detected gene-specific transcripts in all major Arabidopsis tissues tested (Figure 3.19). Multiple microarray datasets show that the expression levels of *FLY1* and its paralog are highest in xylem cells (Brady et al., 2007; Hruz et al., 2008) suggesting a role in vasculature development. Further analysis of the *FLY2* gene function and its relation to *FLY1* is presented in Chapter 4.

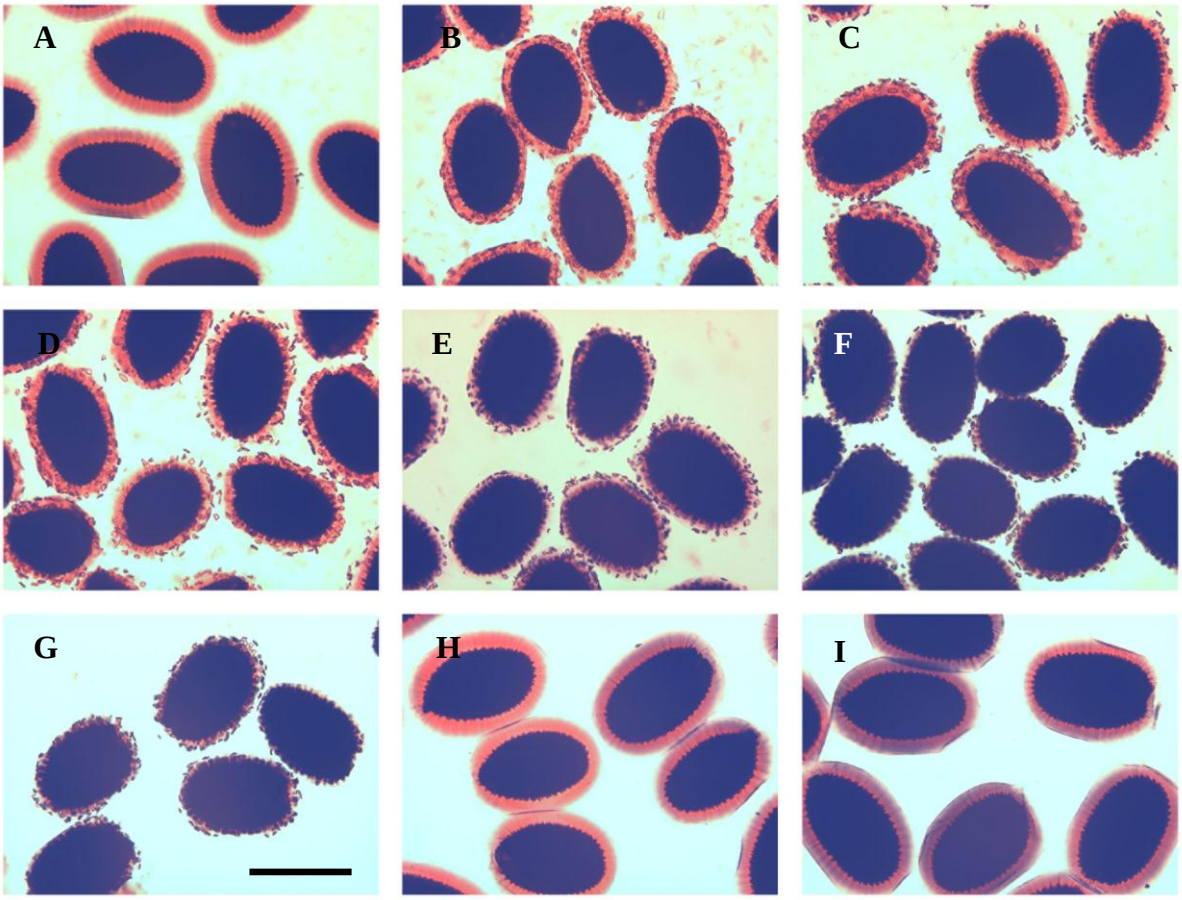

Figure 3.18: Ruthenium Red Staining of *fly1* and *fly2* Seeds Hydrated in Water.
Seed genotypes are Col-2 (A), *fly1-1* to *fly1-6* (B) to (G), *fly2-1* (H) and *fly2-2* (I). Seeds were shaken in water for 2 h and stained with Ruthenium Red for 1 h. Scale bar = 500 µm.

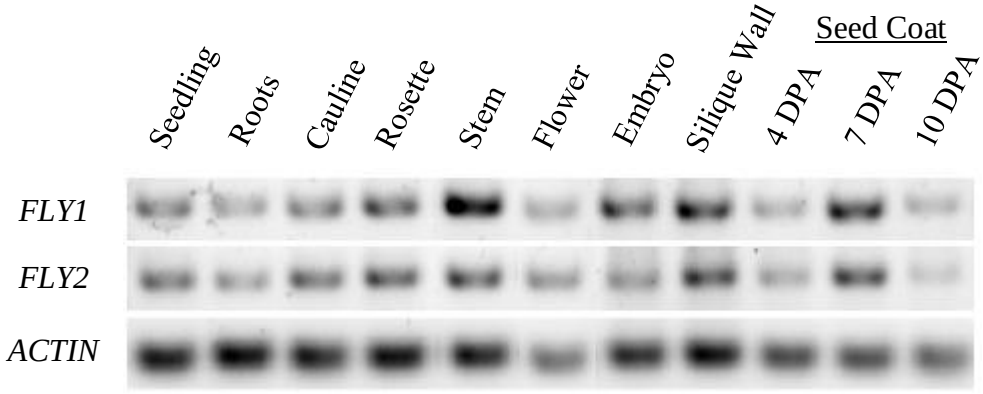

Figure 3.19: RT-PCR Analysis of *FLY1* and *FLY2* Transcripts in Major Tissues. 30 cycles of amplification were performed for all three sets of gene-specific primers. The templates were cDNA samples prepared from Arabidopsis Col-2 tissues, except for the embryos, silique walls, and seed coats, which were dissected from Col-2 siliques. *ACTIN* was used as loading control.

3.4.2 Analysis of the FLY1 Peptide Sequence

Bioinformatic analysis of the FLY1 amino acid sequence was conducted to obtain more information about the structure of this uncharacterized protein that is poorly annotated in the TAIR database (Swarbreck et al., 2007; Lamesch et al., 2011). Figure 3.20 shows a visual summary of the key results of the bioinformatic search, which are described in detail below. Using the ARAMEMNON plant membrane protein database (Schwacke et al., 2003), I determined that FLY1 is an integral membrane protein, which is predicted to have four to eight transmembrane-spanning alpha helices. In addition, FLY1 has an N-terminal signal peptide that is predicted to be cleaved between amino acids 32 and 33 in the ER, and targets the protein to the secretory pathway (Petersen et al., 2011). The large region (approximately 230 aa) between the end of the N-terminal signal peptide and the start of the first transmembrane span does not contain any InterProScan or PROSITE functional domains (Quevillon et al., 2005; Sigrist et al., 2010), or any other conserved motifs (Geer et al., 2002; Marchler-Bauer et al., 2011).

The C-terminal end of the FLY1 protein has a conserved RING finger domain, that coordinates two zinc ions (Quevillon et al., 2005; Sigrist et al., 2010; Lamesch et al., 2011). Although it failed to mention FLY1, a whole-genome study identified FLY2 as containing a RING domain with a C3H2C3 motif (abbreviated RING-H2) based on the arrangement of the 8 zinc-binding Cys and His residues (Kosarev et al., 2002). Manual curation revealed that FLY1 contains a RING-H2 domain whose metal ligand spacing is identical to FLY2. The basic function of this cysteine-rich domain is to facilitate protein-protein interactions (Kosarev et al., 2002), but a genome-wide study has classified the FLY1 protein as a putative RING-type E3 ubiquitin ligase (Stone et al., 2005). The exact orientation of the C-terminal RING finger cannot be determined since 10 out of the 18 independent tools used to examine the FLY1 topology predict an odd number of membrane spans while the remainder predict an even number (Schwacke et al., 2003).

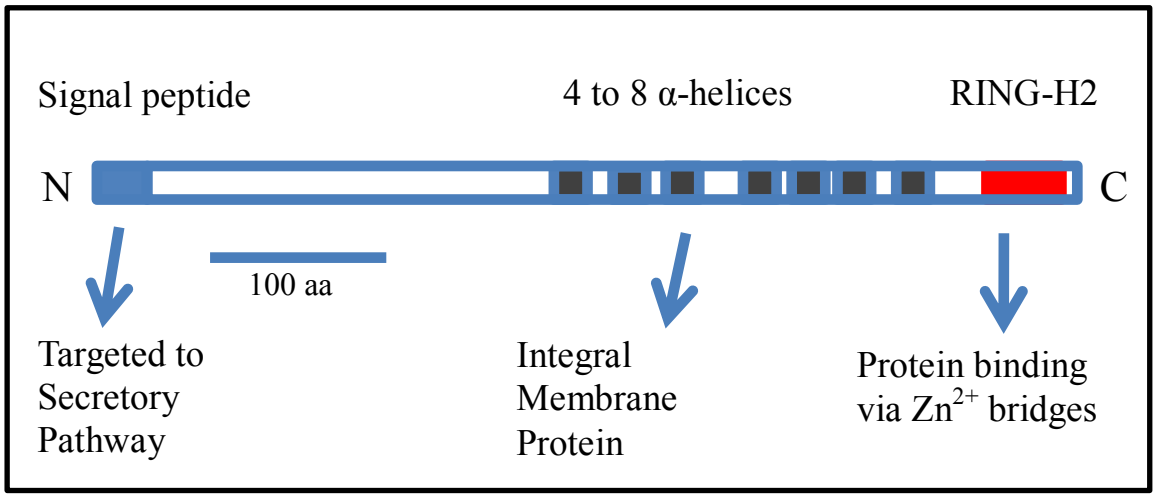

Figure 3.20: Predicted Structure of the FLY1 Protein.
Note that although this image depicts seven transmembrane domains (ARAMEMNON consensus prediction; Schwacke et al., 2003), the FLY1 protein may contain between four and eight alpha helices.

3.5 FLY1 Complementation, Expression and Subcellular Localization

To confirm the identity of *FLY1* and to investigate the expression pattern and subcellular localization of FLY1 proteins, I constructed FLY1-yellow fluorescent protein (YFP) fusions under the control of the native *FLY1* promoter. The *FLY1*$_{pro}$:*FLY1-YFP* transgene was introduced into Arabidopsis *fly1-1* plants, and was shown to rescue the mucilage defects of the mutant (Figure 3.21). Around 30 Basta-resistant *fly1-1* transgenic lines were obtained, and more than a dozen of these had a partially complemented mucilage phenotype, displaying considerably fewer discs (<20 discs/seed) than the mutant (>40 discs/seed), while one line appeared to be fully complemented (Figure 3.21).

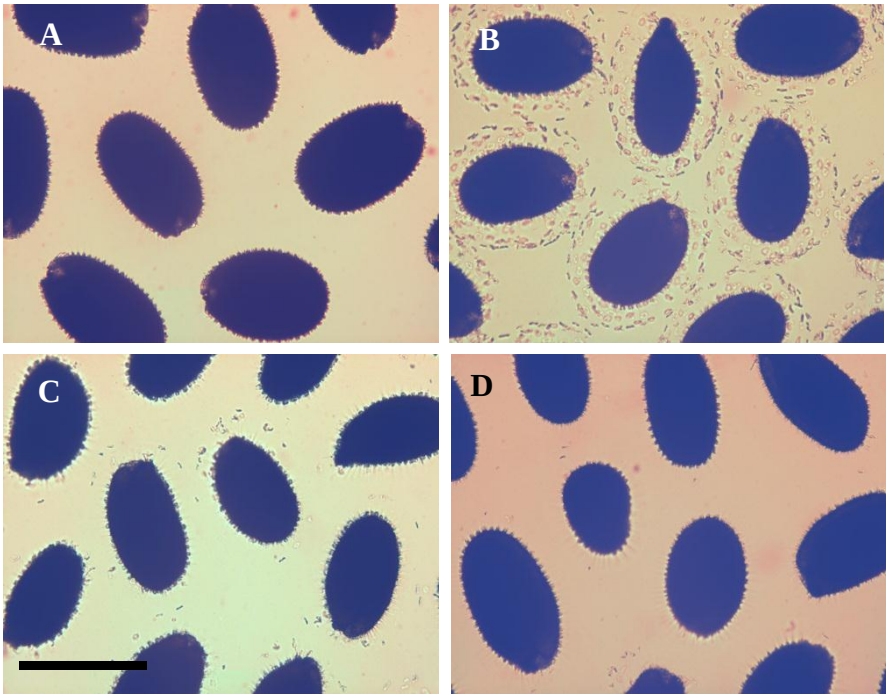

Figure 3.21: Genomic Complementation of *fly1-1* with At4g28370.
Seeds were shaken in water for 1 h. Seeds shown are Col-2 (A), *fly1-1* transformed with empty vector (B), and *fly1-1* transformed with *FLY1*$_{pro}$:*FLY1-YFP* that has a partially (C) or a fully (D) complemented mutant phenotype. Scale bar = 500 µm.

All *fly1-1 FLY1*$_{pro}$*:FLY1-YFP* lines with at least a partially complemented mutant phenotype displayed YFP fluorescence in the epidermal cells of the seed coat (Figure 3.22A and B). Dissected embryos from *FLY1*$_{pro}$*:FLY1-YFP* seeds resembled the negative control and did not show any detectable YFP signal (data not shown). The FLY1-YFP expression in seed coat epidermal cells was highest around 7DPA, the developmental stage where mucilage synthesis and secretion is at its peak. The YFP signal was difficult to detect in seeds after 9 DPA when the cytoplasmic column is displaced by newly deposited secondary cell wall.

The localization of FLY1-YFP fusion proteins was closely examined in Arabidopsis seed coat epidermal cells at 7DPA. No FLY1-YFP signal appears in the mucilage pocket or in the primary cell wall (Figure 3.22D). Instead, FLY1-YFP fusion proteins appear primarily in small, intracellular compartments. In most seed epidermal cells, FLY1-YFP fluorescence is also observed in one or two larger bodies of unknown function (Figure 3.22D). FLY1-YFP proteins are expected to be membrane-bound, and indeed show a more restricted distribution than cytosolic YFP expressed by the seed coat-specific promoter of the *DP1* gene (Elahe Esfandiari, Zhaoqing Jin, Ashraf Abdeen, Jonathan Griffiths, Tamara Western, George Haughn, unpublished results). The center of the cytoplasmic column of seed coat epidermal cells at 7DPA can contain multiple starch granules. These structures exclude the cytosolic YFP signal, appearing as dark circles in the cytoplasm of seed epidermal cells (Figure 3.22C, asterisks). FLY1-YFP bodies are observed mainly along the edges of the cytoplasmic column, and do not co-localize with the amyloplasts (Figure 3.22D, asterisks).

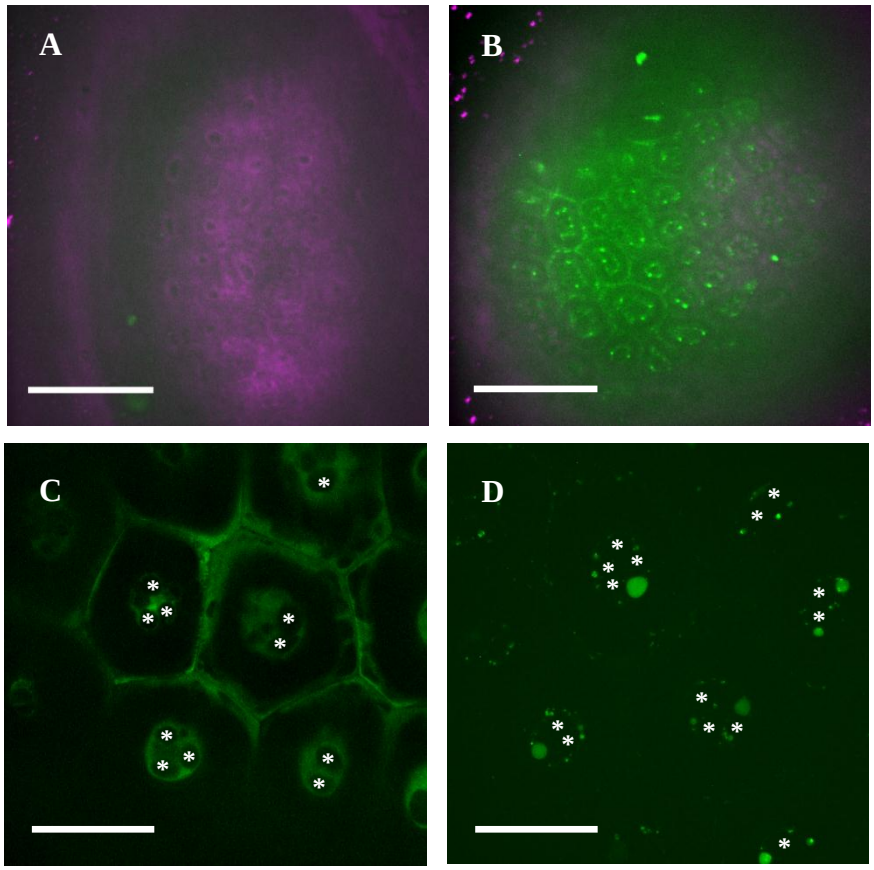

Figure 3.22: Localization of FLY1-YFP in Arabidopsis Seed Coat Epidermal Cells. (A) shows lack of fluorescence in *fly1-1* seeds transformed with empty vector; the magenta background is an artificially colored transmitted light image of the seed. (B) and (D) show green FLY1-YFP signal in intracellular bodies. (C) shows cytosolic YFP signal, driven by the *DP1* seed coat-specific promoter. Asterisks indicate the position of amyloplasts in the cytoplasmic columns (transmitted light images not shown). Scale bars = 100 μm in (A) and (B), and 30 μm in (C) and (D).

3.6 Discussion

Loss-of-function mutations in the *FLY1* gene result in the appearance of two distinct mucilage defects for seeds hydrated in water. The most evident phenotype of *fly1* mutants is the release of unusual disc-like structures, which are mucilage-bound primary cell walls that detach from the columellae of seed coat epidermal cells upon hydration. The second *fly1* phenotype concerns the reduced size of the mucilage capsule, and correlates with a more

adherent pectin gel matrix in the mutant compared to wild type. Hydration of *fly1* seeds in the presence of exogenous Ca^{2+} ions almost completely impairs mucilage release, suggesting that pectin molecules in the mutant can form more calcium-mediated cross-links than Col-2. Calcium bridges are required to cross-link pectin polymers that contain regions of unesterified HG and are one of the key interactions that control the strength of pectin gels (Willats et al., 2001a). EDTA, a cation chelator that can extract the Ca^{2+} ions required for pectin cross-links, completely rescues the *fly1* mutant phenotype including both the size of the mutant capsule and the formation of the discs/primary cell wall detachment from the columella. These data suggest that the *fly1* phenotype is due to increased pectin cohesiveness arising from stronger HG crosslinking by Ca^{2+} ions.

Since pectin with a low DM represents the only cell wall component that uses Ca^{2+} ions as its main mechanism for crosslinking, *fly1-1* mucilage should contain fewer methylester groups than Col-2. Indeed, seed immunolabeling with multiple anti-HG antibodies showed fluorescent patterns consistent the presence of a considerably lower pectin DM in *fly1* mucilage compared to Col-2. Reduced methylesterification would strengthen the pectin gel matrix, and would thereby reduce mucilage expansion and increase its adherence to the seed, consistent with the observed properties of *fly1* mucilage. Extensive calcium bridges within mucilage, and between mucilage and the primary cell wall could generate the necessary pressure for mucilage to lift the primary cell wall off the columella when *fly1* is hydrated in water, leading to the appearance of discs at the edge of the extruded mucilage. Although mucilage is mainly composed of RG-I (Macquet et al., 2007a), modification of HG can have a profound impact on the entire pectin gel matrix if RG-I and HG are covalently bonded to form a high-molecular weight polysaccharide complex, as current models suggest

(Harholt et al., 2010). Overall, the analysis of the *fly1* mutant phenotypes suggests that *FLY1* positively regulates the DM of pectin in seed mucilage.

I identified *FLY1* as At4g28370 using positional cloning, and showed that independent T-DNA insertions in this gene phenocopy the *fly1-1* defects. Crosses between *fly1-1* and selected T-DNA lines (*fly1-2* and *fly1-3*) failed to rescue the seed mucilage phenotype, consistent with the mutants being allelic. Molecular complementation of *fly1-1* with a $FLY1_{pro}$:*FLY1-YFP* transgene containing the wild type At4g28370 coding sequence at least partially rescued the mutant phenotype. The cloned *FLY1* gene encodes an uncharacterized protein with multiple transmembrane spans and a C-terminal RING-H2 domain whose basic function is to facilitate protein-protein interactions.

RING fingers are one of the most abundant domains in the Arabidopsis proteome, and proteins containing this domain have been suggested to function as E3 ubiquitin ligases (Kosarev et al., 2002). E3 ligases provide substrate specificity in the ubiquitin/proteasome pathway since they mediate the transfer of ubiquitin from an E2 ubiquitin-conjugating enzyme to target proteins (Glickman and Ciechanover, 2002). The activity of most E3 ligases is specified by a RING domain, although a variety of other domains may also be involved (Stone et al., 2005; Deshaies and Joazeiro, 2009). In Arabidopsis, more than 70% of 64 RING proteins previously examined (469 in total) showed E2-dependent protein ubiquitination *in vitro* (Stone et al., 2005). FLY1 and FLY2 have been classified as RING E3 ligases in an Arabidopsis genome-wide study (Stone et al., 2005), but their biochemical activities have not been investigated. Moreover, the RING fingers of the FLY proteins could be involved in protein-protein interactions beyond the ubiquitin/proteasome pathway. In the context of cell wall biosynthesis, RING fingers at the N-terminus of cellulose synthase

(CESA) proteins are thought to facilitate the dimerization of the CESA subunits (Kurek et al., 2002). Since FLY1 and FLY2 do not contain any functional domains found in carbohydrate-active enzymes, there is no bioinformatic evidence to suggest that the proteins do not function as E3 ligases.

In addition to the presence of multiple transmembrane spans and a C-terminal RING domain, the FLY1 amino acid sequence contains an N-terminal signal peptide that is predicted to be cleaved in the ER and targets the protein to the secretory pathway (Choo et al., 2009). FLY1-YFP fusion proteins displayed a punctate distribution in the cytoplasm of seed coat epidermal cells at the stage of mucilage biosynthesis. One or two large FLY1-YFP intracellular compartments were also observed in some seed coat cells, but their identity remains to be investigated. One possibility is that the large, unknown compartments are aggregates of misfolded FLY1-YFP fusion proteins. The fusion of YFP to the C-terminal RING finger may disrupt the function of the FLY1 protein, which could explain why most of the *FLY1*$_{pro}$*:FLY1-YFP* transgenic lines isolated only partially rescue the phenotype of the *fly1-1* mutant.

Since FLY1 appears to be localized in the endomembrane system and to positively control pectin methylesterification, this protein may interact with pectin methyltransferase (PMT) enzymes that add methylester groups to galacturonic acids during HG synthesis. HG is synthesized in the Golgi apparatus and is deposited in the apoplast as a fully methylesterified polymer (Goldberg et al., 1996). If FLY1 proteins are required to bind PMTs in the Golgi, then when *FLY1* is genetically disrupted, PMTs may no longer function properly resulting in the secretion of HG that is not fully methylesterified to the cell wall.

FLY1 may be responsible for the anchoring or targeting of PMT enzymes to the Golgi membrane. Although all currently identified Golgi proteins involved in cell wall biosynthesis are thought to be membrane-bound, the mechanisms for the retention of plant proteins in the Golgi are not well understood (Saint-Jore-Dupas et al., 2004). A recent study revealed that the transmembrane domain of GAUT1, the first HG biosynthetic enzyme identified, is cleaved *in vivo* and that the GAUT1 protein is anchored to the Golgi membrane through interactions with GAUT7, a related protein with an intact transmembrane domain (Atmodjo et al., 2011). Proteomic analyses showed that GAUT1 and GAUT7 are at the core of a HG biosynthetic complex composed of 14 different proteins, including two putative PMTs (Atmodjo et al., 2011). Although PMTs are predicted to have a single membrane-spanning domain (Krupková et al., 2007), these enzymes may still have to be anchored by other membrane proteins such as FLY1 to be retained in the Golgi. Alternatively, FLY1 could function as an E3 ligase that uses ubiquitin as a signal that marks PMTs for retention in the Golgi. Although polyubiquitin chains target proteins for degradation, monoubiquitin can play addition roles and has been identified as a signal for membrane protein localization in yeast and animal systems (Reggiori and Pelham, 2002; Hicke and Dunn, 2003; Schnell and Hicke, 2003). In plants, ubiquitin can also alter the localization of modified targets and is required for the internalization of certain plasma membrane proteins (Barberon et al., 2011; Dowil et al., 2011).

The identification of FLY1 as a novel protein that controls pectin methylesterification through protein-protein interactions represents a significant landmark in the study of pectin biosynthesis and modification. Detailed characterization of the seed coat phenotype of the *fly1* mutant revealed an unexpected scenario where primary cell wall detachment appears to

result from the extrusion of mucilage with stronger gelling properties and an increased number of HG cross-links via calcium bridges. Further elucidation of the molecular function of FLY1 may provide new perspectives on cell wall biosynthesis as a whole and on the mechanisms by which enzymes are retained in the Golgi. Although the subcellular localization of FLY1 remains to be confirmed by co-localization with a Golgi marker such as ST-RFP, this protein offers a great window of opportunity to identify additional components of the pectin methylesterification pathway. Future research should include proteomic analyses similar to those used to discover the proteins associated with the GAUT1 and GAUT7 HG biosynthetic enzymes (Atmodjo et al., 2011). Anti-FLY1 and Anti-FLY2 antibodies should be obtained and used to immunoprecipitate protein complexes that contain FLY1 and/or FLY2. Associated proteins will be sequenced by mass spectrometry and their functions will be investigated with bioinformatic tools before being experimentally confirmed.

Chapter 4: Identification of Cell Wall Genes Related to *FLY1*

4.1 Synopsis

FLY1 is an evolutionarily conserved protein that has orthologs in fungi, protists, green algae, mosses, and vascular plant species. TRANSMEMBRANE UBIQUITIN LIGASE 1 (TUL1) is the FLY1 ortholog (28% amino acid identity) in the yeast *Saccharomyces cerevisiae* and was previously shown to be an E3 ligase that is required for sorting Golgi membrane proteins. Since both FLY1 and TUL1 have an N-terminal signal peptide, multiple transmembrane spans, and a C-terminal RING finger domain, FLY1 may use ubiquitin to sort or process cell wall biosynthetic enzymes in the Golgi membrane. FLY1 is proposed bind pectin methyltransferases, but its actual targets are currently unknown. Whether the FLY1 protein has ubiquitin ligase activity remains to be determined and will be the focus of future studies.

FLY1 has a paralog, called *FLY2*, which is highly co-expressed with many genes that encode enzymes involved in cell wall synthesis and modification. T-DNA insertions in this gene fail to show any major morphological defects. Since these homologous genes are highly expressed in xylem cells, they may play partially redundant roles in secondary wall biosynthesis in this cell type. Analysis of *fly1 fly2* double mutants will likely provide more clues about the role of the FLY1 protein beyond the seed coat, and indicate if *FLY1* and *FLY2* function in the same pathway.

KNOTTED1-LIKE HOMEODOMAIN PROTEIN 7 (KNAT7) is top gene co-expressed with *FLY1* and *FLY2* and could be regulating their expression in Arabidopsis since it encodes a transcription factor known to control secondary wall biosynthesis in xylem and seed coat cells. Histological analysis of *knat7* mucilage suggests that KNAT7 may be a negative

regulator of *FLY1*, or a positive regulator of *CESA5*, which is involved in cellulose synthesis in the mucilage pockets of seed epidermal cells.

4.2 Introduction

FLY1 is a novel player required for the biosynthesis of mucilage in Arabidopsis seed coat epidermal cells, but its function at the molecular level is not well understood. In this chapter, I investigate the function of genes related to *FLY1* by sequence homology and/or co-expression in order to learn more about the potential biological and biochemical roles of the encoded protein. I first compare FLY1 to a homologous protein in yeast (TUL1) and present my preliminary analysis of the putative role of *FLY2*, the only paralog of *FLY1*. I also examine the biological roles of genes that show similar expression profiles with *FLY1* and/or *FLY2*, and analyze the seed mucilage phenotype of T-DNA mutants for some of these genes. In particular, I demonstrate that *KNAT7*, the gene that shows the highest co-expression with *FLY1* and its paralog, displays a loss of mucilage adherence to the seed coat.

4.3 Analysis of Genes Homologous to *FLY1*

In order to obtain more clues about role of the *FLY1* gene in plant biology, I conducted a bioinformatic search for homologous genes in Arabidopsis and other organisms. Interestingly, *FLY1* appears to be conserved in most eukaryotes (notably absent in animals) and has at least one ortholog in fungi, protists, green algae, mosses, and vascular plant species with a sequenced genome (Ostlund et al., 2010; Goodstein et al., 2012; Van Bel et al., 2012). The FLY1 has an ortholog (28% aa identity) in the yeast *Saccharomyces cerevisiae*, whose function was previously characterized. TRANSMEMBRANE UBIQUITIN LIGASE 1 (TUL1) is proposed to be a Golgi-localized, membrane-bound E3 ubiquitin ligase involved in the quality control of membrane proteins (Reggiori and Pelham, 2002). TUL1 may sort

misfolded proteins from the Golgi membrane to multivesicular bodies, and may target them for degradation in the vacuole (Reggiori and Pelham, 2002). FLY1 may functionally resemble TUL1 since their protein architectures are remarkably similar and include an N-terminal signal peptide, multiple transmembrane spans, and a C-terminal RING finger.

FLY2 is the only paralog of *FLY1* and resulted from the duplication of a large block of Arabidopsis genes (Tang et al., 2008). FLY2 displays 84.5% aa identity to FLY1, with an N-terminal signal peptide, multiple transmembrane spans and a RING finger for protein-protein interactions. Although both *FLY1* and *FLY2* are preferentially expressed in the seed coat compared to the endosperm and embryo, the *FLY2* transcript level in seeds is significantly lower than that of *FLY1* (Schmid et al., 2005; Winter et al., 2007; Hruz et al., 2008; Le et al., 2010). I obtained and screened five different T-DNA insertional lines disrupting *FLY2* from the ABRC stock center (Figure 4.1). None of the *fly2* mutants had obvious mucilage defects when hydrated in water and stained with Ruthenium Red (*fly2-1* and *fly2-2* are shown in Figure 3.18 H and I; data not shown for remaining alleles). Homozygous *fly2-1* and *fly2-2* lines identified by PCR were further characterized and showed wild type S4B staining, and 2F4, JIM5, and JIM7 immunolabeling (data not shown).

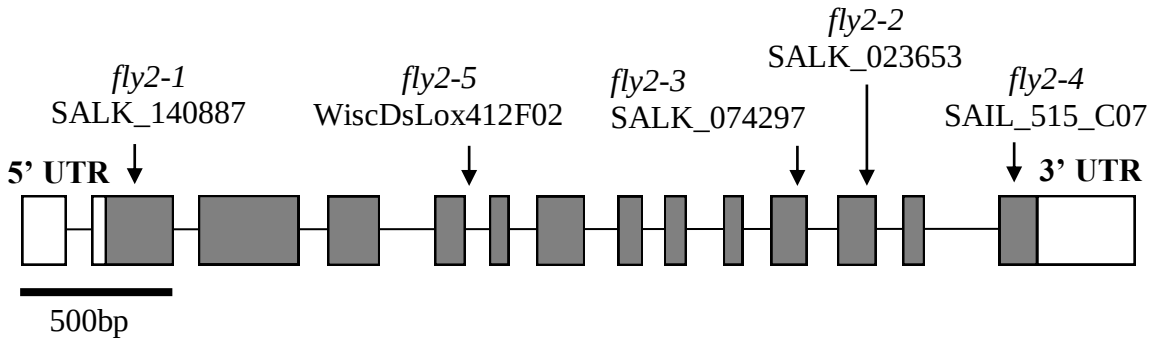

Figure 4.1: *FLY2* Gene Structure and Position of T-DNA Insertions.
Boxes indicate the position of 14 exons. Protein coding regions are shaded, while introns are denoted by the connecting lines. Arrows indicate the location of T-DNA insertions.

Interestingly, the transcript levels of both *FLY1* and *FLY2* are highest in xylem cells (Figure 4.2), suggesting that they play a role in xylem development and possibly affect secondary cell wall biosynthesis. Since both genes display high transcript levels in the base of the stem compared to the stem top in the Arabidopsis eFP Browser (Winter et al., 2007), I prepared cross-sections from the bottom of *fly1* and *fly2* single mutants stems and analyzed the shape and size of xylem cells. The stem cross-sections of *fly1* and *fly2* single mutants resembled wild type (Figure 4.3), and did not show the irregular xylem phenotype characteristic of mutants defective in secondary cell wall biosynthesis (Turner and Somerville, 1997). To examine if the mutants have reduced root elongation, *fly1*, *fly2*, and Col-2 seeds were stratified at 4ºC for 3 d to obtain uniform germination and were then grown in regular conditions and media, on plates in a vertical orientation. The roots of the single mutants were indistinguishable in length from wild type after 7 or 10 d of growth. Due to their high co-expression in xylem cells and their sequence homology, *FLY1* and *FLY2* are likely to play at least partially redundant roles. To test this hypothesis, I have generated F2 segregating populations for *fly1-2* x *fly2-1* and *fly1-2* x *fly2-2* crosses, and I plan to isolate and characterize *fly1 fly2* double mutants.

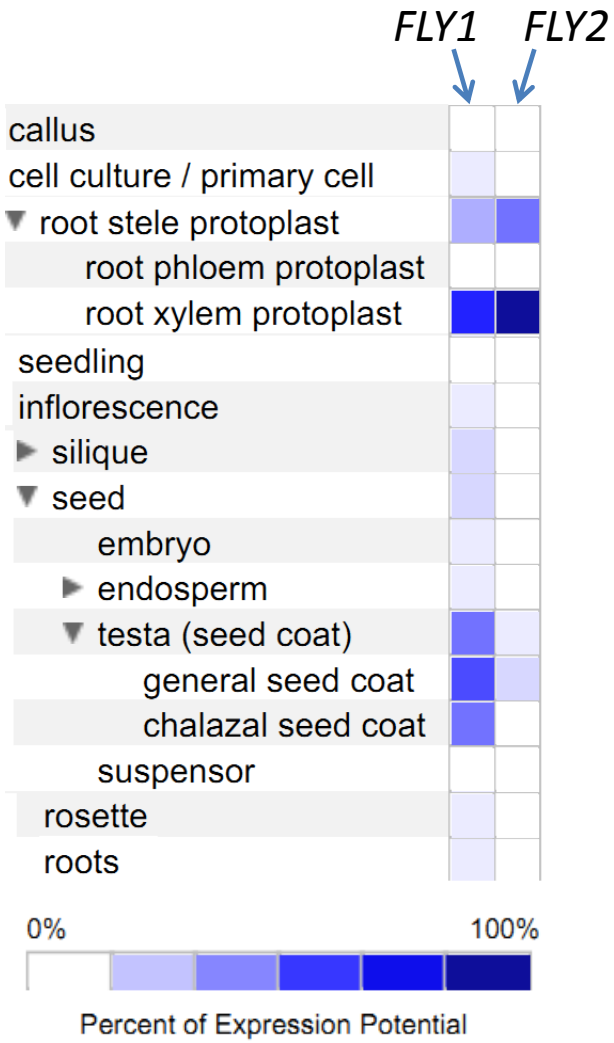

Figure 4.2: *FLY1* and *FLY2* Transcript Levels are Highest in Xylem Cells. Relative transcript levels across Arabidopsis tissues and cell types are shown using a GENEVESTIGATOR heat map (Hruz et al., 2008). Values are normalized to the maximum level of expression (darkest blue color) recorded for each gene.

Figure 4.3: Sections of *fly1* and *fly2* Stems Resemble Wild Type.
The bottom of Col-2 (A), *fly1-1* (B), and *fly2-1* (C) stems were hand-sectioned and stained with phloroglucinol-HCl. Arrows indicate the position of xylem cells, which display a similar morphology in the three genotypes examined. Scale bar = 125 µm.

4.4 Analysis of Genes with Similar Expression Patterns

The top genes expressed concurrently with *FLY1* and/or *FLY2* were identified using the GeneCAT (Mutwil et al., 2008) and ATTED-II databases (Obayashi and Kinoshita, 2010; Obayashi et al., 2011), and the specificity of their expression was verified using GENEVESTIGATOR and the eFP Browser (Winter et al., 2007; Hruz et al., 2008). In the ATTED-II database, *FLY1* is closely linked to *GAE5* (At4g12250), which encodes a UDP-D-glucuronate 4-epimerase proposed to synthesize activated UDP-D-galacturonate precursors necessary for pectin biosynthesis (Usadel et al., 2004b) and with At2g47670, which encodes a putative pectin methylesterase inhibitor. Similarly to *FLY1*, both of these genes are preferentially expressed in the seed coat and in the xylem cells (Brady et al., 2007; Winter et al., 2007). Multiple T-DNA insertions were screened for *GAE5* (Appendix B), but the mutant seeds did not display any mucilage defects, possibly due to redundancy with five other *GAE* genes that are also expressed during silique development (Usadel et al., 2004b).

Interestingly, 15 of the top 20 *FLY2* co-expressed genes in the ATTED-II database encode enzymes involved in cell wall biosynthesis including three polygalacturonases and two cellulose synthases (CESA4 and CESA7). This suggests that despite the lack of obvious

morphological defects in *fly2* single mutants, *FLY2* is involved in cell wall biosynthesis. Co-expression analysis of *FLY1* and *FLY2* using GeneCAT also revealed a large number of cell wall-related genes (Mutwil et al., 2008). *KNOTTED1-LIKE HOMEODOMAIN PROTEIN 7 (KNAT7)* is the top gene co-expressed with both *FLY1* and *FLY2* (Mutwil et al., 2008), and encodes a transcription factor was previously reported to be control cell wall biosynthesis in xylem and seed coat cells (Bhargava, 2010; Li et al., 2011, 2012). From a screen of T-DNA lines for eight genes that are highly co-expressed with *FLY1* in the seed coat (Appendix B), only mutations in *KNAT7* resulted in seed mucilage defects in water with Ruthenium Red staining. To investigate if *KNAT7* is involved in the same pathway for cell wall biosynthesis as the *FLY1* gene, I analyzed the structure of *knat7* mucilage with additional molecular probes.

Although *knat7* seeds release a similar amount of mucilage to wild type when hydrated in water without shaking, the adherent mucilage capsules detach from *knat7* seeds even after gentle mechanical agitation (Bhargava, 2010). This results in the appearance of a smaller mucilage halo compared to wild type after shaking (Figure 4.4), resembling the phenotype of cellulose-deficient *cesa5* mutant seeds (Harpaz-Saad et al., 2011; Mendu et al., 2011; Sullivan et al., 2011). S4B staining of seeds shaken in water revealed that both *knat7* and wild type, unlike *fly1*, have outer tangential primary cell wall fragments attached to the columellae of seed coat epidermal cells. However, *knat7* seeds like the previously described *cesa5* mutant show a reduction of S4B-labelled cellulose microfibrils in the inner mucilage layer compared to wild type (Figure 4.5).

Since *fly1* mucilage was more adherent and displayed a lower degree of pectin methylesterification compared to wild type (Chapter 3), I decided to investigate the pattern of

methylesterification in *knat7* mucilage with anti-pectin antibodies. Although *knat7* still has JIM5-labelled primary cell walls attached to seeds after shaking, the mucilage appears to lack the partially methylesterified homogalacturonan observed in wild type (Figure 4.6). Two additional antibodies, JIM7 and 2F4, also showed reduced mucilage labelling in the mutant compared to wild type (data not shown).

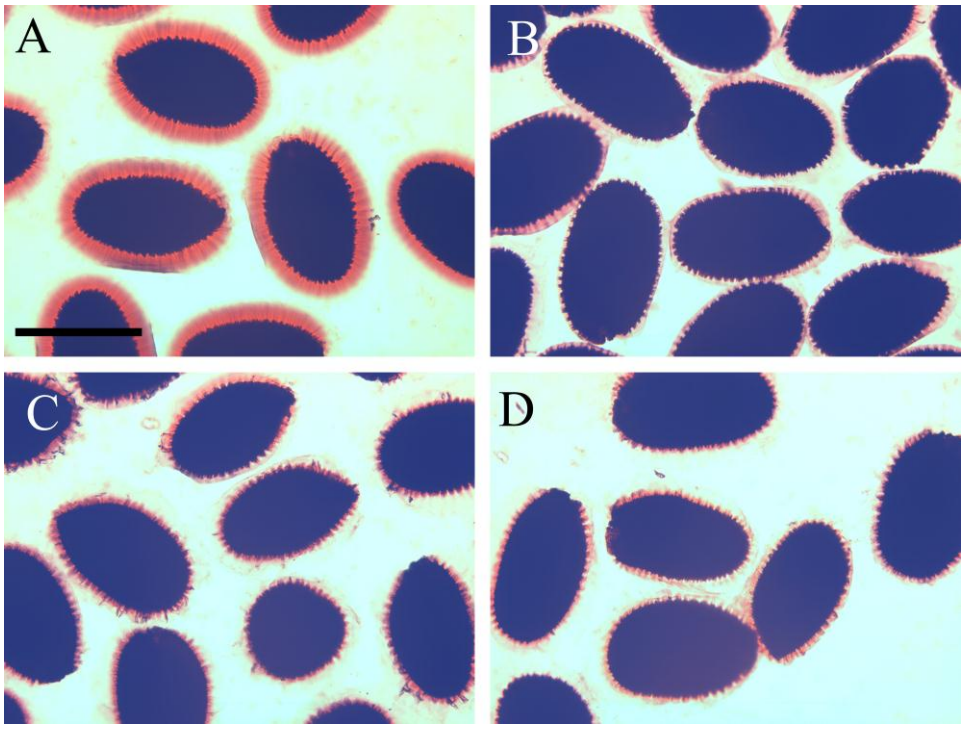

Figure 4.4: Ruthenium Red Staining of *knat7* Seeds Shaken in Water. Col-0 (A), *cesa5-1* (B), *knat7-1* (C), and *knat7-3* (D) were gently shaken for 2 h prior to staining. Note that *knat7* and *cesa5* have smaller mucilage capsules than wild type after mechanical agitation. Scale bar = 500 µm.

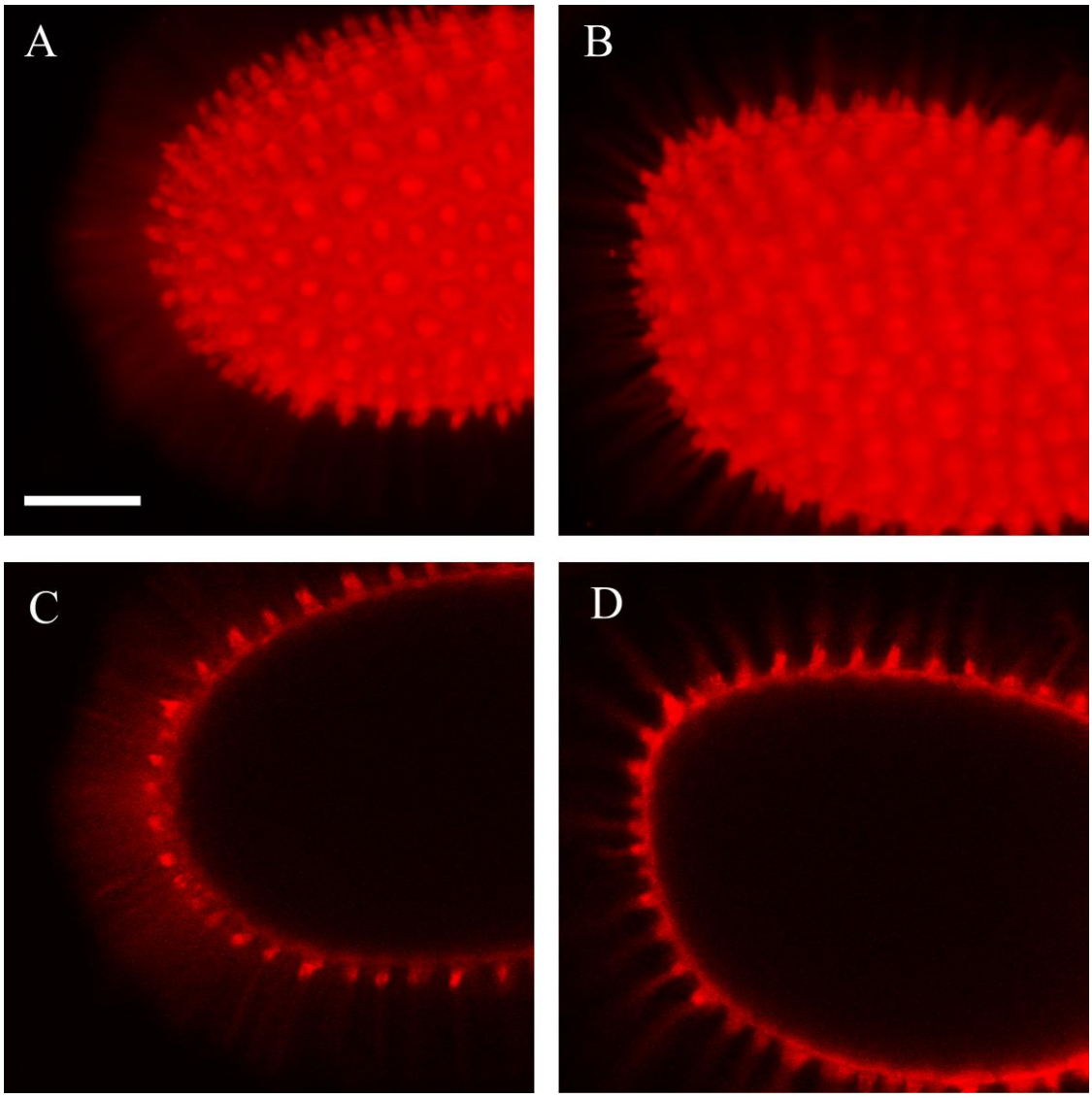

Figure 4.5: S4B Staining of Cellulose in *knat7* Extruded Mucilage.
Col-2 (A) and (C) and *knat7-1* (B) and (D) seeds were shaken in water for 2 h and then stained with S4B. (A) and (B) contain fluorescence from multiple optical sections (rendered using ImageJ, Z-project max intensity method), while (C) and (D) are slices through the middle of seeds. Note the reduction of S4B signal between primary wall fragments in *knat7* mucilage (B) and (D). Scale bar = 100 µm.

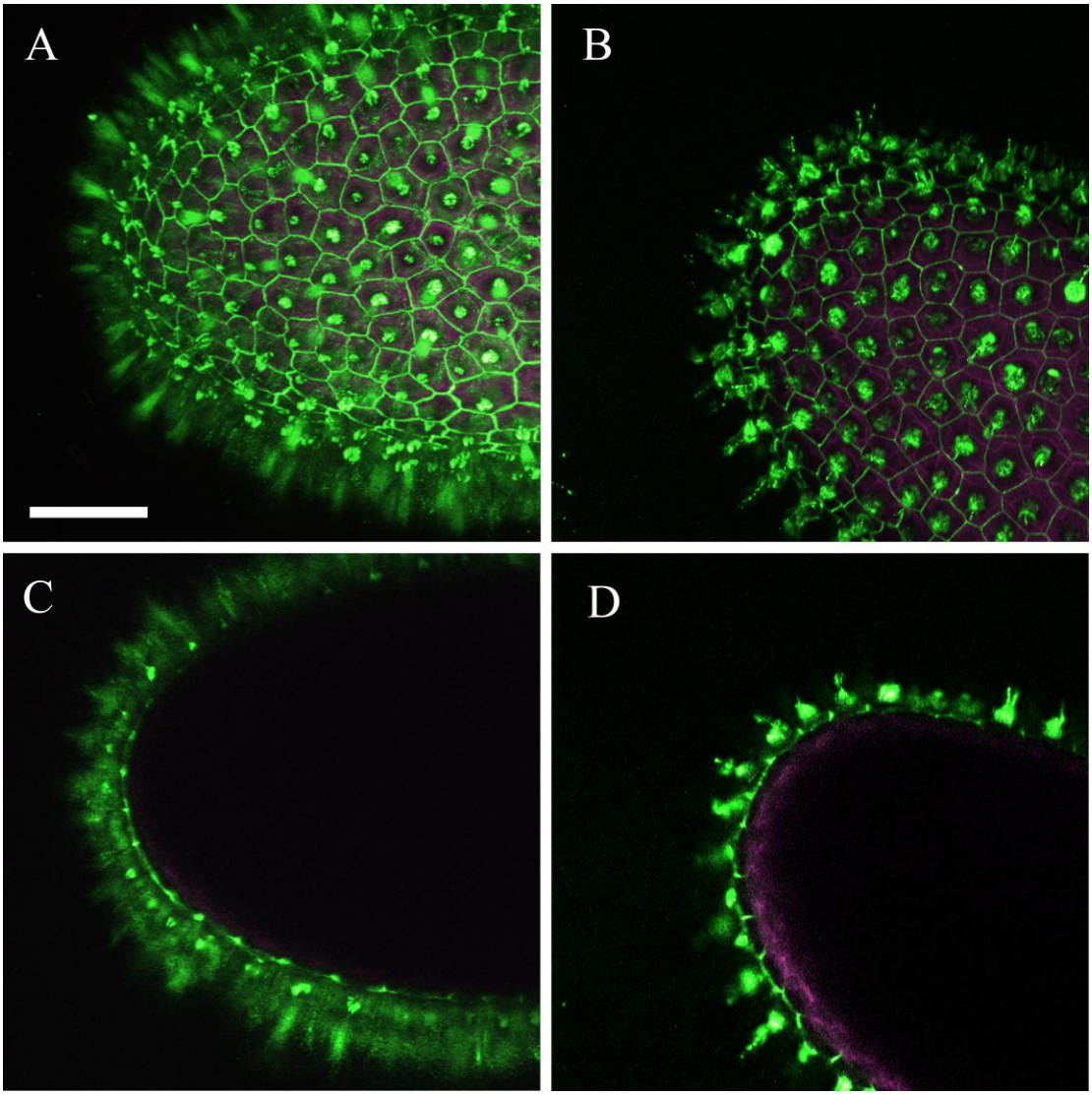

Figure 4.6: JIM5 Immunolabeling of Col-2 and *knat7* Whole Seeds
Col-2 (A) and (C) and *knat7-1* (B) and (D) seeds shaken in water were immunolabeled with JIM5. (A) and (B) contain signals from multiple optical sections (rendered using ImageJ, Z-project max intensity method), while (C) and (D) are slices through the middle of seeds. Note the reduction of JIM5 signal in *knat7* mucilage (B) and (D). Scale bar = 100 µm.

4.5 Discussion

The goal of this chapter was to learn more about the function of *FLY1* through analysis of its homologues and co-expressed genes. FLY1 has a yeast ortholog (TUL1) that displays the same protein structure and also appears to be Golgi-localized (Reggiori and Pelham, 2002). TUL1 was previously shown to act as an E3 ligase that diverts proteins with abnormal transmembrane domains from the Golgi to the vacuole (Reggiori and Pelham, 2002). The function and localization of TUL1 supports the hypothesis proposed in Chapter 3 that FLY1 may be an E3 ligase that processes membrane-bound pectin enzymes in the Golgi. Although protein ubiquitination may have a variety of consequences (Schnell and Hicke, 2003), FLY1 and TUL1 could both be involved in the trafficking of misfolded membrane proteins out of the Golgi. If this scenario were true, pectin methyltransferase (PMT) enzymes with abnormal transmembrane domains may accumulate in the Golgi of *fly1-1* seed coat cells, which could in turn disrupt the methylesterification of galacturonic acids during pectin biosynthesis. Nevertheless, the FLY1 ubiquitin ligase activity, its precise binding partners and the effect of its interactions remain to be determined. To investigate if FLY1 and TUL1 are functionally conserved, future research should include the complementation of the *tul1* mutant phenotype in yeast with a wild type copy of *FLY1* Arabidopsis gene.

Although *FLY2* is the paralog of *FLY1* and is highly co-expressed with many genes that encode enzymes involved in cell wall synthesis and modification, T-DNA insertions in this gene fail to show any major morphological defects. Since *fly2* single mutants do not have seed mucilage defects and *FLY2* appears to have a lower expression in the seed coat compared to *FLY1*, the function of FLY1 proteins may be specialized and distinct from that of FLY2 in this tissue. The homology and expression of the two FLY proteins in xylem cells

suggests that they could play partially redundant roles in secondary wall biosynthesis during xylem development. Analysis of *fly1 fly2* double mutants will likely provide more clues about the role of the FLY1 protein beyond the seed coat, and indicate if *FLY1* and *FLY2* function in the same pathway. In addition, if the two genes are functionally conserved, *FLY2* expressed under the control of *FLY1* promoter should be able to rescue the phenotype of the *fly1-1* mutant.

A T-DNA mutant screen of the top genes co-expressed with *FLY1* in the seed coat identified *KNAT7* as a gene required for the adherence of the inner mucilage layer. KNAT7 is a transcription factor that has been proposed to negatively regulate secondary cell wall formation in the Arabidopsis stem (Li et al., 2011, 2012), but also displays an abnormal seed mucilage phenotype when genetically disrupted (Bhargava, 2010). Since *KNAT7* is highly expressed in xylem and seed coat cells where *FLY1* and *FLY2* transcripts are abundant, KNAT7 could be regulating the expression of these genes. To investigate the likelihood that KNAT7 controls FLY1, I carefully analyzed the mucilage phenotype of *knat7* seeds shaken in water and compared it to that of *fly1* seeds.

The *knat7* seeds release the same amount of mucilage as wild type but display significantly less Ruthenium Red-stained mucilage after mechanical agitation (Bhargava, 2010). This suggests the *knat7* inner mucilage layer is not properly anchored to the seed and represents the opposite phenotype of *fly1* seeds, which have increased mucilage adherence compared to wild type (Chapter 3). The conflicting mucilage phenotypes of *knat7* and *fly1* could be explained if KNAT7 negatively regulates *FLY1* gene expression, which controls mucilage adherence through pectin-pectin interactions. In the *fly1* mutant, pectin has a lower degree of methylesterification, forms more calcium bridges and makes mucilage more

cohesive. If *FLY1* has higher activity in the *knat7* background, mucilage may contain more fully methylesterified pectin and may have a looser structure that detaches easily after mechanical agitation.

In addition, *knat7* seeds have a strikingly similar phenotype to the cellulose-deficient *cesa5* mutant that has decreased attachment of mucilage to the seed epidermis relative to wild type (Mendu et al., 2011; Sullivan et al., 2011). The S4B-staining of mucilage from *knat7* phenocopies *cesa5*, suggesting that mucilage detachment results from a reduction in cellulose. On the other hand, *fly1* and wild type display similar S4B staining of mucilage and the FLY1 protein is not localized at the plasma membrane, where cellulose biosynthesis occurs. Although the transcript levels of *FLY1* and *FLY2* in the *knat7* background still need to be measured, the difference in cellulose staining does not support a role for KNAT7 in the regulation of these genes. The reduced S4B staining in *knat7* mucilage suggests that KNAT7 promotes the expression of *CESA5* and/or other *CESA* genes that are required for mucilage adherence, despite previous evidence that it is a transcriptional repressor (Li et al., 2011, 2012). Additional experiments will be required to test this hypothesis, starting with measuring the levels of *CESA5* transcripts in the *knat7* mutant background. Transcript analysis of other *CESA* genes in the *knat7* seed coat may reveal additional enzymes that are required for cellulose synthesis in mucilage pockets.

Overall, the analysis of homologous and co-expressed genes provided more insight about the biological and biochemical function of the FLY1 protein and indicated that FLY1 and its paralog may play important roles in Arabidopsis xylem development. Nevertheless, additional experiments must be conducted to identify the direct targets of these proteins and to elucidate their biochemical activities. The potential that FLY1 and FLY2 are E3 ligases

involved in the processing or sorting of membrane-bound enzymes in the Golgi makes these proteins attractive candidates for future cell wall research.

Chapter 5: Conclusions

My MSc research employed the Arabidopsis seed coat as a model system to identify new genes involved in the biosynthesis of cell wall polysaccharides, particularly pectin. Pectin and other wall polymers are of significant biological and industrial importance, but their biogenesis is complex and remains poorly understood. The major research objectives of my thesis were:

1. To characterize the seed mucilage phenotype of the *fly1* mutant, to determine the composition of the discs and to discover the underlying cause for these defects.

2. To clone the *FLY1* gene, to confirm its identity, and to analyze its expression, as well as the subcellular localization and the putative functions of the encoded protein.

3. To identify additional genes involved in cell wall biosynthesis, which are related to *FLY1* through sequence homology and/or co-expression.

In Chapter 3, I confirmed that *fly1* discs consist of outer tangential primary cells walls that detach from the columellae upon hydration in water. The detached walls are tightly bound to the *fly1* inner mucilage layer, which appears smaller and is more adherent to the seed than wild type. My results indicate that all *fly1* mucilage defects result from stronger homogalacturonan (HG) crosslinking by Ca^{2+} ions, and suggest that FLY1 promotes pectin methylesterification. FLY1 is a protein with multiple transmembrane spans and a C-terminal RING-H2 finger, which typically facilitates protein binding and frequently appears in E3 ubiquitin ligases. FLY1-YFP fusion proteins localize to small intracellular bodies in seed coat epidermal cells at the stage of mucilage deposition. I hypothesize that FLY1 may interact with pectin methyltransferase enzymes that participate in the biosynthesis of

methylesterified HG in the Golgi. Co-localization of the FLY1-YFP signal with a Golgi marker will be required to confirm the subcellular compartment in which FLY1 proteins reside. Future proteomic analyses of proteins that immunoprecipitate with FLY1 may reveal its direct binding targets and provide more details about its molecular role.

Analysis of genes homologous to *FLY1* in Chapter 4 provided additional clues about the function of the encoded protein. The FLY1 protein is evolutionarily conserved is most eukaryotes with a sequenced genome. Animal cells appear to lack FLY1 homologs, but also do not have polysaccharide-rich cell walls, consistent with FLY1 being involved specifically in cell wall biosynthesis. Interestingly, FLY1 has the same architecture as the yeast TUL1 protein, an E3 ligase that selectively sorts proteins embedded in the Golgi membrane. This suggests that FLY1 may also use ubiquitin molecules to sort or process cell wall biosynthetic enzymes in the Golgi. Experimental evidence to show that FLY1 has the biochemical activity of an E3 ubiquitin ligase is still required. Future studies to investigate if the functions of TUL1 and FLY1 are conserved should include the complementation of *tul1* yeast mutants with a wild type copy of the *FLY1* Arabidopsis gene.

In Chapter 4, I also investigated the function of *FLY2* (the only paralog of *FLY1*) using T-DNA insertional mutants. Despite having some expression in the seed coat, mutations in this gene failed to show any obvious mucilage defects. The results suggest that FLY1 may have a specialized function in pectin biosynthesis in seed coat cells. Due to their sequence homology and very high transcript levels in xylem cells, *FLY1* and *FLY2* may play partially redundant roles in secondary wall biosynthesis in the vasculature. Promoter-swap experiments and the analysis of *fly1 fly2* double mutants will likely provide more clues about

the role of the FLY1 protein beyond the seed coat, and indicate if *FLY1* and *FLY2* function in the same pathway.

The expression profiles of *FLY1* and *FLY2* closely resemble that of *KNAT7*, which encodes a transcription factor involved in secondary cell wall biosynthesis in the xylem and seed coat. Although KNAT7 may regulate the expression of the two *FLY* genes, the reduction of cellulose in *knat7* mucilage suggests that KNAT7 promotes the expression of *CESA5*, a gene involved in the production of cellulose in the mucilage pockets. Future studies should measure the transcript levels of *FLY1*, *FLY2*, *CESA5* and other *CESA* genes in the *knat7* mutant background. This may not only uncover the transcriptional regulatory network of the *FLY* genes, but may also lead to the discovery of novel *CESA* genes involved in mucilage biosynthesis.

Bibliography

Abramoff, M.D., Magalhaes, P.J., and Ram, S.J. (2004). Image Processing with ImageJ. Biophotonics Int. **11**: 36–42.

Alonso, J.M., Stepanova, A.N., Leisse, T.J., Kim, C.J., Chen, H., Shinn, P., Stevenson, D.K., Zimmerman, J., Barajas, P., Cheuk, R., et al. (2003). Genome-Wide Insertional Mutagenesis of Arabidopsis thaliana. Science **301**: 653–657.

Anderson, C.T., Carroll, A., Akhmetova, L., and Somerville, C. (2010). Real-time imaging of cellulose reorientation during cell wall expansion in Arabidopsis roots. Plant Physiol. **152**: 787–796.

Arabidopsis Genome Initiative (2000). Analysis of the genome sequence of the flowering plant Arabidopsis thaliana. Nature **408**: 796–815.

Arsovski, A.A., Haughn, G.W., and Western, T.L. (2010). Seed coat mucilage cells of Arabidopsis thaliana as a model for plant cell wall research. Plant Signal. Behav. **5**: 796–801.

Arsovski, A.A., Popma, T.M., Haughn, G.W., Carpita, N.C., McCann, M.C., and Western, T.L. (2009). AtBXL1 Encodes a Bifunctional β-D-Xylosidase/α-L-Arabinofuranosidase Required for Pectic Arabinan Modification in Arabidopsis Mucilage Secretory Cells. Plant Physiol. **150**: 1219 –1234.

Atmodjo, M.A., Sakuragi, Y., Zhu, X., Burrell, A.J., Mohanty, S.S., Atwood, J.A., Orlando, R., Scheller, H.V., and Mohnen, D. (2011). Galacturonosyltransferase (GAUT)1 and GAUT7 are the core of a plant cell wall pectin biosynthetic homogalacturonan:galacturonosyltransferase complex. Proc. Natl. Acad. Sci. U.S.A. **108**: 20225–20230.

Barberon, M., Zelazny, E., Robert, S., Conéjéro, G., Curie, C., Friml, J., and Vert, G. (2011). Monoubiquitin-dependent endocytosis of the iron-regulated transporter 1 (IRT1) transporter controls iron uptake in plants. Proc. Natl. Acad. Sci. U.S.A. **108**: E450–458.

Bhargava, A. (2010). Functional analysis of the MYB75 transcription factor as a regulator of secondary cell wall formation in Arabidopsis. PhD thesis. University of British Columbia, Vancouver, Canada.

Bouton, S., Leboeuf, E., Mouille, G., Leydecker, M.-T., Talbotec, J., Granier, F., Lahaye, M., Höfte, H., and Truong, H.-N. (2002). QUASIMODO1 encodes a

putative membrane-bound glycosyltransferase required for normal pectin synthesis and cell adhesion in Arabidopsis. Plant Cell **14**: 2577–2590.

Braam, J. (1999). If walls could talk. Curr. Opin. Plant Biol. **2**: 521–524.

Brady, S.M., Orlando, D.A., Lee, J.-Y., Wang, J.Y., Koch, J., Dinneny, J.R., Mace, D., Ohler, U., and Benfey, P.N. (2007). A high-resolution root spatiotemporal map reveals dominant expression patterns. Science **318**: 801–806.

Burton, R.A., Gidley, M.J., and Fincher, G.B. (2010). Heterogeneity in the chemistry, structure and function of plant cell walls. Nat. Chem. Biol. **6**: 724–732.

Caffall, K.H., Pattathil, S., Phillips, S.E., Hahn, M.G., and Mohnen, D. (2009). Arabidopsis thaliana T-DNA Mutants Implicate GAUT Genes in the Biosynthesis of Pectin and Xylan in Cell Walls and Seed Testa. Mol. Plant **2**: 1000 –1014.

Carpita, N.C., and Gibeaut, D.M. (1993). Structural models of primary cell walls in flowering plants: consistency of molecular structure with the physical properties of the walls during growth. Plant J. **3**: 1–30.

Chanliaud, and Gidley (1999). In vitro synthesis and properties of pectin/Acetobacter xylinus cellulose composites. Plant J. **20**: 25–35.

Choo, K.H., Tan, T.W., and Ranganathan, S. (2009). A comprehensive assessment of N-terminal signal peptides prediction methods. BMC Bioinformatics **10**: S2.

Cleland, R. (1971). Cell Wall Extension. Annu. Rev. Plant. Physiol. **22**: 197–222.

Clough, S.J., and Bent, A.F. (1998). Floral dip: a simplified method for Agrobacterium-mediated transformation of Arabidopsis thaliana. Plant J. **16**: 735–743.

Cosgrove, D.J. (2005). Growth of the plant cell wall. Nat. Rev. Mol. Cell Biol. **6**: 850–861.

Dean, G.H., Zheng, H., Tewari, J., Huang, J., Young, D.S., Hwang, Y.T., Western, T.L., Carpita, N.C., McCann, M.C., Mansfield, S.D., et al. (2007). The Arabidopsis MUM2 Gene Encodes a β-Galactosidase Required for the Production of Seed Coat Mucilage with Correct Hydration Properties. Plant Cell **19**: 4007 –4021.

DeBono, A.G. (2012). The role and behavior of Arabidopsis thaliana lipid transfer proteins during cuticular wax deposition. PhD thesis. University of British Columbia, Vancouver, Canada.

Derbyshire, P., McCann, M.C., and Roberts, K. (2007). Restricted cell elongation in Arabidopsis hypocotyls is associated with a reduced average pectin esterification level. BMC Plant Biol. **7**: 31.

Deshaies, R.J., and Joazeiro, C.A.P. (2009). RING domain E3 ubiquitin ligases. Annu. Rev. Biochem. **78**: 399–434.

Dowil, R.T., Lu, X., Saracco, S.A., Vierstra, R.D., and Downes, B.P. (2011). Arabidopsis membrane-anchored ubiquitin-fold (MUB) proteins localize a specific subset of ubiquitin-conjugating (E2) enzymes to the plasma membrane. J. Biol. Chem. **286**: 14913–14921.

Geer, L.Y., Domrachev, M., Lipman, D.J., and Bryant, S.H. (2002). CDART: protein homology by domain architecture. Genome Res. **12**: 1619–1623.

Glickman, M.H., and Ciechanover, A. (2002). The ubiquitin-proteasome proteolytic pathway: destruction for the sake of construction. Physiol. Rev. **82**: 373–428.

Goldberg, R., Morvan, C., Jauneau, A., and Jarvis, M.C. (1996). Methyl-esterification, de-esterification and gelation of pectins in the primary cell wall. In Pectins and Pectinases: Progress in Biotechnology, Vol. 14, J. Visser and A.G.J. Voagen, eds (Amsterdam: Elsevier Science), pp. 151–172.

Goodstein, D.M., Shu, S., Howson, R., Neupane, R., Hayes, R.D., Fazo, J., Mitros, T., Dirks, W., Hellsten, U., Putnam, N., et al. (2012). Phytozome: a comparative platform for green plant genomics. Nucleic Acids Res. **40**: D1178–1186.

Green, P.B. (1980). Organogenesis-A Biophysical View. Annu. Rev. Plant. Physiol. **31**: 51–82.

Griesbeck, O., Baird, G.S., Campbell, R.E., Zacharias, D.A., and Tsien, R.Y. (2001). Reducing the environmental sensitivity of yellow fluorescent protein. Mechanism and applications. J. Biol. Chem. **276**: 29188–29194.

Guerriero, G., Fugelstad, J., and Bulone, V. (2010). What do we really know about cellulose biosynthesis in higher plants? J. Integr. Plant. Biol. **52**: 161–175.

Hamann, T., and Denness, L. (2011). Cell wall integrity maintenance in plants: lessons to be learned from yeast? Plant Signal. Behav. **6**: 1706–1709.

Hamant, O., Traas, J., and Boudaoud, A. (2010). Regulation of shape and patterning in plant development. Curr. Opin. Genet. Dev. **20**: 454–459.

Hanke, D.E., and Northcote, D.H. (1975). Molecular visualization of pectin and DNA by ruthenium red. Biopolymers **14**: 1–17.

Harholt, J., Suttangkakul, A., and Vibe Scheller, H. (2010). Biosynthesis of pectin. Plant Physiol. **153**: 384–395.

Harpaz-Saad, S., McFarlane, H.E., Xu, S., Divi, U.K., Forward, B., Western, T.L., and Kieber, J.J. (2011). Cellulose synthesis via the FEI2 RLK/SOS5 pathway and cellulose synthase 5 is required for the structure of seed coat mucilage in Arabidopsis. Plant J. **68**: 941–953.

Haughn, G., and Chaudhury, A. (2005). Genetic analysis of seed coat development in Arabidopsis. Trends Plant Sci. **10**: 472–477.

Haughn, G.W., and Somerville, C. (1986). Sulfonylurea-resistant mutants of Arabidopsis thaliana. Mol. Gen. Genet. **204**: 430–434.

Hayashi, T., and Kaida, R. (2011). Functions of xyloglucan in plant cells. Mol. Plant **4**: 17–24.

Hématy, K., Cherk, C., and Somerville, S. (2009). Host-pathogen warfare at the plant cell wall. Curr. Opin. Plant Biol. **12**: 406–413.

Heredia, A., Jiménez, A., and Guillén, R. (1995). Composition of plant cell walls. Z. Lebensm. Unters. Forsch. **200**: 24–31.

Hicke, L., and Dunn, R. (2003). Regulation of membrane protein transport by ubiquitin and ubiquitin-binding proteins. Annu. Rev. Cell Dev. Biol. **19**: 141–172.

Hruz, T., Laule, O., Szabo, G., Wessendorp, F., Bleuler, S., Oertle, L., Widmayer, P., Gruissem, W., and Zimmermann, P. (2008). Genevestigator v3: a reference expression database for the meta-analysis of transcriptomes. Adv. Bioinformatics **2008**: 420747.

Huang, J., DeBowles, D., Esfandiari, E., Dean, G., Carpita, N.C., and Haughn, G.W. (2011). The Arabidopsis transcription factor LUH/MUM1 is required for extrusion of seed coat mucilage. Plant Physiol. **156**: 491–502.

Huang, X., and Miller, W. (1991). A time-efficient linear-space local similarity algorithm. Adv. Appl. Math. **12**: 337–357.

Hughes, J., and McCully, M.E. (1975). The use of an optical brightener in the study of plant structure. Stain Technol. **50**: 319–329.

Itoh, K., Hirayama, T., Takahashi, A., Kubo, W., Miyazaki, S., Dairaku, M., Togashi, M., Mikami, R., and Attwood, D. (2007). In situ gelling pectin formulations for oral drug delivery at high gastric pH. Int. J. Pharm. **335**: 90–96.

Jander, G., Norris, S.R., Rounsley, S.D., Bush, D.F., Levin, I.M., and Last, R.L. (2002). Arabidopsis map-based cloning in the post-genome era. Plant Physiol. **129**: 440–450.

Johnson, C.S., Kolevski, B., and Smyth, D.R. (2002). TRANSPARENT TESTA GLABRA2, a Trichome and Seed Coat Development Gene of Arabidopsis, Encodes a WRKY Transcription Factor. Plant Cell **14**: 1359 –1375.

Jolie, R.P., Duvetter, T., Van Loey, A.M., and Hendrickx, M.E. (2010). Pectin methylesterase and its proteinaceous inhibitor: a review. Carbohydr. Res. **345**: 2583–2595.

Joshi, C.P., and Mansfield, S.D. (2007). The cellulose paradox--simple molecule, complex biosynthesis. Curr. Opin. Plant Biol. **10**: 220–226.

Juge, N. (2006). Plant protein inhibitors of cell wall degrading enzymes. Trends Plant Sci. **11**: 359–367.

Kasajima, I., Ide, Y., Ohkama-Ohtsu, N., Hayashi, H., Yoneyama, T., and Fujiwara, T. (2004). A protocol for rapid DNA extraction from Arabidopsis thaliana for PCR analysis. Plant Mol. Biol. Rep. **22**: 49–52.

Keller, B. (1993). Structural Cell Wall Proteins. Plant Physiol. **101**: 1127–1130.

Knox, J.P. (2008). Revealing the structural and functional diversity of plant cell walls. Curr. Opin. Plant Biol. **11**: 308–313.

Knox, J.P. (1997). The use of antibodies to study the architecture and developmental regulation of plant cell walls. Int. Rev. Cytol. **171**: 79–120.

Knox, J.P., Linstead, P.J., King, J., Cooper, C., and Roberts, K. (1990). Pectin esterification is spatially regulated both within cell walls and between developing tissues of root apices. Planta **181**: 512–521.

Kosarev, P., Mayer, K.F.X., and Hardtke, C.S. (2002). Evaluation and classification of RING-finger domains encoded by the Arabidopsis genome. Genome Biol. **3**: research0016.1–research0016.12.

Krogh, A., Larsson, B., von Heijne, G., and Sonnhammer, E.L. (2001). Predicting transmembrane protein topology with a hidden Markov model: application to complete genomes. J. Mol. Biol. **305**: 567–580.

Krupková, E., Immerzeel, P., Pauly, M., and Schmülling, T. (2007). The TUMOROUS SHOOT DEVELOPMENT2 gene of Arabidopsis encoding a putative methyltransferase is required for cell adhesion and co-ordinated plant development. Plant J. **50**: 735–750.

Kurek, I., Kawagoe, Y., Jacob-Wilk, D., Doblin, M., and Delmer, D. (2002). Dimerization of cotton fiber cellulose synthase catalytic subunits occurs via oxidation of the zinc-binding domains. Proc. Natl. Acad. Sci. U.S.A. **99**: 11109–11114.

Lamesch, P., Berardini, T.Z., Li, D., Swarbreck, D., Wilks, C., Sasidharan, R., Muller, R., Dreher, K., Alexander, D.L., Garcia-Hernandez, M., et al. (2011). The Arabidopsis Information Resource (TAIR): improved gene annotation and new tools. Nucl. Acids Res. **40**: D1202-D1210.

Lashbrook, C.C., and Cai, S. (2008). Cell wall remodeling in Arabidopsis stamen abscission zones. Plant Signal. Behav. **3**: 733–736.

Le, B.H., Cheng, C., Bui, A.Q., Wagmaister, J.A., Henry, K.F., Pelletier, J., Kwong, L., Belmonte, M., Kirkbride, R., Horvath, S., et al. (2010). Global analysis of gene activity during Arabidopsis seed development and identification of seed-specific transcription factors. Proc. Natl. Acad. Sci. U.S.A. **107**: 8063–8070.

Lee, I., Ambaru, B., Thakkar, P., Marcotte, E.M., and Rhee, S.Y. (2010). Rational association of genes with traits using a genome-scale gene network for Arabidopsis thaliana. Nat. Biotechnol. **28**: 149–156.

Leon-Kloosterziel, K.M., Keijzer, C.J., and Koornneef, M. (1994). A Seed Shape Mutant of Arabidopsis That Is Affected in Integument Development. Plant Cell **6**: 385–392.

Lerouxel, O., Cavalier, D.M., Liepman, A.H., and Keegstra, K. (2006). Biosynthesis of plant cell wall polysaccharides -- a complex process. Curr. Opin. Plant Biol. **9**: 621–630.

Li, E., Bhargava, A., Qiang, W., Friedmann, M.C., Forneris, N., Savidge, R.A., Johnson, L.A., Mansfield, S.D., Ellis, B.E., and Douglas, C.J. (2012). The Class II KNOX gene KNAT7 negatively regulates secondary wall formation in Arabidopsis and is functionally conserved in Populus. New Phytol. **194**: 102–115.

Li, E., Wang, S., Liu, Y., Chen, J., and Douglas, C.J. (2011). OVATE FAMILY PROTEIN4 (OFP4) interaction with KNAT7 regulates secondary cell wall formation in Arabidopsis thaliana. Plant J. **67**: 328–341.

Liepman, A.H., Wightman, R., Geshi, N., Turner, S.R., and Scheller, H.V. (2010). Arabidopsis - a powerful model system for plant cell wall research. Plant J. **61**: 1107–1121.

Liners, F., Letesson, J.J., Didembourg, C., and Van Cutsem, P. (1989). Monoclonal Antibodies against Pectin: Recognition of a Conformation Induced by Calcium. Plant Physiol. **91**: 1419–1424.

Liu, L., Fishman, M.L., Kost, J., and Hicks, K.B. (2003). Pectin-based systems for colon-specific drug delivery via oral route. Biomaterials **24**: 3333–3343.

Lord, E.M., and Mollet, J.-C. (2002). Plant cell adhesion: A bioassay facilitates discovery of the first pectin biosynthetic gene. Proc. Natl. Acad. Sci. U.S.A. **99**: 15843–15845.

Macquet, A., Ralet, M.-C., Kronenberger, J., Marion-Poll, A., and North, H.M. (2007a). In situ, chemical and macromolecular study of the composition of Arabidopsis thaliana seed coat mucilage. Plant Cell Physiol. **48**: 984–999.

Macquet, A., Ralet, M.-C., Loudet, O., Kronenberger, J., Mouille, G., Marion-Poll, A., and North, H.M. (2007b). A naturally occurring mutation in an Arabidopsis accession affects a beta-D-galactosidase that increases the hydrophilic potential of rhamnogalacturonan I in seed mucilage. Plant Cell **19**: 3990–4006.

Marchler-Bauer, A., Lu, S., Anderson, J.B., Chitsaz, F., Derbyshire, M.K., DeWeese-Scott, C., Fong, J.H., Geer, L.Y., Geer, R.C., Gonzales, N.R., et al. (2011). CDD: a Conserved Domain Database for the functional annotation of proteins. Nucleic Acids Res. **39**: D225–229.

McFarlane, H.E., Young, R.E., Wasteneys, G.O., and Samuels, A.L. (2008). Cortical microtubules mark the mucilage secretion domain of the plasma membrane in Arabidopsis seed coat cells. Planta **227**: 1363–1375.

Mendu, V., Griffiths, J., Persson, S., Stork, J., Downie, B., Voiniciuc, C., Haughn, G., and DeBolt, S. (2011). Subfunctionalization of cellulose synthases in seed coat epidermal cells mediate secondary radial wall synthesis and mucilage attachment. Plant Physiol. **157**: 441-453.

Micheli, F. (2001). Pectin methylesterases: cell wall enzymes with important roles in plant physiology. Trends Plant Sci. **6**: 414–419.

Mohnen, D. (2008). Pectin structure and biosynthesis. Curr. Opin. Plant Biol. **11**: 266–277.

Mohnen, D., and Hahn, M.G. (1993). Cell wall carbohydrates as signals in plants. Semin. Cell Biol. **4**: 93–102.

Moustacas, A.M., Nari, J., Borel, M., Noat, G., and Ricard, J. (1991). Pectin methylesterase, metal ions and plant cell-wall extension. The role of metal ions in plant cell-wall extension. Biochem. J. **279 (Pt 2)**: 351–354.

Mutwil, M., Debolt, S., and Persson, S. (2008). Cellulose synthesis: a complex complex. Curr. Opin. Plant Biol. **11**: 252–257.

Obayashi, T., and Kinoshita, K. (2010). Coexpression landscape in ATTED-II: usage of gene list and gene network for various types of pathways. J. Plant Res. **123**: 311–319.

Obayashi, T., Nishida, K., Kasahara, K., and Kinoshita, K. (2011). ATTED-II updates: condition-specific gene coexpression to extend coexpression analyses and applications to a broad range of flowering plants. Plant Cell Physiol. **52**: 213–219.

Ogawa, M., Kay, P., Wilson, S., and Swain, S.M. (2009). ARABIDOPSIS DEHISCENCE ZONE POLYGALACTURONASE1 (ADPG1), ADPG2, and QUARTET2 are Polygalacturonases required for cell separation during reproductive development in Arabidopsis. Plant Cell **21**: 216–233.

Oka, T., Nemoto, T., and Jigami, Y. (2007). Functional analysis of Arabidopsis thaliana RHM2/MUM4, a multidomain protein involved in UDP-D-glucose to UDP-L-rhamnose conversion. J. Biol. Chem. **282**: 5389–5403.

Ostlund, G., Schmitt, T., Forslund, K., Köstler, T., Messina, D.N., Roopra, S., Frings, O., and Sonnhammer, E.L.L. (2010). InParanoid 7: new algorithms and tools for eukaryotic orthology analysis. Nucleic Acids Res. **38**: D196–203.

Parker, A.J., Haskins, E.F., and Deyrup-Olsen, I. (1982). Toluidine Blue: A Simple, Effective Stain for Plant Tissues. Am. Biol. Teach. **44**: 487–489.

Pattathil, S., Avci, U., Baldwin, D., Swennes, A.G., McGill, J.A., Popper, Z., Bootten, T., Albert, A., Davis, R.H., Chennareddy, C., et al. (2010). A Comprehensive Toolkit of Plant Cell Wall Glycan-Directed Monoclonal Antibodies. Plant Physiol. **153**: 514-525.

Pelletier, S., Van Orden, J., Wolf, S., Vissenberg, K., Delacourt, J., Ndong, Y.A., Pelloux, J., Bischoff, V., Urbain, A., Mouille, G., et al. (2010). A role for pectin de-

methylesterification in a developmentally regulated growth acceleration in dark-grown Arabidopsis hypocotyls. New Phytol. **188**: 726–739.

Pelloux, J., Rustérucci, C., and Mellerowicz, E.J. (2007). New insights into pectin methylesterase structure and function. Trends Plant Sci. **12**: 267–277.

Penfield, S., Meissner, R.C., Shoue, D.A., Carpita, N.C., and Bevan, M.W. (2001). MYB61 Is Required for Mucilage Deposition and Extrusion in the Arabidopsis Seed Coat. Plant Cell **13**: 2777–2791.

Petersen, T.N., Brunak, S., Heijne, G. von, and Nielsen, H. (2011). SignalP 4.0: discriminating signal peptides from transmembrane regions. Nat. Methods **8**: 785–786.

Popper, Z.A. (2008). Evolution and diversity of green plant cell walls. Curr. Opin. Plant Biol. **11**: 286–292.

Prasanna, V., Prabha, T.N., and Tharanathan, R.N. (2007). Fruit ripening phenomena--an overview. Crit. Rev. Food Sci. Nutr. **47**: 1–19.

Quevillon, E., Silventoinen, V., Pillai, S., Harte, N., Mulder, N., Apweiler, R., and Lopez, R. (2005). InterProScan: protein domains identifier. Nucleic Acids Res. **33**: W116–W120.

Rautengarten, C., Usadel, B., Neumetzler, L., Hartmann, J., Büssis, D., and Altmann, T. (2008). A subtilisin-like serine protease essential for mucilage release from Arabidopsis seed coats. Plant J. **54**: 466–480.

Reggiori, F., and Pelham, H.R.B. (2002). A transmembrane ubiquitin ligase required to sort membrane proteins into multivesicular bodies. Nat. Cell Biol. **4**: 117–123.

Reiter, W.D. (2002). Biosynthesis and properties of the plant cell wall. Curr. Opin. Plant Biol. **5**: 536–542.

Rensing, K.H., Samuels, A.L., and Savidge, R.A. (2002). Ultrastructure of vascular cambial cell cytokinesis in pine seedlings preserved by cryofixation and substitution. Protoplasma **220**: 39–49.

Ringli, C., Keller, B., and Ryser, U. (2001). Glycine-rich proteins as structural components of plant cell walls. Cell. Mol. Life Sci. **58**: 1430–1441.

Saint-Jore-Dupas, C., Gomord, V., and Paris, N. (2004). Protein localization in the plant Golgi apparatus and the trans-Golgi network. Cell. Mol. Life Sci. **61**: 159–171.

Sampedro, J., and Cosgrove, D.J. (2005). The expansin superfamily. Genome Biol. **6**: 242.

Sande, S.A. (2005). Pectin-based oral drug delivery to the colon. Expert Opin. Drug Deliv. **2**: 441–450.

Saxena, I.M., and Brown, R.M., Jr (2005). Cellulose biosynthesis: current views and evolving concepts. Ann. Bot. **96**: 9–21.

Scheible, W.-R., and Pauly, M. (2004). Glycosyltransferases and cell wall biosynthesis: novel players and insights. Curr. Opin. Plant Biol. **7**: 285–295.

Schmid, M., Davison, T.S., Henz, S.R., Pape, U.J., Demar, M., Vingron, M., Sch|[ouml]|lkopf, B., Weigel, D., and Lohmann, J.U. (2005). A gene expression map of Arabidopsis thaliana development. Nat. Genet. **37**: 501–506.

Schnell, J.D., and Hicke, L. (2003). Non-Traditional Functions of Ubiquitin and Ubiquitin-Binding Proteins. J. Biol. Chem. **278**: 35857–35860.

Schwacke, R., Schneider, A., van der Graaff, E., Fischer, K., Catoni, E., Desimone, M., Frommer, W.B., Flügge, U.-I., and Kunze, R. (2003). ARAMEMNON, a novel database for Arabidopsis integral membrane proteins. Plant Physiol. **131**: 16–26.

Seifert, G.J., and Roberts, K. (2007). The biology of arabinogalactan proteins. Annu. Rev. Plant Biol. **58**: 137–161.

Sessions, A., Burke, E., Presting, G., Aux, G., McElver, J., Patton, D., Dietrich, B., Ho, P., Bacwaden, J., Ko, C., et al. (2002). A High-Throughput Arabidopsis Reverse Genetics System. Plant Cell **14**: 2985–2994.

Showalter, A.M. (1993). Structure and function of plant cell wall proteins. Plant Cell **5**: 9–23.

Sigrist, C.J.A., Cerutti, L., de Castro, E., Langendijk-Genevaux, P.S., Bulliard, V., Bairoch, A., and Hulo, N. (2010). PROSITE, a protein domain database for functional characterization and annotation. Nucleic Acids Res. **38**: D161–166.

Somerville, C. (2006). Cellulose Synthesis in Higher Plants. Annu. Rev. Cell Dev. Biol. **22**: 53–78.

Somerville, C., Bauer, S., Brininstool, G., Facette, M., Hamann, T., Milne, J., Osborne, E., Paredez, A., Persson, S., Raab, T., et al. (2004). Toward a systems approach to understanding plant cell walls. Science **306**: 2206–2211.

Sorensen, A.E. (1986). Seed Dispersal by Adhesion. Annu. Rev. Ecol. Evol. Syst. **17**: 443–463.

Spurr, A.R. (1969). A low-viscosity epoxy resin embedding medium for electron microscopy. J. Ultrastruct. Res. **26**: 31–43.

Sriamornsak, P. (2011). Application of pectin in oral drug delivery. Expert Opin. Drug Deliv. **8**: 1009–1023.

Steele, N.M., McCann, M.C., and Roberts, K. (1997). Pectin Modification in Cell Walls of Ripening Tomatoes Occurs in Distinct Domains. Plant Physiol. **114**: 373–381.

Sterling, J.D., Atmodjo, M.A., Inwood, S.E., Kumar Kolli, V.S., Quigley, H.F., Hahn, M.G., and Mohnen, D. (2006). Functional identification of an Arabidopsis pectin biosynthetic homogalacturonan galacturonosyltransferase. Proc. Natl. Acad. Sci. U.S.A. **103**: 5236–5241.

Stone, S.L., Hauksdóttir, H., Troy, A., Herschleb, J., Kraft, E., and Callis, J. (2005). Functional analysis of the RING-type ubiquitin ligase family of Arabidopsis. Plant Physiol. **137**: 13–30.

Stork, J., Harris, D., Griffiths, J., Williams, B., Beisson, F., Li-Beisson, Y., Mendu, V., Haughn, G., and DeBolt, S. (2010). CELLULOSE SYNTHASE9 Serves a Nonredundant Role in Secondary Cell Wall Synthesis in Arabidopsis Epidermal Testa Cells. Plant Physiol. **153**: 580 –589.

Sullivan, S., Ralet, M.-C., Berger, A., Diatloff, E., Bischoff, V., Gonneau, M., Marion-Poll, A., and North, H.M. (2011). CESA5 is required for the synthesis of cellulose with a role in structuring the adherent mucilage of Arabidopsis seeds. Plant Physiol. **156**: 1725–1739.

Swarbreck, D., Wilks, C., Lamesch, P., Berardini, T.Z., Garcia-Hernandez, M., Foerster, H., Li, D., Meyer, T., Muller, R., Ploetz, L., et al. (2007). The Arabidopsis Information Resource (TAIR): gene structure and function annotation. Nucleic Acids Res. **36**: D1009–D1014.

Szymanski, D.B., and Cosgrove, D.J. (2009). Dynamic coordination of cytoskeletal and cell wall systems during plant cell morphogenesis. Curr. Biol. **19**: R800–811.

Tang, H., Bowers, J.E., Wang, X., Ming, R., Alam, M., and Paterson, A.H. (2008). Synteny and collinearity in plant genomes. Science **320**: 486–488.

Taylor, N.G. (2008). Cellulose biosynthesis and deposition in higher plants. New Phytol. **178**: 239–252.

Thakur, B.R., Singh, R.K., and Handa, A.K. (1997). Chemistry and uses of pectin--a review. Crit. Rev. Food Sci. Nutr. **37**: 47–73.

Thierry-Mieg, D., and Thierry-Mieg, J. (2006). AceView: a comprehensive cDNA-supported gene and transcripts annotation. Genome Biol. **7**: S12.

Tsukamoto, T., Qin, Y., Huang, Y., Dunatunga, D., and Palanivelu, R. (2010). A role for LORELEI, a putative glycosylphosphatidylinositol-anchored protein, in Arabidopsis thaliana double fertilization and early seed development. Plant J. **62**: 571–588.

Turner, S.R., and Somerville, C.R. (1997). Collapsed xylem phenotype of Arabidopsis identifies mutants deficient in cellulose deposition in the secondary cell wall. Plant Cell **9**: 689–701.

Usadel, B., Kuschinsky, A.M., Rosso, M.G., Eckermann, N., and Pauly, M. (2004a). RHM2 is involved in mucilage pectin synthesis and is required for the development of the seed coat in Arabidopsis. Plant Physiol. **134**: 286–295.

Usadel, B., Schlüter, U., Mølhøj, M., Gipmans, M., Verma, R., Kossmann, J., Reiter, W.-D., and Pauly, M. (2004b). Identification and characterization of a UDP-D-glucuronate 4-epimerase in Arabidopsis. FEBS Lett. **569**: 327–331.

Van Bel, M., Proost, S., Wischnitzki, E., Movahedi, S., Scheerlinck, C., Van de Peer, Y., and Vandepoele, K. (2012). Dissecting plant genomes with the PLAZA comparative genomics platform. Plant Physiol. **158**: 590–600.

VandenBosch, K.A., Bradley, D.J., Knox, J.P., Perotto, S., Butcher, G.W., and Brewin, N.J. (1989). Common components of the infection thread matrix and the intercellular space identified by immunocytochemical analysis of pea nodules and uninfected roots. EMBO J. **8**: 335–341.

Verollet, R. (2008). A major step towards efficient sample preparation with bead-beating. Biotechniques **44**: 832–833.

Volkmann, D., and Baluska, F. (2006). Gravity: one of the driving forces for evolution. Protoplasma **229**: 143–148.

Warde-Farley, D., Donaldson, S.L., Comes, O., Zuberi, K., Badrawi, R., Chao, P., Franz, M., Grouios, C., Kazi, F., Lopes, C.T., et al. (2010). The GeneMANIA

prediction server: biological network integration for gene prioritization and predicting gene function. Nucleic Acids Res. **38**: W214–220.

Western, T.L., Burn, J., Tan, W.L., Skinner, D.J., Martin-McCaffrey, L., Moffatt, B.A., and Haughn, G.W. (2001). Isolation and Characterization of Mutants Defective in Seed Coat Mucilage Secretory Cell Development in Arabidopsis. Plant Physiol. **127**: 998–1011.

Western, T.L., Skinner, D.J., and Haughn, G.W. (2000). Differentiation of Mucilage Secretory Cells of the Arabidopsis Seed Coat. Plant Physiol. **122**: 345–356.

Western, T.L., Young, D.S., Dean, G.H., Tan, W.L., Samuels, A.L., and Haughn, G.W. (2004). MUCILAGE-MODIFIED4 Encodes a Putative Pectin Biosynthetic Enzyme Developmentally Regulated by APETALA2, TRANSPARENT TESTA GLABRA1, and GLABRA2 in the Arabidopsis Seed Coat. Plant Physiol. **134**: 296 –306.

Willats, W.G., McCartney, L., Mackie, W., and Knox, J.P. (2001a). Pectin: cell biology and prospects for functional analysis. Plant Mol. Biol **47**: 9–27.

Willats, W.G.T., McCartney, L., and Knox, J.P. (2001b). In-situ analysis of pectic polysaccharides in seed mucilage and at the root surface of Arabidopsis thaliana. Planta **213**: 37–44.

Willats, W.G.T., Orfila, C., Limberg, G., Buchholt, H.C., van Alebeek, G.-J.W.M., Voragen, A.G.J., Marcus, S.E., Christensen, T.M.I.E., Mikkelsen, J.D., Murray, B.S., et al. (2001c). Modulation of the Degree and Pattern of Methyl-esterification of Pectic Homogalacturonan in Plant Cell Walls. J. Biol. Chem. **276**: 19404 –19413.

Winter, D., Vinegar, B., Nahal, H., Ammar, R., Wilson, G.V., and Provart, N.J. (2007). An "Electronic Fluorescent Pictograph" Browser for Exploring and Analyzing Large-Scale Biological Data Sets. PLoS ONE **2**: e718.

Wojtaszek, P. (2001). Organismal view of a plant and a plant cell. Acta Biochim. Pol. **48**: 443–451.

Wolf, S., Hématy, K., and Höfte, H. (2011). Growth Control and Cell Wall Signaling in Plants. Annual Review of Plant Biology. PMID: 22224451.

Wolf, S., Mouille, G., and Pelloux, J. (2009). Homogalacturonan Methyl-Esterification and Plant Development. Mol. Plant **2**: 851–860.

Woody, S.T., Austin-Phillips, S., Amasino, R.M., and Krysan, P.J. (2007). The WiscDsLox T-DNA collection: an arabidopsis community resource generated by

using an improved high-throughput T-DNA sequencing pipeline. J. Plant Res. **120**: 157–165.

Xu, C., Zhao, L., Pan, X., and Šamaj, J. (2011). Developmental Localization and Methylesterification of Pectin Epitopes during Somatic Embryogenesis of Banana (Musa spp. AAA). PLoS ONE **6**: e22992.

York, W.S., Darvill, A.G., McNeil, M., Stevenson, T.T., and Albersheim, P. (1986). Isolation and characterization of plant cell walls and cell wall components. Plant Mol. Biol. **118**: 3–40.

Young, J.A., and Evans, R.A. (1973). Mucilaginous Seed Coats. Weed Sci. **21**: 52–54.

Young, R.E., McFarlane, H.E., Hahn, M.G., Western, T.L., Haughn, G.W., and Samuels, A.L. (2008). Analysis of the Golgi Apparatus in Arabidopsis Seed Coat Cells during Polarized Secretion of Pectin-Rich Mucilage. Plant Cell **20**: 1623–1638.

Zandleven, J., Sørensen, S.O., Harholt, J., Beldman, G., Schols, H.A., Scheller, H.V., and Voragen, A.J. (2007). Xylogalacturonan exists in cell walls from various tissues of Arabidopsis thaliana. Phytochemistry **68**: 1219–1226.

Zimmermann, P., Hirsch-Hoffmann, M., Hennig, L., and Gruissem, W. (2004). GENEVESTIGATOR. Arabidopsis Microarray Database and Analysis Toolbox. Plant Physiol. **136**: 2621 –2632.

Appendices

Appendix A : List of Arabidopsis T-DNA Lines Used for *FLY1* Positional Cloning

Gene	Polymorphism	Location	Gene Annotation
At4g28070	GK-957G01	exon	AFG1-like ATPase family protein
At4g28080	SALK_131234	exon	Tetratricopeptide repeat (TPR)-like
At4g28080	SALK_020337C	intron	Tetratricopeptide repeat (TPR)-like
At4g28085	SALK_065775	5' UTR	unknown
At4g28085	SALK_046516C	promoter	unknown
At4g28088	none available		salt responsive protein family
At4g28090	SALK_080944	exon	SKU5 similar 10 (SKS10)
At4g28100	SALK_022056C	1st exon	unknown
At4g28100	SALK_022926	1st exon	unknown
At4g28100	SALK_022930	1st exon	unknown
At4g28110	SALK_014739C	exon	MYB41
At4g28110	SALK_142422	promoter	MYB41
At4g28130	SALK_054320	1st exon	diacylglycerol kinase 6 (DGK6)
At4g28130	SALK_016285C	7th exon	diacylglycerol kinase 6 (DGK6)
At4g28140	SAIL_73_C12	exon	DREB subfamily A-6 TF
At4g28140	SAIL_73_C12	exon	DREB subfamily A-6 TF
At4g28140	SAIL_512_B08	exon	DREB subfamily A-6 TF
At4g28150	SALK_087120C	4th exon	unknown
At4g28150	SALK_106384C	5' UTR	unknown
At4g28160	SALK_016246C	5' UTR	HPRG family protein

Gene	Polymorphism	Location	Gene Annotation
At4g28160	SALK_020715C	5' UTR	HPRG family protein
At4g28170	SALK_150390	first exon	unknown
At4g28170	SALK_021906	3' UTR	unknown
At4g28180	SALK_022090	exon	N-terminal protein myristoylation
At4g28180	SALK_021906	3' UTR	N-terminal protein myristoylation
At4g28181	SAIL_874_E05	exon	unknown
At4g28190	SALK_074642C	first exon	ULTRAPETALA1 (ULT1)
At4g28190	SALK_003061	5' UTR	ULTRAPETALA1 (ULT1)
At4g28200	SALK_035072	3' UTR	involved in RNA processing
At4g28200	SALK_122771C	5' UTR	involved in RNA processing
At4g28200	SALK_108952C	5' UTR	involved in RNA processing
At4g28210	SALK_122771C	exon	embryo defective 1923 (emb1923)
At4g28210	SALK_108952C	exon	embryo defective 1923 (emb1923)
At4g28210	GK-065A09	exon	embryo defective 1923 (emb1923)
At4g28220	SALK_087720C	5' UTR	NAD(P)H dehydrogenase B1
At4g28220	GK-297C02	6th exon	NAD(P)H dehydrogenase B1
At4g28220	GK-764B10	5th exon	NAD(P)H dehydrogenase B1
At4g28230	SALK_030161	exon	unknown
At4g28230	SALK_097811C	5' UTR	unknown
At4g28240	SALK_068672C	5' UTR	wound-responsive protein-related
At4g28240	SAIL_520_B05	exon	wound-responsive protein-related
At4g28250	GK-494A04	3rd exon	β-expansin/allergen protein

Gene	Polymorphism	Location	Gene Annotation
At4g28250	SALK_124760	5' UTR	β-expansin/allergen protein
At4g28260	SALK_036374C	promoter	unknown
At4g28260	SALK_080639C	promoter	unknown
At4g28270	SALK_136700	exon	RING finger E3 ubiquitin ligase
At4g28280	none available		LLG2
At4g28290	GK-054E08	5' UTR	unknown
At4g28290	SALK_086732	5' UTR	unknown
At4g28300	SALK_048257C	3rd exon	putative cel wall protein
At4g28300	GK-108A02	3rd exon	putative cel wall protein
At4g28300	SALK_080244C	promoter	putative cel wall protein
At4g28300	SAIL_711_D11	exon	putative cel wall protein
At4g28310	SALK_068367C	exon	unknown
At4g28310	SALK_151600C	5' UTR	unknown
At4g28320	SALK_059047C	4th intron	endo-β-mannanase 5 (MAN5)
At4g28320	SALK_015220C	5' UTR	endo-β-mannanase 5 (MAN5)
At4g28320	SALK_068367C	5' UTR	endo-β-mannanase 5 (MAN5)
At4g28330	SALK_058771C	5' UTR	unknown
At4g28330	SALK_106684	5' UTR	unknown
At4g28330	GK-752D02	exon	unknown
At4g28340	SALK_033839C	5' UTR	unknown
At4g28340	SALK_082582C	5' UTR	unknown
At4g28340	SALK_147260	exon	unknown

Gene	Polymorphism	Location	Gene Annotation
At4g28350	GK-523C11	5' UTR	lectin protein kinase family
At4g28350	SALK_141841C	5' UTR	lectin protein kinase family
At4g28360	SALK_012199	exon	ribosomal protein L22 family
At4g28362	SALK_069743	5' UTR	pre-tRNA; tRNA-Lys
At4g28365	GK-956B01	5' UTR	early nodulin-like protein 3
At4g28365	SALK_069743	5' UTR	early nodulin-like protein 3
At4g28370	SALK_067290	13th exon	protein binding /zinc ion binding
At4g28370	SALK_144822	6th exon	protein binding /zinc ion binding
At4g28370	SALK_139154	10th exon	protein binding /zinc ion binding
At4g28380	SALK_053581	promoter	Leucine-rich repeat (LRR) protein
At4g28390	SALK_053581	3rd exon	ADP/ATP CARRIER 3 (AAC3)
At4g28390	WiscDsLox387B07	3rd exon	ADP/ATP CARRIER 3 (AAC3)
At4g28395	GK-288A12	2nd exon	related to lipid transfer proteins
At4g28395	SALK_094117	5' UTR	related to lipid transfer proteins
At4g28397	GK-322G03	exon	related to ATA7, lipid transporter
At4g28400	SALK_127487C	5' UTR	protein phosphatase 2C (PP2C)
At4g28400	SALK_070725C	5th exon	protein phosphatase 2C (PP2C)
At4g28405	GK-033G01	5' UTR	unknown
At4g28405	SALK_018252	exon	unknown
At4g28410	SALK_011695C	4th exon	aminotransferase-related
At4g28420	SALK_056023	5' UTR	aminotransferase, putative
At4g28430	SAIL_178_G04	4th exon	reticulon family protein

Gene	Polymorphism	Location	Gene Annotation
At4g28430	SALK_083406C	intron	reticulon family protein
At4g28440	SALK_073625	intron	DNA-binding protein-related
At4g28440	SALK_091487	2nd exon	DNA-binding protein-related
At4g28450	SALK_036856	13th exon	protein with a DWD motif
At4g28460	SALK_119896	promoter	unknown
At4g28470	SALK_064700C	17th exon	RPN subunit of 26S proteasome
At4g28470	SALK_115981	4th exon	RPN subunit of 26S proteasome
At4g28480	SAIL_232_G06	first exon	DNAJ heat shock family protein
At4g28480	WiscDsLox477-480J10	first exon	DNAJ heat shock family protein
At4g28485	SALK_039261C	3rd exon	unknown
At4g28490	SALK_105975C	1st exon	Receptor kinase-like protein
At4g28490	GK-148C12	1st exon	Receptor kinase-like protein
At4g28500	SM_3_31925	3rd exon	NAC domain containing protein 73
At4g28500	SM_3_37337	1st exon	NAC domain containing protein 73
At4g28510	SALK_071668C	promoter	prohibitin 1 (Atphb1)
At4g28510	SAIL_895_H10	promoter	prohibitin 1 (Atphb1)
At4g28520	SM_3_36286	5' UTR	12S seed storage protein
At4g28520	GK-283D09	1st exon	12S seed storage protein
At4g28530	SALK_094441C	2nd intron	NAC domain containing protein 74
At4g28530	SALK_149691C	1st intron	NAC domain containing protein 74
At4g28540	SAIL_209_G07	14th exon	CASEIN KINASE I-LIKE 6
At4g28550	SALK_136344	exon	RabGAP/TBC domain protein

Gene	Polymorphism	Location	Gene Annotation
At4g28556	GK-062G02	intron	RIC7
At4g28560	SALK_117755C	exon	CRIB motif-containing protein 7
At4g28560	SM_3_30368	exon	CRIB motif-containing protein 7
At4g28564	SALK_119099C	exon	unknown
At4g28570	SALK_124354C	2nd exon	alcohol oxidase-related
At4g28570	SALK_081176C	2nd exon	alcohol oxidase-related

Appendix B : Arabidopsis T-DNA Insertions for Genes Related to *FLY1*

Gene	Polymorphism	Location	Gene Annotation
At1g06780	CS836723	7th exon	Galacturonosyltransferase 6 (GAUT6)
At1g06780	SALK_056646C	7th exon	Galacturonosyltransferase 6 (GAUT6)
At1g06780	SALK_007987	7th exon	Galacturonosyltransferase 6 (GAUT6)
At1g62990	SALK_002098C	4th exon	KNAT7
At1g62990	SALK_110899C	3rd intron	KNAT7
At1g77280	SALK_107837C	10th exon	protein serine/threonine kinase
At1g77280	SALK_047814C	intron	protein serine/threonine kinase
At2g45220	SALK_059908C	1st intron	plant invertase/PMEI
At2g45220	CS919451	1st intron	plant invertase/PMEI
At3g18230	SALK_032655C	1st exon	Octicosapeptide/Phox/Bem1p protein
At3g18230	SALK_071226C	1st exon	Octicosapeptide/Phox/Bem1p protein
At4g12250	CS859567	1st exon	GAE5
At4g12250	SALK_042836C	5' UTR	GAE5
At4g12250	CS871149	1st exon	GAE5
At5g62150	CS858663	exon	cell wall macromolecule catabolism
At5g62150	SALK_144729C	exon	cell wall macromolecule catabolism
At5g62150	CS904799	exon	cell wall macromolecule catabolism
At5g63760	SALK_085636C	1st exon	ARIADNE 15, zinc ion binding
At5g63760	CS877417	5' UTR	ARIADNE 15, zinc ion binding
At5g63760	SALK_106047	promoter	ARIADNE 15, zinc ion binding